Ana Cristina Rocha da Silva Cortez das Neves

Licenciada em Ciências de Engenharia do Ambiente

Photochemical degradation of triclosan: a comparison between different light sources

Dissertação para obtenção do Grau de Mestre em Engenharia do Ambiente, perfil Engenharia Sanitária

Orientador: Profª. Doutora Ana Isabel Espinha da Silveira, Professora Auxiliar, Faculdade de Ciências e Tecnologias – Universidade Nova de Lisboa

Co-orientador: Prof. Doutor Roberto Raga, Assistant Professor, DII – Università degli Studi di Padova

Júri:

Presidente: Profª. Doutora Maria da Conceição Raimundo dos Santos
Arguente: Doutor Eduardo Manuel Hipólito Pires Mateus
Vogal: Profª. Doutora Ana Isabel Espinha da Silveira

FACULDADE DE CIÊNCIAS E TECNOLOGIA
UNIVERSIDADE NOVA DE LISBOA

Dezembro 2014

Ana Cristina Rocha da Silva Cortez das Neves

Licenciada em Ciências de Engenharia do Ambiente

Photochemical degradation of triclosan: a comparison between different light sources

Dissertação para obtenção do Grau de Mestre em Engenharia do Ambiente, perfil Engenharia Sanitária

Orientador: Profª. Doutora Ana Isabel Espinha da Silveira, Professora Auxiliar, Faculdade de Ciências e Tecnologias – Universidade Nova de Lisboa

Co-orientador: Prof. Doutor Roberto Raga, Assistant Professor, DII – Università degli Studi di Padova

Júri:

Presidente: Profª. Doutora Maria da Conceição Raimundo dos Santos
Arguente: Doutor Eduardo Manuel Hipólito Pires Mateus
Vogal: Profª. Doutora Ana Isabel Espinha da Silveira

FACULDADE DE CIÊNCIAS E TECNOLOGIA
UNIVERSIDADE NOVA DE LISBOA

Dezembro 2014

Photochemical degradation of triclosan: a comparison between different light sources

“Valeu a pena? Tude vale a pena se a alma não é pequena.”

Fernando Pessoa

Acknowledgments

Firstly I would like to thank Professor Ana Silveira the initial stimulus to embark in this adventure. Again to Professor Ana Silveira and Professor Roberto Raga I thank for the opportunity to accomplish this investigation and thesis on an international context, invaluable for my Academic and Human formation.

To Professor Roberta Bertani a special thanks for all the guidance and advice throughout the elaboration of the thesis, for the tireless support and attention given even in busy times. The remarkable passion for Chemistry and work is evident and contagious.

A special note of appreciation to my teachers in FCT/UNL who have contributed to my academic accomplishment.

I would also like to thank the wonderful welcome to the Italian laboratory and the technical support from Paolo, Fabio and Flavio. To Riccardo, Luca and Ivo, thank you for the contribution given to this work. To my Italian friends a special thank you, to Elisa Burigo and Bianca Bresolin for all the good and fun times. Also to my ERASMUS and Residenzia Colombo friends, you have been my family during this endeavour.

To all my friends that direct and indirectly contributed to this work. Additionally Gil Gonçalves and João Lourenço thank you for the fellowship during these years of Academia and for the ever growing friendship.

A special thank you note to Tiago Nunes for the infinite love and patience; for the support, advice and motivation, in particular for reviewing the English of this thesis.

Finally to my family, a very special token of gratitude and appreciation, you have always primed for the best in my education. To Filipa we are more than friends we are sister`s. To my Father that does not ever let me give up of anything and always seems to find the right combination of support and independence that I need to carry on and to my Mother whom has always revealed to be a great woman especially during the bleaker of times, you are my inspiration.

Resumo

O surgimento de novos contaminantes pode representar um perigo para o ambiente e para a Humanidade com repercussões ainda desconhecidas. Uma das maiores produções mundiais de produtos farmacêuticos e de higiene pessoal são produtos antimicrobianos. Triclosan é um agente antimicrobiano presente na maioria dos produtos. Apesar da alta eficiência de remoção de triclosan nas Estações de Tratamento de Águas Residuais, os seus níveis estão em franco aumento nos ecossistemas, através de descargas de efluentes domésticos e lamas utilizadas em aplicações no terreno. Regulado pela norma EC/1272/2008 (anexo VI, tabela 3.1), este composto é considerado muito tóxico para a vida aquática com efeitos a longo prazo, tendo também sido reportado que a sua transformação fotoquímica deriva em dioxinas.

Neste trabalho foram definidos três objectivos. Determinar o processo fotoquímico mais eficiente na degradação do triclosan, comparando diversas fontes de luz; identificação dos subprodutos principais que se formam durante a degradação do triclosan e por último o estudo da influência das reacções Fenton e foto-Fenton.

Foram comparados métodos de degradação fotoquímica tais como: fotocatálise com recurso a luz ultravioleta (UV), fotocatálise com recurso a luz solar, fotocatálise com recurso a LEDs, reacção Fenton e foto-Fenton. A degradação do triclosan foi observada através de cromatografia de gás/espectrometria de massa (GC/MS).

Os resultados obtidos com a reacção foto-Fenton demonstram sucesso na oxidação do triclosan em H_2O e CO_2 sem a formação de nenhum subproduto ao fim de duas horas. Foi possível a foto degradação do triclosan com recurso a dióxido de titânio (TiO_2) e LEDs, obtendo uma taxa de degradação de 53% num ensaio com a duração de 8 horas. A taxa de degradação da reacção Fenton, luz UV e luz solar demonstraram uma degradação entre os 90% e 95%. Os resultados são reportados aos dados observados sem suporte estatístico, uma vez que tal não foi possível no decorrer do período do trabalho. Foram identificados subprodutos como hidroquinona e 2,4-diclorofenol durante a primeira hora de reacção de fotocatálise por UV. Um composto identificado possivelmente como C_7O_4H estava transversalmente presente na degradação por UV, luz solar e LEDs concluindo-se que se tratava de um contaminante.

Estudos futuros sobre a utilização de LEDs devem ser considerados, não só pelas suas vantagens de longa durabilidade e baixo consumo energético, mas também em substituição às lâmpadas UV. O potencial de contaminação ambiental das lâmpadas UV levou a que estas estejam a ser progressivamente retiradas dos mercados pelos governos. As reacções Fenton e foto-Fenton não são alternativa pois são processos custosos devido aos reagentes envolvidos.

Palavras-chave: Triclosan, dióxido de titânio, fotoquímico, fotocatálise, foto degradação, luz fluorescente, LEDs, foto-Fenton.

Abstract

New emerging contaminants could represent a danger to the environment and Humanity with repercussions not yet known. One of the major worldwide pharmaceutical and personal care productions are antimicrobials products, triclosan, is an antimicrobial agent present in most products. Despite the high removal rate of triclosan present in wastewater treatments, triclosan levels are on the rise in the environment through disposal of wastewater effluent and use of sewage sludge in land application. Regulated in the EC/1272/2008 (annex VI, table 3.1), this compound is considered very toxic to aquatic life and it has been reported that photochemical transformation of triclosan produces dioxins.

In the current work it was defined three objectives; determination of the most efficient process in triclosan degradation, recurring to photochemical degradation methods comparing different sources of light; identification of the main by-products formed during the degradation and the study of the influence of the Fenton and photo-Fenton reaction.

Photochemical degradation methods such as: photocatalysis under florescent light (UV), photocatalysis under visible light (sunlight), photocatalysis under LEDs, photo-Fenton and Fenton reaction have been compared in this work. The degradation of triclosan was visualized through gas chromatography/mass spectrometry (GC/MS).

In this study photo-Fenton reaction has successfully oxidized triclosan to H_2O and CO_2 without any by-products within 2 hours. Photocatalysis by titanium dioxide (TiO_2) under LEDs was possible, having a degradation rate of 53% in an 8 hours essay. The degradation rate of the Fenton reaction, UV light and sunlight showed degradation between 90% and 95%. The results are reported to the data observed without statistic support, since this was not possible during the work period. Hydroquinone specie and 2,4-dichlorophenol by-products were identified in the first hour of photocatalysis by UV. A common compound, possibly identified has C_7O_4H , was present at the degradation by UV, sunlight and LEDs and was concluded to be a contaminant.

In the future more studies in the use of LEDs should be undertaken given the advantages of long durability and low consumption of energy of these lamps and that due to their negative impact on the environment fluorescent lamps are being progressively made unavailable by governments, requiring new solutions to be found. Fenton and photo-Fenton reactions can also be costly processes given the expensive reagents used.

Keywords: Triclosan, titanium dioxide, photochemical, photocatalysis, photodegradation, fluorescent light, LEDs, photo-Fenton.

Contents List

Figures list

Tables list

Acronyms List

2,4–DCP	2,4-dichlorophenol
2,8–DCDD	2,8–dicholorodibenzo-p-dioxin
AOPs	Advanced oxidation processes
^{13}C	Carbon 13 isotope
CO_2	Carbon Dioxide
δ	Chemical shift
ESI	Electrospray ionization
ESI–MS	Electrospray ionization mass spectrometry
$[FeO_4]^{2-}$	Ferrate (VI)
$FeSO_4.7H_2O$	Iron (II) sulfate heptahydrate
GC/ITMS	Gas chromatography/ion trap mass spectrometry
GC/MS	Gas chromatography/mass spectrometry
^1H	Proton
^1H NMR	Proton nuclear magnetic resonance
H_2O	Water
H_2O_2	Hydroxide peroxide
H_2SO_4	Sulfuric acid
HPLC	High performance liquid chromatography
HPLC/MS/MS	Liquid chromatography/tandem mass spectrometry
HRGC/MS	High resolution gas chromatography/mass spectrometry
K_2CO_3	Potassium carbonate
LED	Light emitting diode
MSTFA	N-Methyl-N Trifluoroacetamida
m/z	Mass-to-charge ratio
Na_2SO_4	Sodium sulfate (anhydrous form)
NaCl	Sodium chloride
NIST	National Institute of Standards and Technology
NMR	Nuclear magnetic resonance
O_3	Ozone
$OH^{\bullet}$	Hydroxyl radical
PoI	Pollutant
Pt	Platinum
RRLC – MS/MS	Rapid resolution liquid chromatography – tandem mass spectrometry
$SO_4^{\bullet -}$	Sulfate radical anion
TCS	Triclosan
TEM	Transmission Electron Microscopy
TiO_2	Titanium Dioxide
TMS	Tetramethylsilane
UV	Ultraviolet light

XRD	X Ray Diffraction

1 Introduction

Our society has thrived to great extent due to antimicrobial products which allow for a longer life-span for Humanity and greater comfort in treatment of the sick. Triclosan (5 – chloro – 2 – [2,4 – dichlorophenoxy] – phenol) is an antimicrobial agent widely used in various consumer products of health and personal care (Yang *et al*., 2011). Globally the production of triclosan is over 1500 tons per year (Dann & Hontela, 2011), available in more than 2 000 antimicrobial products in the U.S, representing only in this country a market of $1.4 billion in 2014 (Halden, 2014).

Regulated in the EC/1272/2008 (annex VI, table 3.1), this compound is considered very toxic to aquatic life with long lasting effects causing serious irritation to the skin and irritation to the eyes. A final classification has not yet been established. The main sources of contamination in the environment are the release of wastewater effluent and the use of sewage sludge in land application (Dann & Hontela, 2011; Ricart *et al*., 2010; Thompson *et al*., 2005).

There is a growing concern regarding the persistence of triclosan in the environment and its potential adverse impacts, such as bacteria resistance (Yazdankhah *et al*., 2006), endocrine disruptive chemical (Dann & Hontela, 2011; Foran *et al*., 2000) and acute and chronic toxicity (Nassef *et al*., 2010; Chalew & Halden, 2009; Orvos *et al*., 2002).
Structurally related to toxic and carcinogenic dioxins for instance 2,3,7,8–tetrachlorodibenzo–p–dioxin and 2,3,7,8–tetrachlorodibenzofuran, triclosan has been labeled has a predioxin (Halden, 2014). Higher toxicity intermediates and by-products formed during triclosan degradation, as the phototransformation of triclosan to produce 2,8–dicholorodibenzo–p–dioxin (2,8–DCDD) are the major hazards and reasons for alarm (Mezcua *et al*., 2004).

Advanced oxidation processes (AOPs), can be defined as systems that produce strong reactivity species, precisely the hydroxyl radical ($OH^{\bullet}$) or sulfate radical anion ($SO_4^{\bullet -}$) to oxidize or degrade micropollutants such as endocrine disrupting chemicals and pharmaceutical and personal care products (Júnior. *et al*., 2012; Song *et al*., 2012). Catalysis under light irradiation has received great attention for pollution control, has the advantages of use inexpensive photocatalyst (TiO_2), operations conditions such as room temperature and atmospheric pressure, and nearly complete oxidation of carbon and hydrogen containing pollutants to CO_2 and H_2O (Shie *et al*., 2008).

The use of mercury discharge lamps to conduct irradiation is the traditionally used method in TiO_2 photocatalysis (Yu *et al*., 2014), however this process has the disadvantages of the short life, energy cost, the instability of the output power and the hazardous materials from the emitted wastes from the lamps (Yu *et al*., 2014; Shie *et al*., 2008). The handling of UV lamps

should be taken with care because of the UV emission from the UV lamps are harmful to humans eyes (Shie *et al*., 2008).

The LEDs offer numerous advantages: long lifetime, lower power, inexpensive installation, possibility of selective monochromatic light, more effectiveness converting electricity to light with little or no heating and the use of direct current power which offers greater flexibility for field applications, especially for remote areas (Ghosh *et al*., 2009; Shie *et al*., 2008).

LEDs are a reliable competitor to florescent lamp. There are only a limited number of papers that study the LED photocatalysis applied in the field of environmental engineering (Yu *et al*., 2014). No paper on LED photocatalysis in triclosan was found at the time of this written study.

1.1 Thesis Objectives

The main aim of this thesis was to study methods of degradation applied to the environmental contaminant triclosan using traditional light sources (UV and sunlight), as well as the Light Emitting Diode (LEDs). An additional aim was to study the influence of the Fenton and photo Fenton reaction. The objectives were:

i) To analyze which is the best degradation method based on the degradation rate;
ii) To identify the main by-products formed during the degradation.

1.2 Thesis Organization

This thesis was divided in five chapters, and respective subchapters.

1. Introduction, establishes the context and aim of the dissertation.
2. Literature Review, characterization and description of the environmental problems and concerns about triclosan. The state of the art of the photocatalytic process as well as case-studies of other degradation processes are presented.
3. Methodology, the experimental methodology is described. The instruments explored and the analytical treatment methods are defined.
4. Results and discussion, the results are exposed according to the degradation variables and characterization of the standard solution agreeing to the analytical instruments was done. In this chapter a comparison between degradation methods and identification of by-products was presented in order to achieve a response to the thesis objectives.
5. Conclusions and future recommendations, the accomplishment of the objectives is evaluated and futures recommendations to improve results towards and theme development are proposed.

2 Literature Review

2.1 The compound triclosan

Triclosan (TCS) is a broad-spectrum antimicrobial, widely used as main ingredient in various consumer products as disinfectant, preservative or antiseptic. It is used in personal care and household products like: soaps, deodorant soaps, mouthwash, toothpastes, shampoos, body lotions and detergents. It is also used in clinical settings, medical devices, plastic materials and toys (Dann & Hontela, 2011; SCCS, 2010; Fang *et al*., 2010; Bhargava & Leonard, 1996).

TCS was first synthesized by the chemical company Cyba-Geigy in Basel, Switzerland. Firstly registered as a pesticide in 1969, it was later on introduced to the healthcare industry in 1972 and it met widespread use throughout Europe in toothpastes during the 80`s (Kola *et al*., 2013; Fang *et al*., 2010; Bhargava & Leonard, 1996).

According to the European Union in the Scientific Committee on Consumer Safety (SCCS, 2010) apud The European Association of the Cosmetics Industry (COLIPA, 2007) indicates that about 85% of the total of volume of triclosan is used in personal care products, 5% in textiles and 10% for plastics and food contact materials.

Over the years consumer demand for antimicrobials products has increased and so has the amount of triclosan (Figure 2.1). Between 1976 and 2008 the US Patent and Trademark Office issued a total of 2385 patents containing the word triclosan. The production of TCS has now exceeded 1500 tons per year, with Europe having a part of 350 tons of total production. In the U.S over 2 000 antimicrobials products are available with TCS representing a market of $1.4 billion (Halden, 2014; Dann & Hontela, 2011; Fang *et al*., 2010; ; Singer *et al*., 2002).

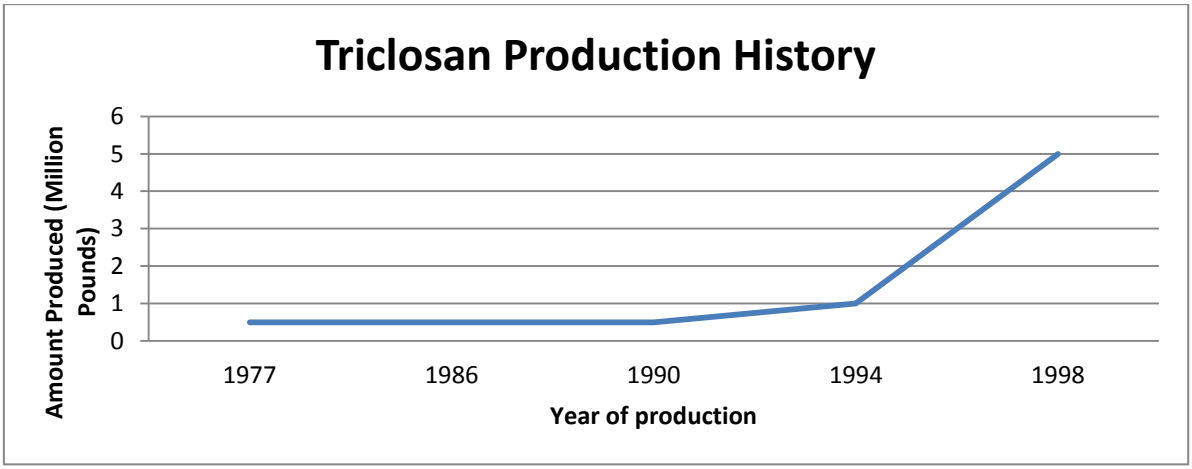

Figure 2.1 Historic evolution of triclosan (Adapted from: Fang *et al*., 2010)

The widespread use and mass production of TCS brings new concerns to human health and to the environment that must be studied (Fang *et al*., 2010).

Triclosan is the name given by the Internacional Nomenclature of Cosmetic Ingredient (INCI), but TCS takes on many different trade names: Irgasan; CH 3565; Irgasan DP300; Ster-Zac; Aquasept; Sapoderm; Irgacare MP; Lexol 300 and Cloxifenolum. In fibres and other materials it can take the name of Ultra-Fresh, Amicor, Microban, Monolith, Bactonixans Sanitized (Dann & Hontela, 2011).

2.1.1 Physico-chemical properties

This nonionic antibacterial agent, is a halogenated phenol with a molecular weight of 289,55 $gmol^{-1}$ and its molecular structure is represented in Figure 2.2.

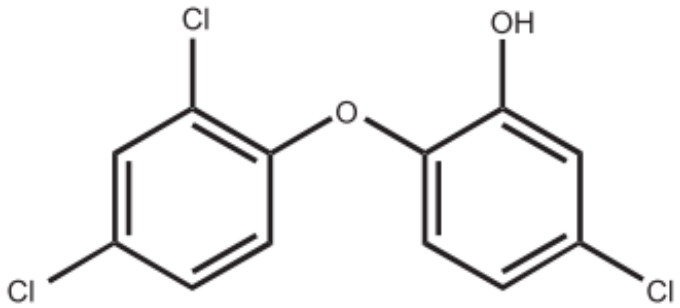

Figure 2.2 Molecular structure of triclosan (Adapted from: Fang *et al*., 2010)

On the Table 2.1 are gathered the most important physico-chemical features of TCS.

Table 2.1 Chemical Properties of triclosan (Adapted from: Dann & Hontela, 2011; Fang *et al*., 2010)

INCI name	Triclosan
Synonymous	5-cloro-2-(2,4-dichlorophenoxy)phenol or 2,4,4`-trichloro-2`hydroxydiphenyl ether
Chemical abstracts service registry number	3380–34–5
Formula	$C_{12}H_7Cl_3O_2$
Molecular Weight	289,55 $gmol^{-1}$
Specific gravity	1,55 x 10^3 kg/m^3 at 22ºC
Melting point	54-57ºC
Vapor Pressure	4 x 10^{-6} mm Hg at 20ºC
Octanol – water partition constant (log K_{ow})	4,76
Boiling point	280 – 290ºC
Physical state	Colorless to off white crystalline powder
Solubility	Water (20ºC): 0,01 g/l ; n–Hexane (25ºC): 85 g/l; Other solvents such as ethanol; acetone, Tween 20 are highly soluble (25ºC) : >1000 g/l

2.1.2 Antibacterial properties

The first action of TCS is on the cytoplasmic membrane, directed to the RNA and protein synthesis (Bhargava & Leonard, 1996). In addition TCS demonstrates a tendency to disorder membrane activities, compromising the functional activity without causing leakage of intracellular components (Villalaín *et al*., 2001).

Triclosan inhibits bacterial fatty acid biosynthesis by inhibiting the enzyme enoyl–acyl–carrier protein (ACP) reductase or FabI (Russell, A.D., 2004, Heath *et al*., 1999). This enzyme catalyzes chemical reactions essential in the synthesis of fatty acid. The bacterial enzyme ACP sequence and structural organization are different from those of mammalian fatty acid biosynthesis enzymes (Ling *et al*., 2004). So the efficacy and specificity of triclosan against bacteria's making this compound an antibacterial.

Triclosan has different reactions depending on its concentration (SCCS, 2010). At low concentrations triclosan is bacteriostatic, inhibiting the enzyme ACP; at higher concentrations it becomes bactericidal, destabilizing the membrane structure and compromising the functional integrity of those membranes (SCCS, 2010; Villalaín *et al*., 2001). According to Heidler & Halden, (2007) and Bhargava & Leonard, (1996) referring Regos *et al*., 1979 triclosan is effective at low concentrations against a broad spectrum of gram-negative and gram-positive bacteria.

2.2 The environmental problem of triclosan

2.2.1 Sources of contamination

The main sources identified of contamination of the environment are (Dann & Hontela, 2011; Ricart *et al*., 2010; Thompson *et al*., 2005):

1) The release of wastewater effluent into the receiving waters;
2) The use of sewage sludge in land application.

Biological wastewater treatment is currently considered the principal destructive mechanism limiting dispersal of and environmental contamination of TCS (Heidler & Halden, 2007).

Removal efficiencies are between 95% to 98% for activated sludge plants (Heidler & Halden, 2007; Thompson *et al*., 2005; Bester, 2003; McAvoy *et al*., 2002), 58% to 96% for rotating biological contactors and 86% to 97% for trickling filter (Thompson *et al*., 2005). Activated sludge treatment had the higher removal efficiencies because it is maintained in high dissolved

oxygen levels (Thompson *et al*., 2005). TCS shows no biodegradation under anaerobic conditions (McAvoy *et al*., 2002).

According with Bester, (2003) in a study performed in a German activated sludge sewage treatment plant that processed 200 000 m^3 wastewater per day, about 5% of TCS was dissolved in the effluent and 30% was absorbed to the sludge. It was considered that the other 65% was transformed into unknown metabolites or strongly bound residues. There are four process that could remove TCS from the liquid phase: volatilization, photolysis, sorption to wastewater sludge and biodegradation (Thompson *et al*., 2005). Volatilization could be considered refutable since triclosan vapor pressure is 4×10^{-6} mm Hg (Heidler & Halden, 2007; Thompson *et al*., 2005). TCS is mostly in its photostable form in the pH range that normally wastewater treatment works, from 6.5 to 8.5, therefore photolysis is minimal (Thompson *et al*., 2005). TCS is a hydrophobic compound, and hydrophobic compounds tend to adsorb to primary sludge (Thompson *et al*., 2005).

In a deep research, Chalew & Halden, (2009) found the maximum amount detected in rivers in the U.S was 2.3 µg/l. The potential environmental risk is higher in waters with low dilution capacity (Ricart *et al*., 2010).

Currently there are some methods available to remove TCS from the water, like advanced oxidation or granular activated carbon. Unfortunately these methods are expensive to install and operate (Thompson *et al*., 2005).

2.2.2 Environmental fate

TCS`s trichlorinated binuclear aromatic structure shares similarities with dioxins, suggesting potentially problematic properties, including persistence and bioaccumulation (Heidler & Halden, 2007). Bioaccumulation in tissue, opens a potential pathway for chemical biomagnification up the food chain (Chalew & Halden, 2009).

Photodegradation seems to be the major route of elimination of triclosan in aquatic environments (Latch *et al*., 2003; Singer *et al*., 2002). It takes place at low intensity under UV light (254, 313 or 365 nanometer), simulated solar light or artificial white light under laboratory assays. In Figure 2.3 is showed the photodecomposition pathways of TCS.

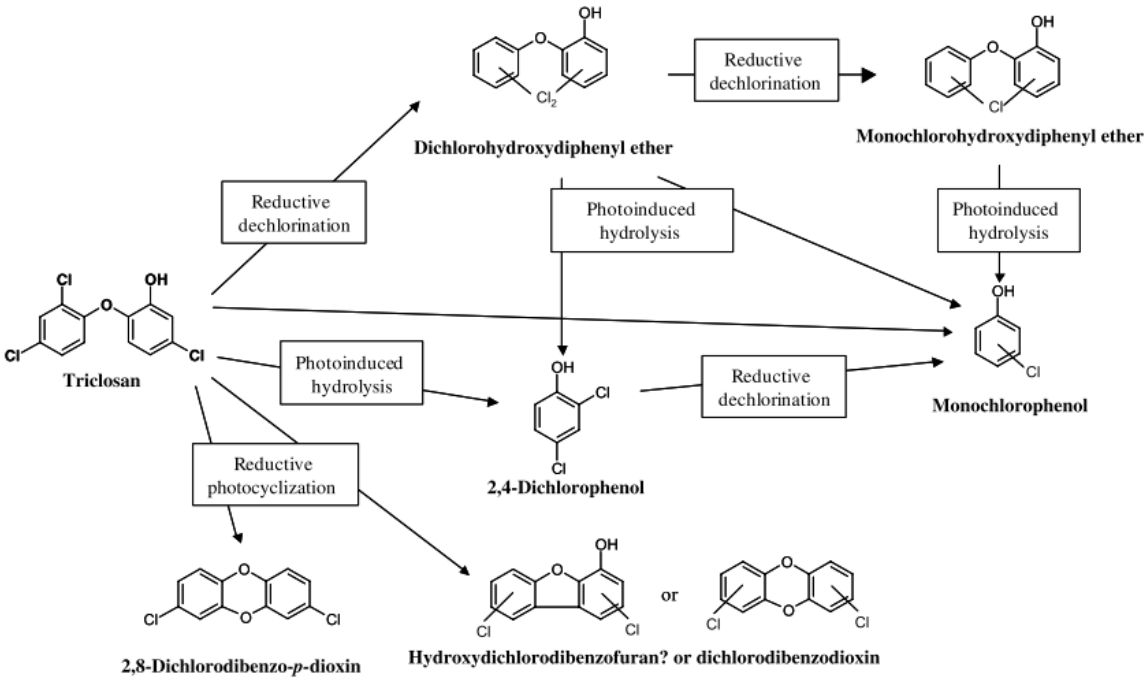

Figure 2.3 Photodecomposition pathways of TCS (Adapted from: Sanchez-Prado *et al*., 2006)

Tixier *et al*., (2002) concluded that photochemical transformation of TCS accounts for up 80% of its loss from the epilimnion in Lake Greifensee during summer months. Dioxins accumulate in the water due to the TCS photodegradation (Aranami & Readman, 2007).

2.2.3 Toxicity

Since TCS is an anthropogenic chemical, its presence in the environment derives directly from human activities. TCS it is an apolar molecule (log K_{ow} = 4,8), and is likely to bioaccumulate (Thompson *et al*., 2005).

The main concerns originated by the TCS compound are:

1. Resistance of bacteria

Antibacterials are similar to antibiotics in the point that both inhibit bacterial growth. One concern is bacteria will become resistant to antibacterial products like TCS. Another concern is bacteria that becomes resistant to TCS can also become resistant to antibiotics (Yazdankhah *et al*., 2006).

2. Endocrine disruptive chemical

The molecular structure of TCS is very similar to non-steroidal estrogens and the thyroid hormones (Dann & Hontela, 2011; Foran *et al*., 2000), molecules with two aromatic rings (Figure 2.4).

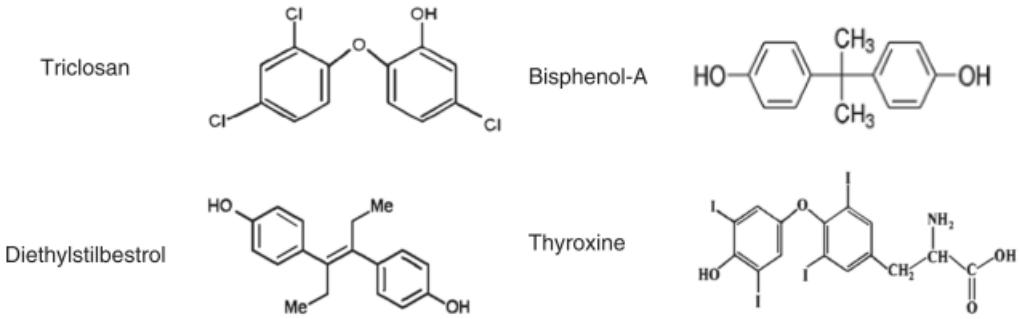

Figure 2.4 The structural similarity of TCS to Bisphenol A, Diethylstillbestrol and the thyroid hormone thyroxine (Adapted from: Dann & Hontela, 2011)

3. Acute and chronic toxicity

Higher toxicity intermediates and by-products are produced during TCS degradation in the environment bring new concerns to its degradation mechanism in the environment. TCS has been detected in water, sediments, biosolids, soils, aquatic species and humans (Dann & Hontela, 2011). Worldwide TCS survey indicates a large dispersion being referred in aquatic environments and organisms from the United States, to Germany and Australia (Katz *et al*., 2013; Xie *et al*., 2008; Coogan *et al*., 2007; Ying & Kookana, 2007).

In humans, exposure and bioaccumulation were registered by detection of TCS in human breast milk in the United States, Sweden and Australia (Toms *et al*., 2011; Dayan, 2007; Allmyr *et al*., 2006; Adolfsson-Erici *et al*., 2002). In China and Korea it was detected in urine (Li *et al*., 2013; Kim *et al*., 2011). Human blood and plasma samples with the presence of TCS were reported in Sweden and Australia (Allmyr *et al*., 2006; Adolfsson-Erici *et al*., 2002).

An in vitro study revealed that the exposure to TCS inhibits phase II enzyme metabolism in human liver (Wang *et al*., 2004). Other studies (SCCS, 2010; Dayan, 2007) conclude that TCS is rapidly absorbed from the gastrointestinal tract and although at a lower rate is also absorbed through the skin.

The route of administration and the kind of species has a substantial influence on the toxicity of triclosan (Fang *et al*., 2010; Bhargava & Leonard, 1996). TCS inhibited plant growth with a half maximal effective concentration (EC_{50}) between 57 mg/kg to 108 mg/kg. Soil respiration was inhibited in treatments with triclosan at concentrations more than 10 mg/kg (Liu *et al*., 2009). At concentrations below 10 mg/kg, TCS can disturb the nitrogen cycle in some soils (Waller & Kookana, 2009).

TCS has the potencial to bioaccumulate in aquatic organisms and exert adverse physiological effects (Hontela & Habibi, 2013). From the studied aquatic species, the ones that appeared most vulnerable are crustacea and algae species, with growth inhibition occurring at

concentrations measured in surface waters (Dann & Hontela, 2011; Chalew & Halden, 2009; Tatarazako *et al*., 2004; Orvos *et al*., 2002).

- **Algae**

In Tatarazako *et al*., 2004 the microalga *Selenastrum capricornutum* was about 30 to 80 times more sensitive to Triclosan toxicity than the bacterium (*Vibrio fisheri*) and fish (*Danio rerio* and *Oryzias latipes*). The half maximal inhibitory concentration (IC_{50}) growth inhibition of microalga *Selenastrum capricornutum* was 4,7 µg/l while fish *Danio rerio* and *Oryzias latipes* were respectively 220 µg/l and 400 µg/l.

Another algae, *Scenedesmus subspicatus*, revealed a EC_{50} (96h) of 1,4 µg/l (Orvos *et al*., 2002). Chalew & Halden, (2009) performed a study where the summary of occurrence data for TCS and contrasts of toxicity thresholds for aquatic organisms were gathered. According to this study the toxic concentrations to algae lays in the range of 0,2 µg/l to 2,8 µg/l. The increased of concentration of TCS affects the viability of the diatom cell (Ricart *et al*., 2010).

The influence that TCS has on algae, important organisms for being the first-step producers in the ecosystem, opens the possibility for the destruction of the ecosystem's balance if a high volume discharge in the environment occurs (Tatarazako *et al*., 2004).

- **Crustacea**

Orvos *et al*., 2002 studied the aquatic toxicity of triclosan using activated sludge microorganisms, algae, invertebrates and fish. The *Daphnia magna* acute toxicity EC_{50} (48h) was 390 µg/l and to the Ceriodaphnia was 184,7 µg/l. The study of Chalew & Halden, (2009) stated acute toxicity for crustacea lays in the range from 185 µg/l to 390 µg/l and chronic toxicity lower levels initiate from 6 µg/l to 182 µg/l.

- **Fish**

Fish show a great vulnerability to TCS too. Nassef *et al*., 2010, measured the effects on feeding behavior and swimming speed in adult Japanese medaka fish (*Oryzias latipes*). Exposure to 0,17 mg/l TCS in nine days resulted in a decrease in the mean of the swimming performance, but not in the feeding behavior. However, swimming performance is closely related to food capture and is considered to be a primary determinant of survival in many species of fish and other aquatic animals. Other study performed by Foran *et al*., 2000, in a exposure of 14 days with 1,10 µg/l and 100 µg/l TCS in Japanese medaka fish (*Oryzias latipes*), suggested TCS may act as an environmental anti-estrogen or androgen. At lower concentrations swimming

performance and feeding behaviors were affected. At high concentrations it was lethal to medaka infant fish, calculating the lethal concentration at 50% (LC_{50}) in 48h of 352 µg/l.

For the zebrafish (*Danio rerio*), the effects of TCS count teratogenic effects and delaying embryo development, resulting in mortality within 48h (Nassef *et al*., 2009 apud Dann & Hontela, 2011). The acute toxicity levels in fish have been determined to range from 260 µg/l to 440 µg/l and the chronic toxicity range from 34 µg/l to 290 µg/l (Chalew & Halden, 2009). Aquatic invertebrates also exhibit vulnerability to TCS (Dann & Hontela, 2011).

Due to the large increase of exposure, even if a product is non-toxic, the accumulation of TCS from different sources in the environment can have a greater effect of which exposure dangers are not yet known.

2.3 Different processes studied for degradation. Triclosan case studies

AOPs, can be defined as systems that produce strong reactivity species, precisely $OH^{\bullet}$ or $SO_4^{\bullet-}$ to oxidize or degrade micropollutants such as endocrine disrupting chemicals and pharmaceutical and personal care products (Júnior *et al*., 2012; Song *et al*., 2012).

AOPs recognized examples are (Júnior *et al*., 2012; Bauer & Fallmann, 1997):

- Oxidant (catalyst, when used)/ light: H_2O_2/UV; O_3/UV; O_3-H_2O_2/UV; (TiO_2)/UV; Fe(III)/(TiO_2)/UV;
- Fenton-reaction or H_2O_2-Fe(III);
- Photo-Fenton reaction or H_2O_2 [Fe (II)/(Fe(III)]/UV.

The generation of $OH^{\bullet}$ radicals in AOPs is very important because it affects not only the decay rate of the parent compound triclosan but also the accumulation of toxic intermediates (Song *et al*., 2012). One usual problem for the AOPs is the high demand of electrical energy for ozonizers and/or UV lamps. The pursuance for a total cost reduction process can be possible by using the catalyst TiO_2 that used 5% of the solar spectrum and the photo-Fenton reaction, since O_3 and H_2O_2 alone don't absorb light of wavelength superior to 300 nanometers (nm), having the main precondition the use of sunlight (Bauer & Fallmann, 1997).

Triclosan case studies

2.3.1 Photocatalysis perform under ultraviolet light (UV)

Sankoda *et al*., 2011 performed one study through TiO_2 photocatalysis by UV light with the objective of identify structures of intermediates and evaluate the endocrine disrupting activities from TCS treated with TiO_2 during the oxidative reactions.

The conditions of the photo reactor are exposed in the Table 2.2. It should be noted that experiments to measure the photodegradation rate of the TCS used smaller volume of sample than the experiments to analyze the intermediates.

Table 2.2 Main conditions of the photodegradation of TCS experiment made by Sankoda *et al*., 2011

Light	Solution (ml)	Water	TCS (mg/l)	Sample (ml)	Analysis	Time experiment (h)
UV	500	Deionized	1	5 and 400	GC/MS after derivatization	4

The main achievements and conclusions of the study are:

- Identified intermediates: dichlorophenols, specially 2,4-dichlorophenol (2,4-DCP); tetraclosans, mono-chlorinated derivative of TCS, hydroxylated triclosan and 2,8–DCDD;
- TCS was hardly decomposed by TiO_2 without UV irradiation;
- TiO_2 degraded approximately 90% of the initial concentration within 2h of irradiation;
- Tetraclosan and 2,4-DCP have stronger thyroid hormone activities than triclosan in the presence of postmitochondrial supernatant fraction, known as S9, prepared from rat liver.

Some carcinogenic chemicals, such aromatic amines and polycyclic aromatic hydrocarbons, are biologically inactive unless they are metabolized to active forms (Mortelmans & Zeiger, 2000). In humans and lower animals like rats, the cytochrome P450 enzymes, important to oxidase xenobiotic compounds are mainly present in the liver and are capable of metabolizing these carcinogenic chemicals. Since bacteria do not have this metabolic capability, an exogenous mammalian organ activation needs to be add to the assay. Human or rat S9 liver fraction are the typical metabolic activation preparation used in this type mutagenicity of assays for being rich in metabolizing enzymes (Hakura *et al*., 2002; Mortelmans & Zeiger, 2000; Hakura *et al*., 1999).

Rafqah *et al*., 2006 conducted a study with the objective to investigate the photocatalytic degradation of TCS using different types of TiO_2 (Degussa P25, PC50 and PC500). TiO_2

Degussa P25 used a mixture of anatase/rutile (80/30) and PC50 and PC500 which are 100% of anatase. Table 2.3 resumes the main experimental:

Table 2.3 Main conditions of the photodegradation of TCS made by Rafqah *et al*., 2006

Light (nm)	Solution (ml)	Water	TCS (mg/l)	TiO_2 (g/l)	Sample (ml)	Analysis	Time experiment (h)
300 - 450	150	Deionized and Natural (River)	4 to 11	1	0,2	HPLC/MS/MS	1 and 0,5

The main achievements and conclusions of the study performed were:

- Identified intermediates: 2,4–DCP, chlorocatechol hydroxylated triclosan and 5–chloro–2–(4–chlorophenoxyl)phenol;
- The direct photolysis on the degradation of TCS was negligible;
- Photolysis accounted less than 8% after 60 minutes (min) and TiO_2 P25 photocatalysis showed a total disappearance of TCS in the same time;
- TiO_2 P25 was by far the more efficient catalyst;
- The p-dioxin derivatives (2,8–DCDD and 2,7-dicholorodibenzo-p-dioxin) were not detected;
- The degradation of TCS in the presence of TiO_2 was efficient but at a slower initial rate when compared with natural water.

Yu *et al*., 2006 study the destruction of TCS in aqueous solution using TiO_2 (Degussa P25) at two different wavelengths in the UV spectral region (254 and 365 nm). The experimental conditions are exposed at the Table 2.4.

Table 2.4 Main conditions of the photocatalysis degradation experiment performed by Yu *et al*., 2006

Light (nm)	Solution (ml)	Water	TCS (mg/l)	TiO_2 (g/l)	Sample (ml)	Analysis	Time experiment (h)
254 and 365	600	Deionized	9	0,1	10 and 2,5	GC/ITMS and GC/MS	6

The main achievements and conclusions of the study performed were:

- Identified intermediates: 2,4–DCP, quinone of triclosan (2-chloro-5-(2,4-dichlorophenoxy)-[1,4]benzoquinone) and hydroquinone of triclosan (2-chloro-5-(2,4-dichlorophenoxy)benzene-1,4-diol);
- No chlorinated dibenzo-p-dioxin congener was detected at 365 nm, however a chlorinated dibenzo-p-dioxin was found in samples exposed to 254 nm UV light, indicating wavelength dependency;

- 2,4–DCP is the major intermediate;
- Photocatalytic degradation of TCS over TiO_2 was 95% over 6h.

Latch *et al*., 2003 used water samples from the Mississippi river to comprehend the photochemical behavior of TCS. The water river was spiked with 4,7 mg/l of TCS and analyzed the presence of dioxins trough GC/MS, HPLC and NMR. This work concludes that TCS is likely to be converted to 2, 8 – DCDD in sunlight – irradiated surface waters.

2.3.2 Sunlight

Sanchez-Prado *et al*., 2006 observed the photochemical degradation of TCS samples non-spiked with TCS from a wastewater treatment plant located in Galicia, in the northwest of Spain. The estimated concentration of TCS was in the order of the nanograms per mililiter. The samples were submitted at UV lamp in a wavelength equal to 254 nm and to a solar simulator photo reactor. The same experiment was made in ultrapure water, with the influence of the pH also studied. The experimental conditions are exposed at the Table 2.5.

Table 2.5 Main conditions of the experiment performed by Sanchez-Prado *et al*., 2006

Water	Sample (ml)	Analysis	Time experiment (h)
wastewater and deionized	5	GC/MS	0,5

The main achievements and conclusions of the study performed were:

- Identified intermediates: 2,8–DCDD, another di-chlorinated dioxin or dichlorohydroxydibenzofuran, dichlorohydroxydiphenyl ether, monochlorophenol and dichlorophenol;
- TCS photodegradation occurred in both light sources;
- TCS degradation altought fast, is slower in wastewater than in ultrapure water;
- Photodegradation of TCS and formation of 2,8–DCDD occurred independently of the pH;
- The photodegradation in basic pH solutions is faster than in acidic pH solutions.

2.3.3 Fenton and photo-Fenton reaction

Fenton is a simple redox reaction in which Fe^{2+} is oxidized to Fe^{3+} and H_2O_2 is reduced to hydroxide ion (OH^-) and $OH^\bullet$ (eq.2.1) (Júnior. *et al*., 2012):

$$Fe^{2+} + H_2O_2 \rightarrow Fe^{3+} + OH^- + OH^\cdot \qquad \text{(eq.2.1)}$$

In the absence of light, the Fe^{3+} can be reduced to ferrous ion by a second molecule of H_2O_2 (eq.2.2), (Júnior. *et al*., 2012):

$$Fe^{3+} + H_2O_2 + H_2O \rightarrow Fe^{2+} + H_3O^+ + HO_2^{\cdot -} \quad \text{(eq.2.2)}$$

For the degradation of organic molecules, the optimum pH for the Fenton reaction is in the range of pH of 2-4 (Júnior *et al*., 2012; Bauer & Fallmann, 1997). One way to accelerate the Fenton reaction is thought the irradiation of ultraviolet light, giving the name photo-assisted Fenton or photo-Fenton reaction (Júnior *et al*., 2012). The photo-reaction produces additional $OH^{\bullet}$ radicals and leads to the recycling of the Fe^{2+} catalyst (Bauer & Fallmann, 1997). The general mechanism is show in the eq.2.3.

$$Fe^{3+} + H_2O \xrightarrow{h\nu} Fe^{2+} + OH^{\cdot} + H^+ \quad \text{(eq.2.3)}$$

Yang *et al*., 2011 determined the rate constants and identified intermediates for the reaction of Fe (VI) with triclosan and evaluated the toxicity changes during the Fe (VI) oxidation of triclosan using algal toxicity tests. The conditions of the Fenton reaction experiment are reported in the Table 2.6. For the identification of the intermediate products samples were adjusted to a pH equal to 2.

Main conditions are presented in the Table 2.6.

Table 2.6 Main conditions of the Fenton reaction experiment performed by Yang *et al*., 2011

Solution (ml)	pH	Water	TCS (mg/l)	$[FeO_4]^{2-}$ (mg/l)	Analysis	Time experiment (h)
150	7 - 10	Deionized	0,87	5	GC/MS and RRLC – MS/MS	1,5

The main achievements and conclusions of the study performed were:

- Identified intermediates: 2,4–DCP, 2-chlorobenzoquinone, chlorophenol and hydroquinone of triclosan;
- The proposed mechanism for the oxidation of triclosan by the Fe(VI) involves the scission of the ether bond and phenoxy radical addition reaction;
- The degradation processes of triclosan resulted in a significant decreased of algal toxicity.

Son *et al*., 2010 studied the degradation efficiency of TCS in the Fenton reaction, photo-Fenton reaction and photolysis (UV-C only). In this work it was estimated the participation of $OH^{\bullet}$ radicals into the reactions by adding methanol, a radical scavenger. In all the reactions the concentration of TCS and the duration of the experiments were identical; in the photolysis experiment the UV-C lamps had a wavelength of 254 nm. The main conditions of the Fenton and photo-Fenton reaction are reported in the Table 2.7 and Table 2.8.

Table 2.7 Main conditions of the Fenton reaction performed by Son *et al*., 2010

Solution (ml)	pH	Water	TCS (mg/l)	$FeSO_4.7H_2O$ (mg/l)	H_2O_2 (mg/l)	Analysis	Time experiment (h)
1500	3	Deionized	5	556	180	GC/MS	2

Table 2.8 Main conditions of the photo-Fenton reaction experiment performed by Son *et al*., 2010

Light (nm)	Solution (ml)	Water	TCS (mg/l)	$FeSO_4.7H_2O$ (mg/l)	Analysis	Time experiment (h)
365	1500	Deionized	5	556	GC/MS	2

The main achievements and conclusions of the study performed were:

- Identified intermediates: Chloride (ionic intermediate of TCS);
- TCS was completely degraded after 90 min under photolysis (UV-C), and after 30 min in the Fenton and photo-Fenton.
- The primary degradation mechanism in both Fenton and photolysis is oxidation by $OH^{\bullet}$ radicals. The presence of methanol, considerably reduced the degradation rate of TCS in all tree reactions, but with more expression in the Fenton and photolysis reactions;
- The reversible reaction of Fe^{2+} to Fe^{3+} occurs in the photo-Fenton reaction, but not in the Fenton reaction;
- The photo-Fenton reaction can overcome the disadvantages of the Fenton reaction like sludge production, the use of expensive H_2O_2 and pH adjustment.

Degradation products

Dioxins, specifically 2,8–DCDD, are one of the most dangerous by-products produced in the photodegradation of TCS. Dioxin can be highly carcinogenic and can cause health problems as severe as weakening of the immune system, decreased fertility, altered sex hormones, miscarriage, birth defects and cancer (Glaser, 2004).

The by-product 2,4–DCP is considered a priority pollutant by the US EPA (United States Environmental Protection Agency), suspected to be a carcinogenic compound.

2.4 Mechanism of photocatalysis. The catalyst TiO_2

The inspiration to the conception of the photocatalysis came from the natural photosynthesis from plants. Plants use sunlight energy to grow, this process is possible by the oxidation of water, producing O_2 and the reduction of CO_2 through solar energy (Kaneko & Okura, 2002).

By analogy to the natural photosynthesis, A. Fujishima and K. Honda investigated the photoelectrolysis of water using light energy. The now called Honda-Fujishima effect, first tried in 1972, consisted in a system with a TiO_2 semiconductor electrode and a Pt electrode connected by an electrical circuit (Figure 2.5). When TiO_2 is irradiated with light of wavelengths shorter than ~ 415 nm, photocurrent flowed from the platinum counter to the TiO_2 electrode thought the external circuit. The direction of the current reveals that the oxidation reaction (oxygen evolution) occurs at the TiO_2 electrode and the reduction reaction (hydrogen evolution) at the Pt electrode. This proved that water can be decomposed, using UV visible light, into oxygen and hydrogen, without the application of an external voltage (Kaneko & Okura, 2002).

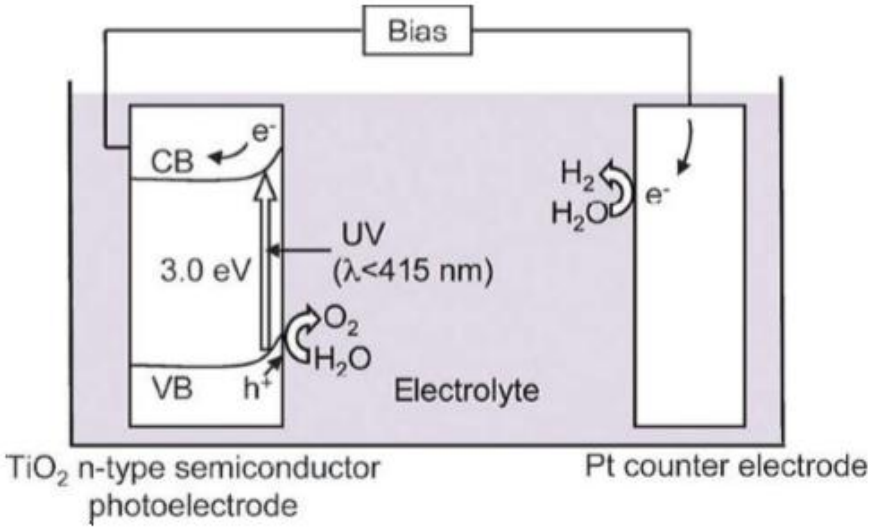

Figure 2.5 Honda – Fujishima effect – water splitting using a TiO_2 photoelectrode, demonstrating the valence band (VB) and the conduction band (CB) (Adapted from: Kudo & Miseki, 2009)

Photocatalysis is an oxidative decomposition activated by light, which uses a semiconductor or a catalyst to accelerate the chemical reaction without being consumed as a reactant.

TiO_2 photocatalysis was performed in this work. The TiO_2 photocatalysis process can be described as follows (Nakata & Fujishima, 2012; Kaneko & Okura, 2002):

- Illumination of TiO_2 by light with energy larger than the band gap energy elevates electron in the valence band to the conduction band; a positive hole (h^+) is formed in the valence band after elevated electron (e^-). Following the reaction:

$$TiO_2 \xrightarrow{h\nu} e^- + h^+ \qquad \text{(eq. 2.4)}$$

- Photogenerated holes in the valence band diffuse to the TiO_2 surface and react with adsorbed water molecules, forming hydroxyl radicals ($OH^\bullet$) or directly to the pollutant, according to the following reactions:

$$h^+ + H_2O \rightarrow OH\cdot + H^+ \quad \text{(eq. 2.5)}$$

$$h^+ + Pol \rightarrow CO_2 \quad \text{(eq.2.6)}$$

- In the meantime, electrons in the conduction band typically react with molecular oxygen in the air to produce superoxide radical anions (O_2^-), following the reaction:

$$e^- + O_2 \rightarrow \cdot O_2^- \quad \text{(eq.2.7)}$$

- These strong reactive oxygen species oxidize and decompose organic substances (Figure 2.6); when the degradation is complete the final products are CO_2 and H_2O.

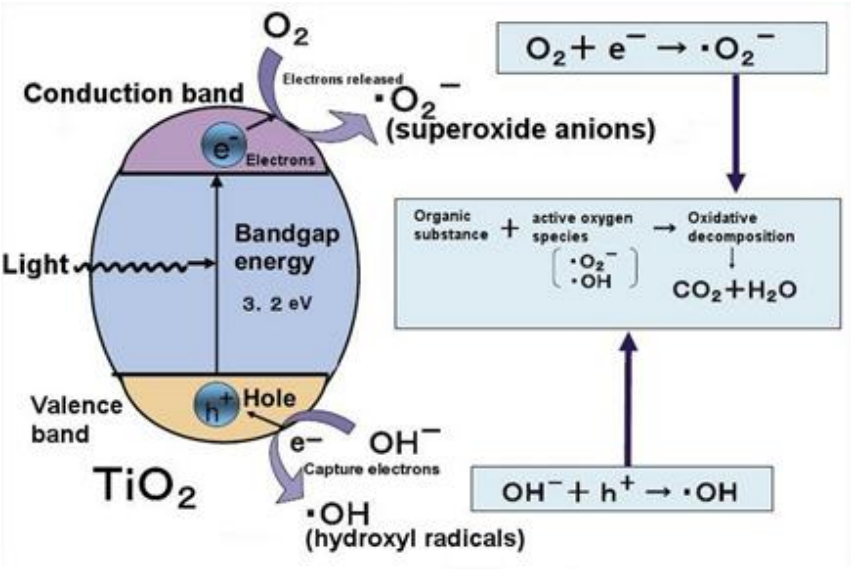

Figure 2.6 Principles of oxidative decomposition of TiO_2 photocatalysis (Adapted from: Fujishima & Murakami, 2010)

The most difficult problem in photocatalysis is the rapid recombination of separated positive and negative charges, the oxidant–reduction process should occur simultaneously, otherwise electrons accumulate in the conduction band and the recombination between electron and positive hole increase. For this reason an effective consumption of electrons is essential to achieve efficient photocatalysis (Kaneko & Okura, 2002).

Currently many applications exist for photocatalysis technology like self-cleaning materials, air cleaning, water purification, antitumor activity and self-sterilizing (Figure 2.7).

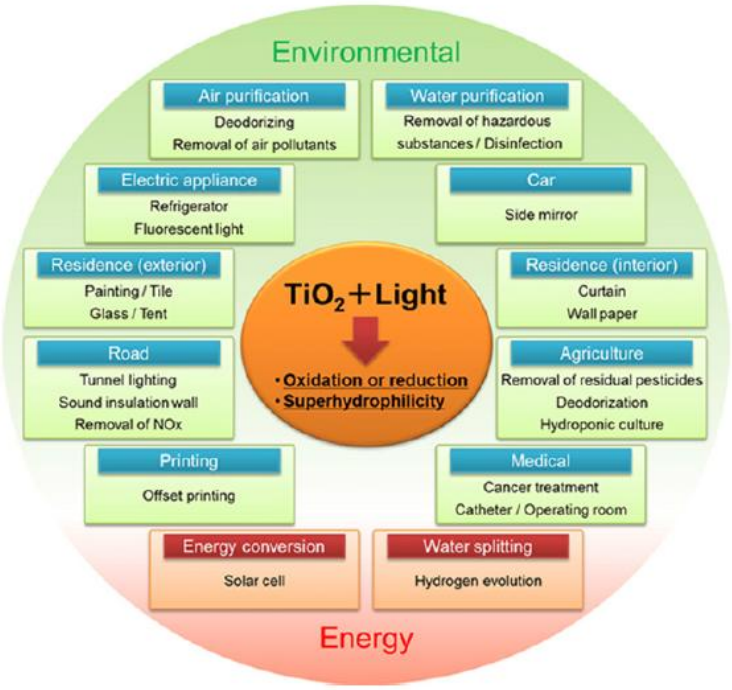

Figure 2.7 Applications of TiO_2 photocatalysis (Adapted from: Nakata & Fujishima, 2012)

The catalyst: TiO_2

The ideal catalyst is the one that makes strong oxidizing species and uses light energy with high efficiency. The semiconductor should be chemically and biologically inert, photocatalyst stable, easy to produce, efficiently activated by sunlight, able to efficiently catalyze reactions, cheap, and without risks to the environment and humans (Carp *et al*., 2004).

TiO_2 has become the principal photocatalyst in environmental decontamination for a huge variety of organics, viruses, bacteria, fungi, algae, and cancer cells that can be totally degraded and mineralized to CO_2, H_2O and harmless inorganic compounds (Carp *et al*., 2004). The TiO_2 demonstrates many advantages towards its use in environmental photocatalysis and over other semiconductors: availability of the catalyst; availability in nature; high chemical stability; relatively inexpensiveness; nontoxic and high photoactivity (Kaneko & Okura, 2002).

TiO_2 can crystalize in three main polymorphs: rutile, anatase and brookite. In the Figure 2.8 are represented the structures of the polymorphs; rutile (a in Figure 2.8) and anatase (b in Figure 2.8) have a tetragonal structure, brookite has a orthorhombic form (c in Figure 2.8). These structures can be defined in by the distortion of TiO_6 octahedrals, where each Ti^{4+} ion is surrounding by six O^{2-} in the positions of the vertices (Fuertes *et al*., 2013; Carp *et al*., 2004). Red spheres are Ti^{4+}, blue spheres are O^{2-} and the yellow lines represent the unit cell.

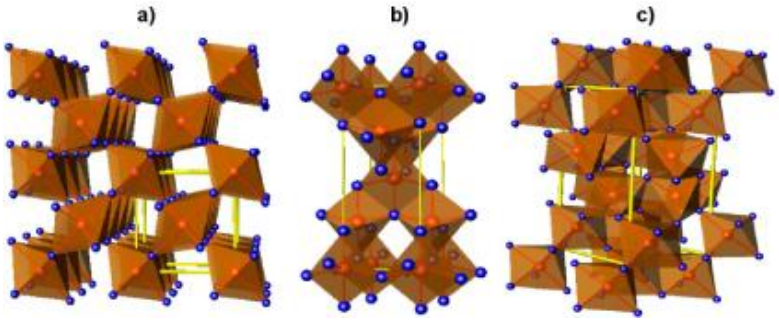

Figure 2.8 Crystal structures of TiO_2 polymorphs, (a) rutile, (b) anatase and (c) brookite (Adapted from: Fuertes *et al*., 2013).

Differences in lattice structures are responsible for different mass densities and electronic band structures among the polymorphs (Fuertes *et al*., 2013). Anatase has a larger photocatalytic activity, explained by a higher band gap then rutile, as reported in Table 2.9.

Nevertheless a mixture of anatase and rutile, like commercial Degussa "TiO_2 P25", is claimed to be more active than anatase (Sun & Xu, 2010; Kaneko & Okura, 2002).

Table 2.9 Some properties of the main polymorphs of TiO_2 (Adapted from: Carp *et al*., 2004)

	Rutile	**Anatase**	**Brookite**
Polymorph form	tetragonal	tetragonal	orthorhombic
Density (kg/m3)	4240	3830	4170
Band Gap (eV)	3,05	3,26	-

3 Methodology

3.1 Experimental setup

The Figure 3.1 demonstrates the experiments based in advanced oxidation process made to recognize the degradation degree of triclosan and identification of the main products. An additional experiment was done, with Rhodamine B as a control to the operation system reactor.

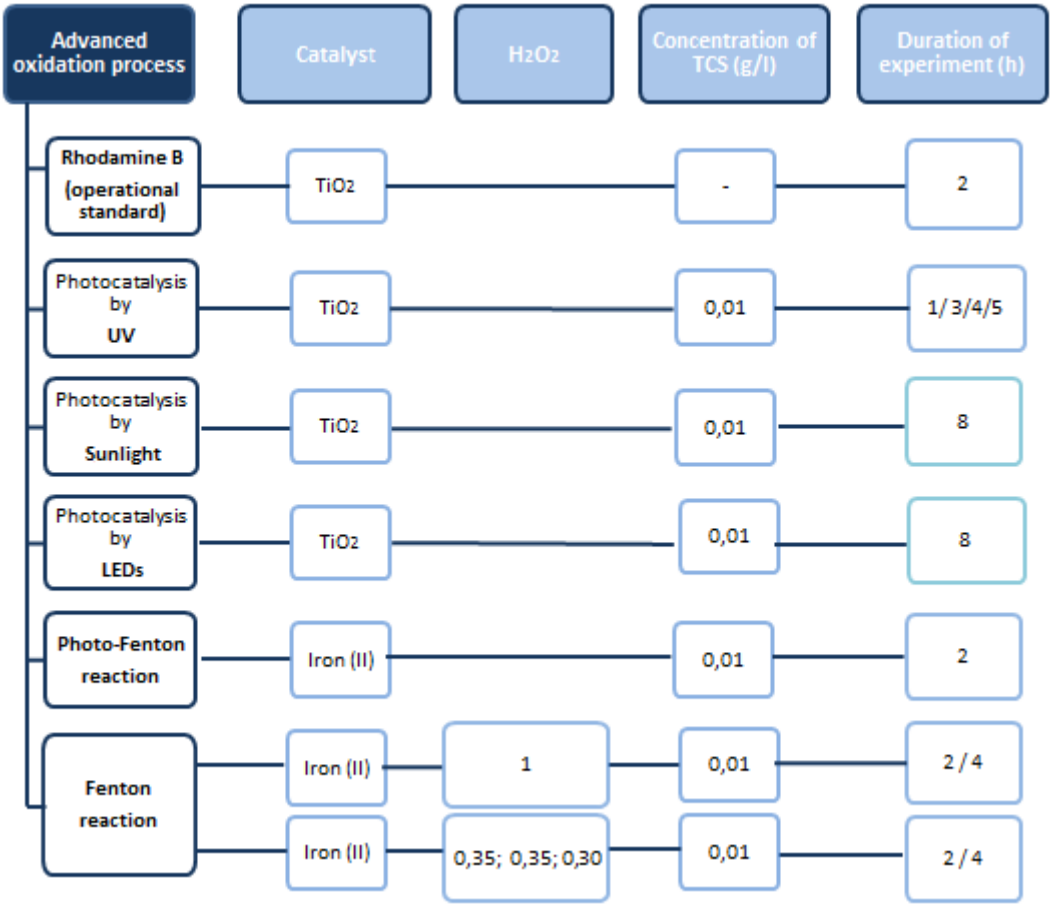

Figure 3.1 Advanced oxidation process experiments carried out to the degradation of TCS

To fully understand the triclosan molecule and the standard solution, GC/MS, NMR, ESI-MS and UV-VIS spectrometry analysis were performed (Figure 3.2).

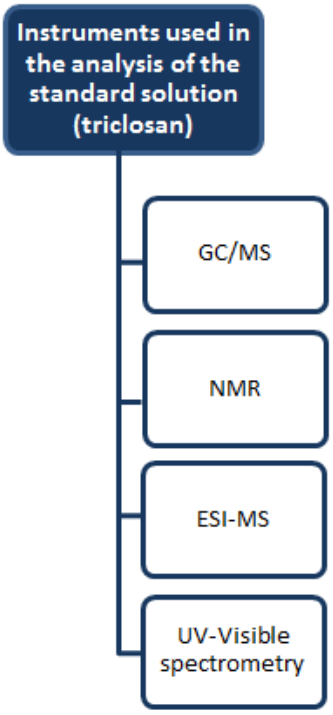

Figure 3.2 Advanced oxidation process experiments carried out to the degradation of TCS

Commercial Aeroxide "TiO_2 P25" purchased from Evonik Degussa was used in this work. The "TiO_2 P25" it is well known for his composition of anatase and rutile crystallites, but it seems that some absence of information about the exact crystalline composition exists (Ohtani *et al.*, 2010). The powder was characterized with a Transmission Electron Microscopy (TEM) and with X Ray Diffraction (XRD) and this information was shared by Professor R. Bertani in personal communication, March 2014, from the chemistry laboratories of Università degli Studi di Padova. The TEM allows evaluation of the particle dimension and the XRD the composition of TiO_2 and the ratio between anatase and rutile.

TEM analysis showed the most of the particles has a diameter of 20 nm, illustrated in Figure 3.3.

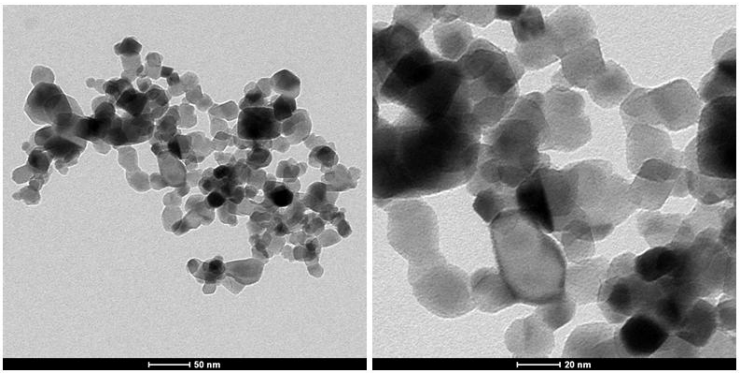

Figure 3.3 TEM images of commercial "TiO_2 P25"

The XRD analysis reveals two main peaks related to the crystallographic plane, peak 25.3 related to the anatase phase (red line Figure 3.4) and peak 27.45 to the rutile phase (green line Figure 3.4). The blue line in the Figure 3.4 refers to the diffractogram of TiO_2.

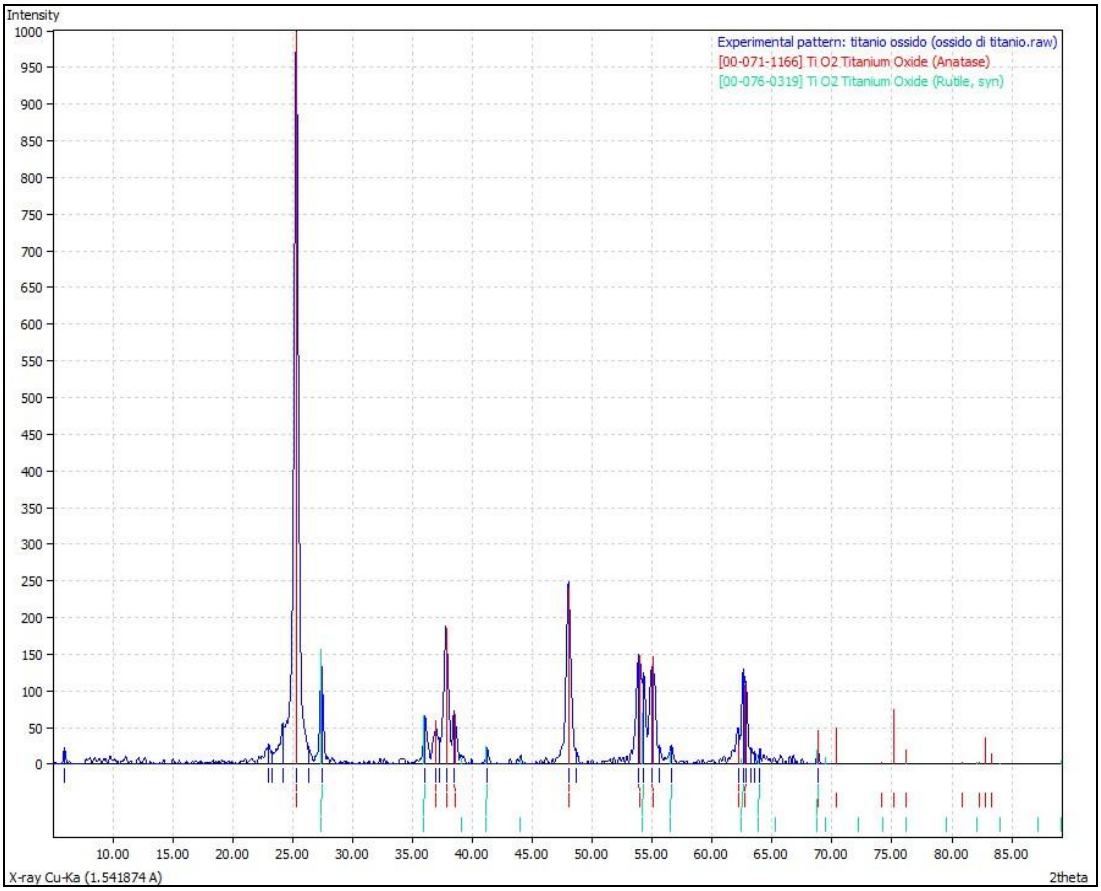

Figure 3.4 XRD spectrum of commercial "TiO_2 P25"

Comparing the intensity values, in the table 3.1; the content of rutile is 15.8% as show by the ratio of the intensities signals appearing at 2theta 25.3 peak (anatase) and 2theta 27.45 peak (rutile).

Table 3.1 XRD peaks of commercial "TiO_2 P25"

2theta	intensity
25.3	995.43
27.45	153.73
36.04	78.45
37.8	192.52
38.5	85.27
48.03	276.48
53.98	160.29
54.26	139.09
54.99	140.36
56.66	35.2
62.83	129.76
68.97	72.51

According to the information in the label product the specific surface area is 50 ± 15 m^2/g, the percentage in weight of TiO_2 is 99.5% and the typical crystalline composition was 70-78% anatase, 10-15% rutile and 7-20% amorphous phase.

In all the experiments the maximal amount of solubility of TCS in water was chosen given the difficulties of determination in the GC/MS analysis. The maximum solubility of TCS in distilled water is 0,01 g/l at 20ºC (SCCS, 2010; Yu *et al*., 2006).

The amount of TiO_2 was chosen based on literature, Rafqah *et al*., 2006, compared different concentrations of commercial "TiO_2 P25" (0.2, 0.5, 1, and 2.5 g/l) concluded that the most efficient concentration was 1 g/l. Since the concentration of 0,5 g/l in this study yielded approximated values of efficiency has the concentration 1 g/l, the concentration of 0,5 g/l of TiO_2 was used. The standard solution was prepared by dissolving triclosan in deionized laboratory water.

3.1.1 Rhodamine B as operational control

Photocatalytic degradation of Rhodamine B

To verify the efficiency of the photocatalytic system constructed a first experiment was done with Rhodamine B. This experiment was common to students who were using the same system created for photocatalysis but were studying other proposed selections.

The degradation of the Rhodamine B by photocatalysis using commercial "TiO_2 P25" from Degussa was proven by Aliabadi & Sagharigar, (2011), the Rhodamine B changed color in function of the UV exposition time due of it destruction. Therefore the same was tried to confirm if the system worked. The Rhodamine B aqueous solution was placed in the beaker with 100 mg of TiO_2 and placed in the reactor (a) in Figure 3.5). A continuous mixing was ensure by the magnetic stirred. The experiment had a duration of 2 hours (b) in Figure 3.5) and samples of 1 ml were collected every 5 min.

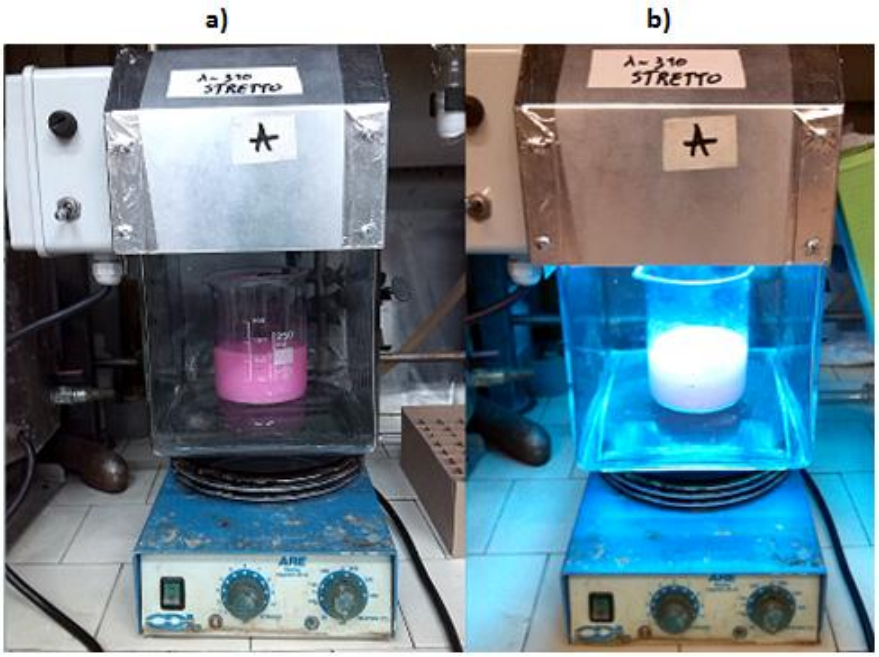

Figure 3.5 Picture of the photocatalytic degradation of Rhodamine B, a) in the beginning with UV lights of, b) in the end of the experiment

Two blanks experiments were effectuated in the same conditions although blank 1 was performed on an dark room and blank 2 was performed in the absence of TiO_2. The blank experiments were run during 2 hours and every 30 minutes 1 ml of solution was collected.

The conditions that have been respected for the elaboration of the assay were:

- Volume of solution: 100 ml
- Concentration of Rhodamine B: 48 g/l
- Concentration of TiO_2: 1 g/l
- Time of experiment: 2 hours

3.1.2 Photocatalysis by UV light

The photocatalytic degradation under UV light was performed in a glass structure, covert with a quartz plaque. A beaker, containing the suspension was placed inside the glass structure (Figure 3.6). Two parallel lamps at a distance of 5,5 cm from each other and at 23,5 cm to the surface of the suspension were placed on the top of the quartz plaque (a) and b) in Figure 3.7). The lamps used were from Philips model PL –S 9W /01 /2P 1CT with maximum wavelength at 310 nm corresponding to 90 $\mu W/mm^2$ (c) in Figure 3.7). Technical manufacture features are presented in the Figure 3.8. The quartz plaque permits the transmission of UV light inside the glass structure.

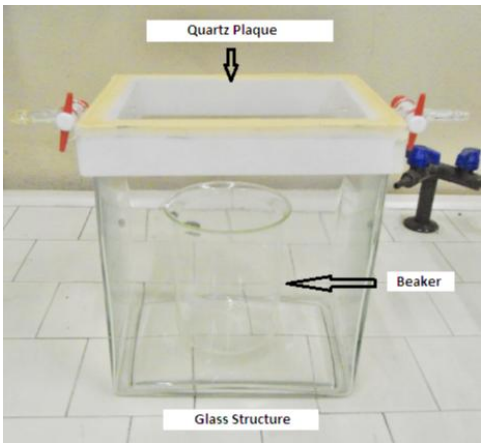

Figure 3.6 Picture in detail of the glass structure, beaker and quartz plaque used in the reactor

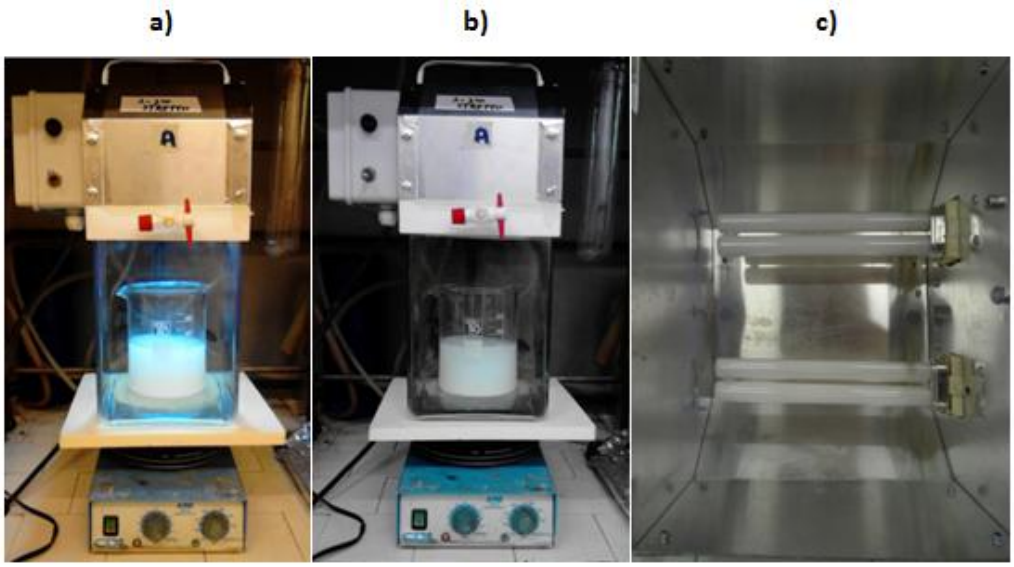

Figure 3.7 Pictures of the reactor under the photocatalysis by UV experiment and detail of the UV lamps, a) experimental setup with UV lights on, b) experimental set up with UV lights of, c) UV lamps

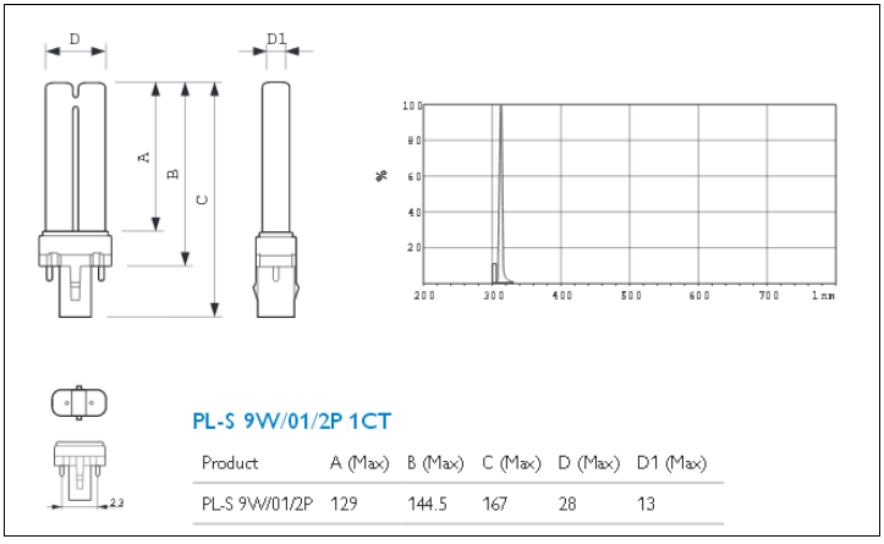

Figure 3.8 Emission spectra of the UV lamps used and technical features according to the manufacture

The suspension with TCS was allocated inside the structure of glass and covered with the quartz plaque and the UV light (a) in Figure 3.7). Contents were stirred during an hour in dark conditions to guarantee maximum absorption of the catalyst and during the time of the experiment to maintain uniformity of the suspension. After this hour the lights were turned on to begin the process of photocatalysis. This process was replicated four times to gather samples of 1, 3, 4 and 5 hours.

The conditions that have been respected for the elaboration of the assay were:

- Volume of solution: 250 ml
- Concentration of TCS: 0,01 g/l
- Concentration of TiO_2: 0,5 g/l
- Time of experiment: 1, 3, 4 and 5 hours

3.1.3 Photocatalysis by sunlight

This experiment was chosen to be done under the best weather conditions; a sunny and clouds-free day during the time of the experiment. One crystallizer with 1 l of the suspension was placed on the top of the floor of the industrial engineering department tower in the Università degli Studi di Padova, and left under the sun for 8h (Figure 3.9). No stirred conditions were possible to maintain.

Figure 3.9 Picture of the crystallizer ready to place on the top of the tower

The conditions that have been respected for the elaboration of the assay were:

- Volume of solution: 1 l
- Concentration of TCS: 0,01 g/l
- Concentration of TiO_2: 0,5 g/l
- Time of experiment: 8 hours

3.1.4 Photocatalysis by LEDs

To perform the photocatalytic degradation under LEDs, sixteen LEDs in a current of 0.1 A and a voltage of 24 V were placed on the top of a crystallizer with 60 ml of suspension (Figure 3.10 and a) in Figure 3.11). The LEDs were at a distance of 1,2 cm from the surface of the suspension (b) in Figure 3.11).

One hour before the experiment started, the suspension was maintained in the dark, under stirring, to improve the absorption of the catalyst. During the time of the experiment, the rate of stirring was cut down to avoid splashes to the LEDs while keeping the suspension mixtured.

Figure 3.10 Picture of the LEDs experiment (system of volt-ammeter and LEDs connection)

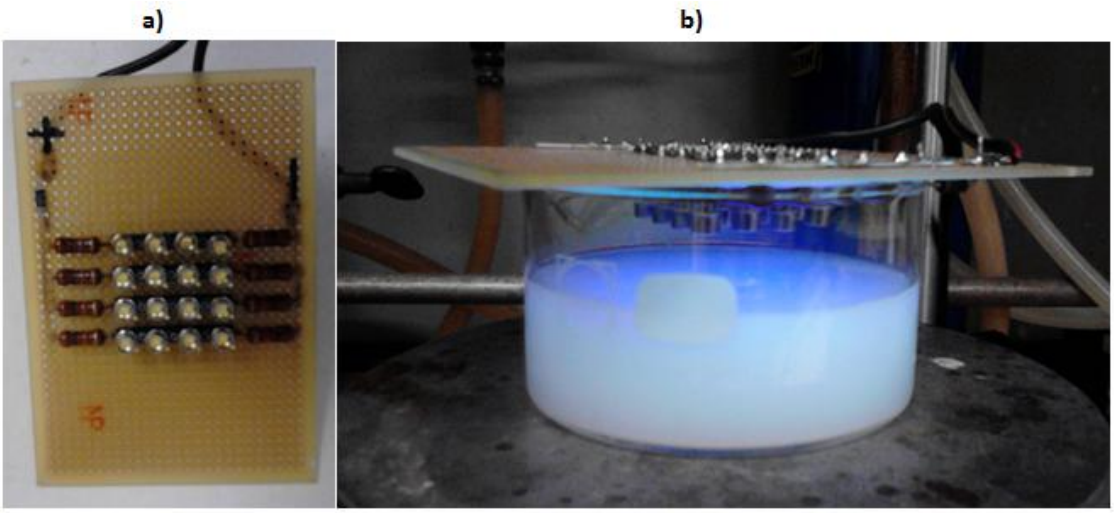

Figure 3.11 Picture in detail of the sixteen LEDs and photocatalytic experiment

The conditions that have been respected for the elaboration of the assay were:

- Volume of solution: 60 ml
- Concentration of TCS: 0,01 g/l
- Concentration of TiO_2: 0,5 g/l
- Time of experiment: 8 hours

3.1.5 Photo-Fenton reaction

A beaker was ready with a solution of TCS and $FeSO_4.7H_2O$. The pH was measured by a universal pH indicator stripes and is dropped until around 3 by adding H_2SO_4 96%. H_2O_2 30% is added to the suspension and UV lights are turn on for 2 hours of experiment.

The conditions that have been respected for the elaboration of the assay were:

- Volume of solution: 250 ml
- Concentration of TCS: 0,01 g/l
- $FeSO_4.7H_2O$: 77,7 mg
- H_2O_2 (30%): 1 ml
- Time of experiment: 2 hours

3.1.6 Fenton Reaction

- Degradation under addition of H_2O_2 at once

The $FeSO_4.7H_2O$ was weighed and placed in a balloon and 250 ml of volume suspension was added to the balloon (Figure 3.12). The Fenton-reaction was initiated. A magnetic stirrer device was turned on to ensure complete mixing of the reagents during the time of the experiments. The pH was measured by a universal pH indicator stripe and the pH was decreased about 3 by adding H_2SO_4 96%, respecting the optimal pH for the Fenton reaction found in the literature (between 2-4) (Júnior *et al*.,2012; Bauer & Fallmann, 1997). The addition of H_2O_2 at 30% ensued. The reaction stopped when the extraction with n-hexane began. The Fenton reaction was replicated to gather samples for 2 and 4 hours.

Figure 3.12 Picture of the development of the Fenton reaction experiment

The conditions that have been respected for the elaboration of the assay were:

- Volume of solution: 250 ml
- Concentration of TCS: 0,01 g/l
- $FeSO_4.7H_2O$: 77,7 mg
- H_2O_2 (30%): 1 ml
- Time of experiment: 2 and 4 hours

- Degradation under addition of H_2O_2 in 3 instants of time

The $FeSO_4.7H_2O$ was weigh and placed in a balloon, 250 ml of volume suspension was added to the balloon. The magnetic stirrer device ensured complete mixing of the reagents during the experiments time (2 and 4 hours). The pH was measured by a universal pH indicator stripe and is dropped until around 3 by adding H_2SO_4 96% and the addition of H_2O_2 30% was made in 3 separate times during the duration of the experiment. For instance in the 2h experiment, the addition of H_2O_2 was made at 20 min (0,35 ml), 60 min (0,35 ml) and at 100 min (0,30 ml).

The concentration of $FeSO_4.7H_2O$ and H_2O_2 are based on the concentrations adopted in the studies of I. Casalatina (I. Casalatina, personal communication, May 2014) in the Laboratory of the Università degli Studi di Padova and it was respected in the photo-Fenton and Fenton reaction to maintain uniformity in the experiments.

The conditions that have been respected for the elaboration of the assay were:

- Volume of solution: 250 ml
- Concentration of TCS: 0,01 g/l
- $FeSO_4.7H_2O$: 77,7 mg
- H_2O_2 (30%): 1 ml (0,35 ml + 0,35 ml + 0,30 ml)
- Time of experiment: 2 and 4 hours

3.2 Determination of phenols and TCS by GC/MS

On the analytical determination of phenols, specifically triclosan, one obstacle was encountered in the collection of the results:

- **Derivatization:** the OH group can be attached to the internal solid phase of the GC/MS; the strong iteration can interdict the OH group to leave the column and consequently not show in the mass spectra. To avoid this problem, derivatization is necessary.

Several methods of treatment of analysis based in the literature were tested in this work but did not succeed, like: chloroform extraction by Yu *et al*., 2006; n-hexane extraction and addition of NaCl to facilitate the extraction and passage of the organic phase in Na_2SO_4 by Gómez *et al*., 2009; n-hexane extraction and derivatization with N-Methyl-N Trifluoroacetamida (MSTFA) by Catrinescu *et al*., 2012. The analytical method founded that suit better are described hereafter.

- **Derivatization with acetic anhydride acid**

The best method found for identification of triclosan and respective byproducts was in Czaplicka, (2001). In all experiments all the volume was treated to analysis in the GC/MS.

Firstly, in the end of the experiments and after measurement of the pH, the volume of solution was filtered with a filtering round paper (pore size 4 - 7 µm) (Whatman filter n° 597) to remove TiO_2. This step was not taken in experiments without TiO_2. The pH was measured in each experiment by a universal pH indicator stripes of Macherey – Nagel, reference 921 10, pH from 0 to 14.

This method encloses extraction, derivatization and quantitative/qualitative determination using GC/MS.

- **Extraction**

Three extractions of the solution with n-hexane were performed. The n-hexane quantity was chosen respecting a ratio of 2:1 (volume of solution / volume n-hexane) divided by the three extractions. The remaining aqueous solution was discarded, while combined n-hexane extracts were concentrated in a nitrogen stream until a volume of 2 ml was reached.

- **Derivatization**

To the n-hexane extract sample after nitrogen concentration, 3 ml of 0.1 M K_2CO_3 were added, followed by 2 ml of n-hexane containing 100 µl of acetic anhydride. Triclosan molecule contains a phenolic hydroxyl group. The hydroxyl group was functionalized with acetic anhydride acid. The solution was mixed intensively and then was left to settle until the layers were separated. After 30 minutes the layer of water was discarded. The n-hexane layer was dried and concentrated in a stream of nitrogen to 200 µl and then analyzed.

- **Quantitative and qualitative determination on GC/MS**

To perform the quantitative analysis, 1µl of benzonitrile (the internal standard) was added in all samples, having a retention time of about 4 minutes, ensuring that the peak did not coelute. The integration of the area of the peaks and a comparison with the area of the internal standard allowed a quantitative analysis. The retention time and the respective mass spectra of the peaks allowed a qualitative analysis.

3.3 Instruments

3.3.1 GC/MS: Gas chromatography/mass spectrometer

Gas chromatography is based upon the partition of the analyte between a gaseous mobile phase and a liquid phase immobilized on the surface of an inert solid by adsorption or chemical bonding. Mass spectrometer measures the mass to charge ratio (m/z) of ions produced from the sample. The GC/MS is a hyphenated technique; it is an analytical method in which two instrumental techniques are coupled combining the separation capabilities of chromatography with the capacity detection of electrical or spectral methods (Skoog *et al*., 2004).

The schematic representation of the GC/MS system is represented in the Figure 3.13, here the sample is injected into the capillary column, where the separation of the components occurs. After the fragmentation they are ionized, mass analyzed, and then detected by the electron multiplier. The separated ions are recognized and a plot of the ion intensity versus m/z value is produced by the data-system (Skoog *et al*., 2004).

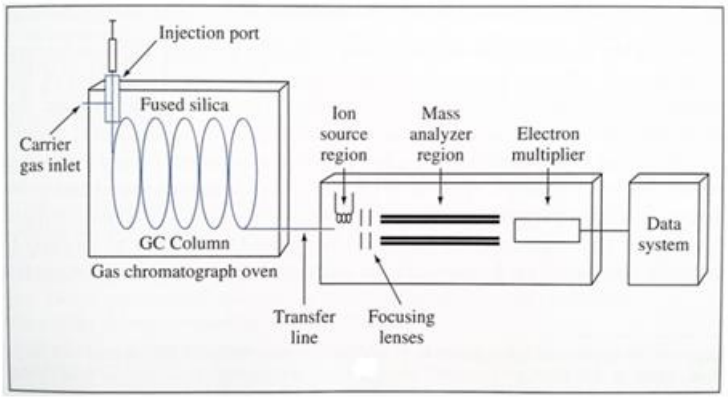

Figure 3.13 Schematic of a typical capillary GC/MS instrument (Adapted from: Skoog *et al*., 2004)

From the chromatogram is possible to make a qualitative and quantitative analysis. The retention time, the time between injection of a sample and the appearance of a solute peak at the detector of a chromatographic column, was valuable to the identifications of the components. The comparison of the area of an analyte peak with an internal standard allows to make a quantitative analysis. The internal standard method offers a highest precision analysis, because uncertainties introduced by sample injection, flow rate, and variations in column conditions are minimized (Skoog *et al*., 2004).

Analysis by the GC/MS were run using an AUTO HRGC/MS Carlo Erba gas chromatograph spectrometer equipped with an Agilent DB-5MS column (diameter of 0,25 mm, length of 30 m and film thickness of 0,25 µm), helium as gas carrier (He flow rate = 4 ml/min) and coupled to a QMD 1000 Carlo Erba mass spectrometer as detector. The injector temperature was 280°C and the GC temperature program ranged from 80°C (2 min) at 10°C/min to 280°C (15 min). All samples were analyzed by direct injection of 1 µl with a microsyringe (mode splitness). The internal standard used was benzonitrile. The interpretation of the chromatogram was performed with the aid of the program management of the instrument, the mass lab, equipped with the National Institute of Standards and Technology (NIST) and Wiley libraries. The instrument used is show in the Figure 3.14.

Figure 3.14 Carlo Erba GC/MS

3.3.2 ESI–MS: Electrospray ionization mass spectrometry

ESI uses electrical energy to assist the transfer of ions from solution into the gaseous phase before they are subjected to mass spectrum analysis (Ho *et al*., 2003).

The electrospray ionization process stated in the Figure 3.15 starts when a stream of liquid solution is pumped through a stainless quartz silica capillary tube which is at a high voltage relative to the wall of the surrounding chamber. A mist of highly charged droplets with the same polarity as the capillary voltage is generated from the Taylor cone. The application of a nebulizing gas (e.g. nitrogen), which shares around the eluted sample solution, develops a higher sample flow rate. These droplets are continuously reduced as the solvent evaporate and as they move towards the entrance to the mass spectrometer. Finally it yields free charged analyte molecules that can be analyzed for their molecular mass and ion intensity (Ho *et al*., 2003; Cech & Enke, 2002; Bruins, 1998).

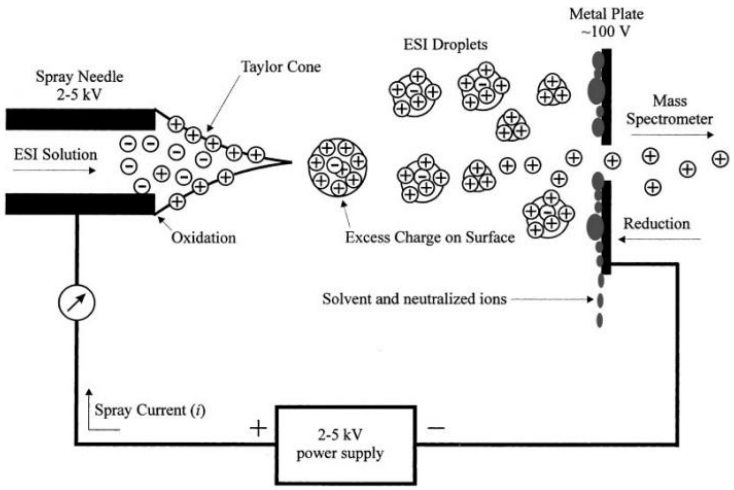

Figure 3.15 Schematic of the electrospray ionization process (Adapted from: Cech & Enke, 2002)

The ESI-MS analyses were performed using a Thermo-Finnigan LCQ-Duo spectrometer operating in positive ion mode (Figure 3.16). Instrumental parameters: capillary voltage 10 V, spray voltage 4.5 kV; capillary temperature 200 °C; mass scan range from 150 to 2000 amu; N_2 was used as sheath gas; the He pressure inside the trap was kept constant. The pressure read directly by an ion gauge (in the absence of the N_2 stream) was 1.33×10^{-5} Tor. Sample solutions were prepared by dissolving the compounds in acetonitrile. Sample solutions were directly infused into the ESI source by a syringe pump at 8 µl/min flow rate.

Figure 3.16 Thermo-Finnigan LCQ-Duo spectrometer

3.3.3 UV-Vis spectrophotometer: Ultraviolet–Visible Spectrophotometer

The UV-Vis spectrophotometer equipment performs quantitative analysis by the absorption of spectral radiation based on the Beer–Lambert law which states that the absorption is proportional to the concentration of the analyte.

The beam of selected wavelength reaches the beam splitter and one beam passes through the reference solution to a photodetector, and the second passes through the sample to other photodetector. The two outputs are amplified and their ratio or the log ratio is obtained by computer and displayed. This process is illustrated in Figure 3.17.

The UV-Visible spectra were recorded at a Perkin-Elmer Lambda 25, showing in Figure 3.18, a double been spectrophotometer in the range 190-800 nm with 1 cm light path cuvettes made of UV grade silica (quartz).

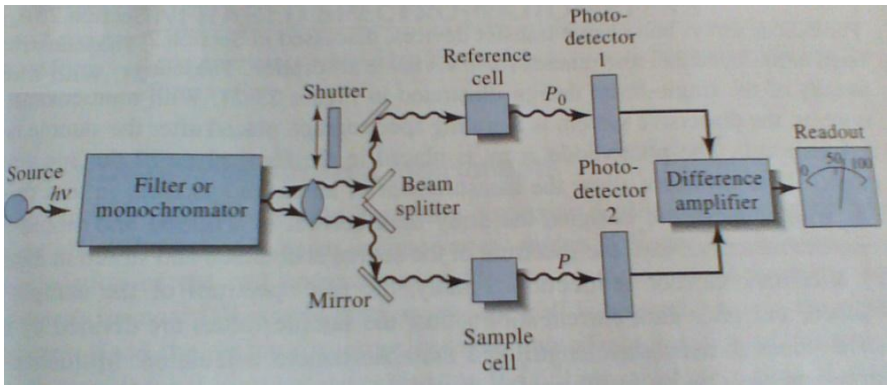

Figure 3.17 Optical Path in UV-Vis spectrophotometer (Adapted from: Skoog *et al*., 2004)

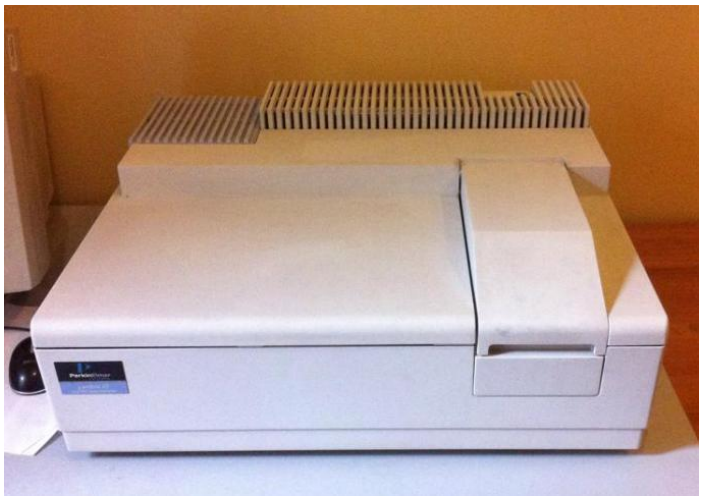

Figure 3.18 Perkin-Elmer Lambda 25

3.3.4 ^{1}H NMR Spectrometry: Proton Nuclear Magnetic Spectrometry

Nuclear magnetic resonance (NMR) is another form of absorption spectrometry. All nuclei carry a charge and a mass; some isomers possess spin or angular momentum. Spinning charge on proton generates magnetic field, where there is associated an magnetic moment (Silverstein *et al*., 2005).

The magnetic moment of the spinning charge can be described in terms of its quantum spin number. The spin number determines the number of orientations a nucleus can assume in an external nuclear field. For a nucleus with spin ½, two levels of energy are possible. In the absence of magnetic field the state of energy returns to the ground state (Silverstein *et al*., 2005; Bovey *et al*., 1988).

In the schematic presented in a) Figure 3.19, the sample tube is placed in the field of a strong magnet (the superconducting solenoid), then radio frequency transmitter applies a radio frequency sufficiently wide to cover the entire range of magnetic field strength. This pulse simultaneously excites all of the nuclei in the sample. Immediately following this pulse, the

excited nuclei begin to return to the ground state and radiate the absorbed energy. A detector collects this energy producing free induction decay (FID) which is the sum of all the nuclei radiating over time. By Fourier transform the information in the FID is converted in a spectrum in function of the frequency (Silverstein *et al*., 2005; Bovey *et al*., 1988).

The ^{1}H NMR spectra were run at 298 K on a Bruker 200 AC spectrometer, presented in b) Figure 3.19, operating at 200.13 MHz, respectively; δ values are given in ppm. Peak positions are relative to TMS and were calibrated against residual solvent resonance (^{1}H) or the deuterated solvent multiplet (^{13}C).

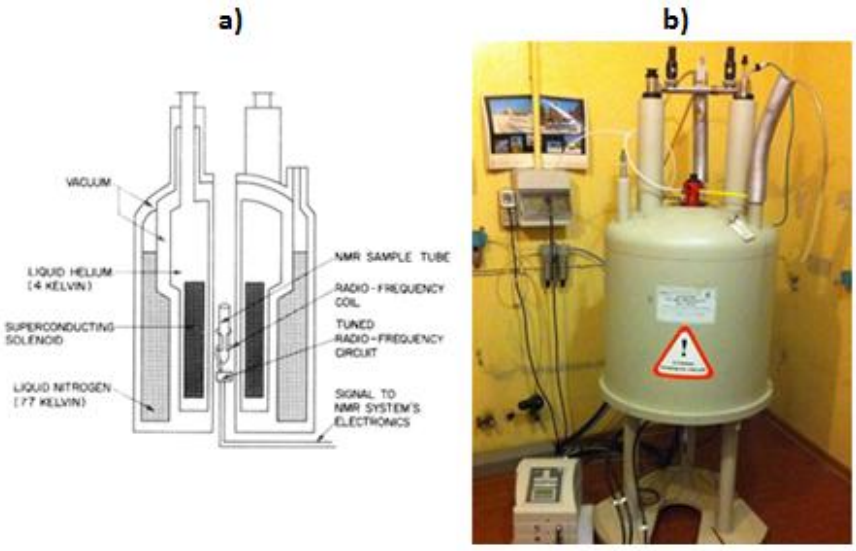

Figure 3.19 Bruker 200 AC spectrometer and cross section of superconductive magnet for ^{1}H NMR spectroscopy (Adapted from: Bovey *et al*., 1988)

3.3.5 Liquid/liquid extraction

Solvent extraction is an operation based on the limited miscibility and the distribution of the solute between two liquid phases (Jabrou, 2012). The solute is in an aqueous solution and an organic solvent (in this work, n-hexane) immiscible with water is added.

The two immiscible liquids were strongly mixed in a magnetic stirrer with the objective to have good dispersion of the solvents in each other (a) in Figure 3.20). Since the solubility of the solute is different in the two solvents, a transition occurred, from the water to the n-hexane. The separation between the solvents is performed in a separation funnel (b) in Figure 3.20); the two layers have to be visibly separated to ensure the success of the extraction. The yield is enhanced when the process is repeated on the water layer. The extraction was repeated three times.

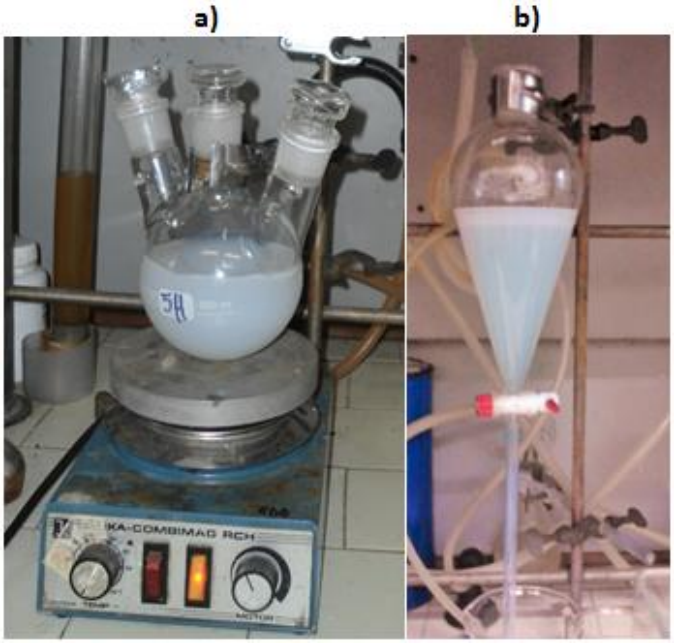

Figure 3.20 Liquid/liquid extraction **a)** Mixing of the solvents, b) separation funnel

4 Results and discussion

4.1 Characterization of the TCS standard solution by analytical instruments

To fully understand the triclosan molecule and the standard solution, GC/MS, ^{1}H NMR, ESI-MS and UV-Vis spectrometry analysis were performed. The standard solution consisted in water and triclosan in a concentration of 0,01 g/l (maximum solubility of TCS in water at 20°C).

- **GC/MS**

The GC/MS analysis of TCS (Figure 4.1), shows two major peaks at the retention time 20.396 and 21.046 min in the abundance of 100% and 50%. Other two peaks of lower strength appear in the retention times 18.812 and 19.863 min with 8% and 11%. All these peaks reveal very similar mass spectra, the mass spectra of the most abundant species are presented in Figure 4.2 and 4.3. The less abundance peaks mass spectra are in the Figure I.1 and I.2, in the Appendix I. As an example, the presence of one chloride is visible in the TCS ($C_{12}H_7Cl_3O_2$), mass spectrum characterized by the base peaks ions m/z 288 and 290, corresponding to the molecular ions $[M]^+$ and $[M + 2]^+$, which represent a typical chlorine signature.

The ion peak m/z 218 and 220 reveal the presence of other chloride. Mezcua *et al.*, 2004 made a GC/MS analysis under electron impact ionization, the same performed in this work, the resulting mass spectrum is illustrated in the Figure 4.4 and shows the stronger base peaks ions at m/z 288, 290 and 218. The ions peaks of m/z 51, 63, 114 and 146 are always present in both analysis, also characterizing the TCS compound.

Presence of the same molecular base peak ions in all the mass spectra, determined the presence of isomers which constitute the commercial mixture.

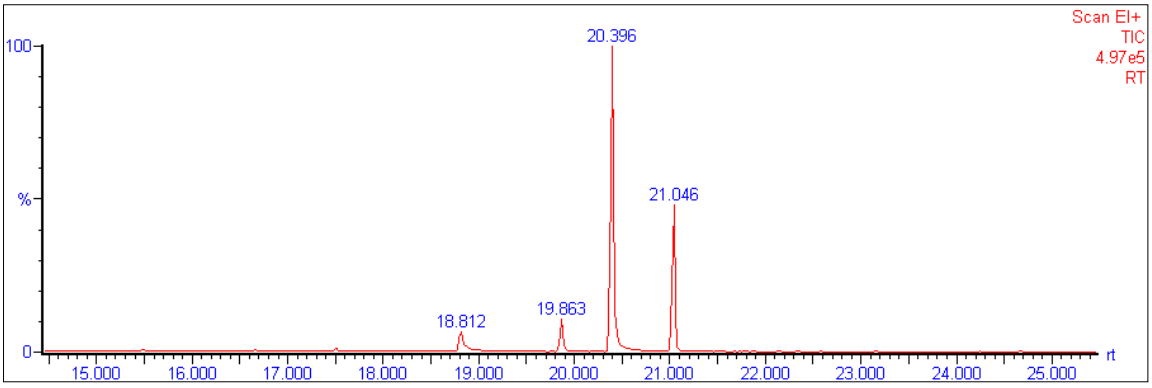

Figure 4.1 Triclosan chromatogram

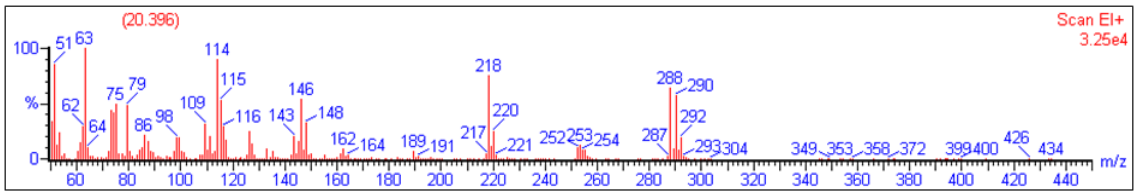

Figure 4.2 Peak at 20.396

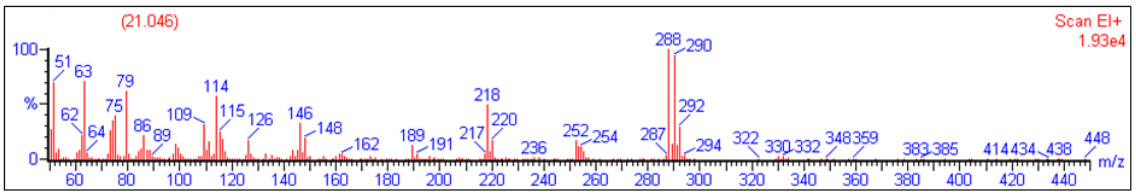

Figure 4.3 Peak at 21.046

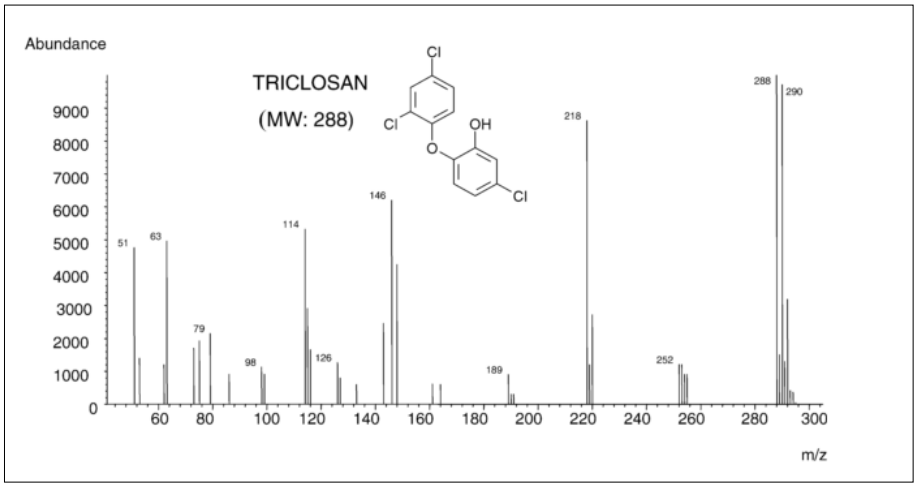

Figure 4.4 Triclosan chromatogram by Mezcua *et al*., 2004

- **^{1}H NMR Spectroscopy**

The analysis of the ^{1}H NMR spectra of the TCS (Figure 4.5) reveals six protons plus one referring to the OH group. Only the signals due to the most abundant isomer are visible in the spectrum.

The six protons were identified and located in the molecular structure of triclosan reported in Figure 4.6, as H1, H2, H3, H4, H5 and H6.

The J-coupling is the frequency difference in Hz between the component peaks. The J-coupling is calculated by the following equation:

$$J(Hz) = Chemical\ Shift\ difference\ (ppm) * Field\ strength\ (MHz) \qquad \text{(eq. 4.1)}$$

The H6 is a doublet centered at δ 7.54 ppm with a J-coupling of $^{4}J_{H5H6}$ 4 Hz, the H5 is a doublet of doublets centered at δ 7.225 ppm with a J-coupling of $^{3}J_{H4H5}$ 4 Hz and a J-coupling of $^{4}J_{H5H6}$ 2 Hz, the H1 is a triplet at δ 7.05 ppm with a J-coupling of $^{4}J_{H1H2}$ ~ 1 Hz. The H2 and H3 are centered at δ 6.875 ppm with a J-coupling with H1 about 1Hz and the H4 is a duplet centered at δ 6.775 ppm with a J-coupling of $^{3}J_{H5H4}$ 8 Hz. The OH is at δ 7.66 ppm.

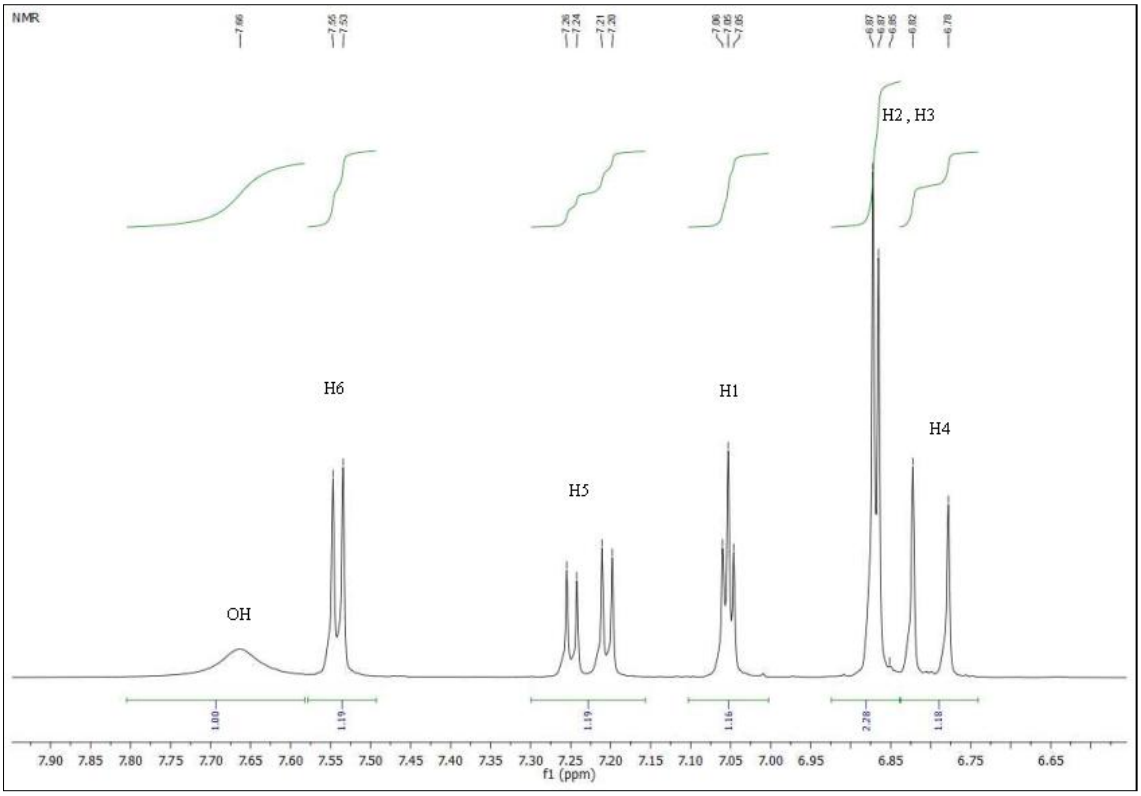

Figure 4.5 ^{1}H NMR spectra of triclosan

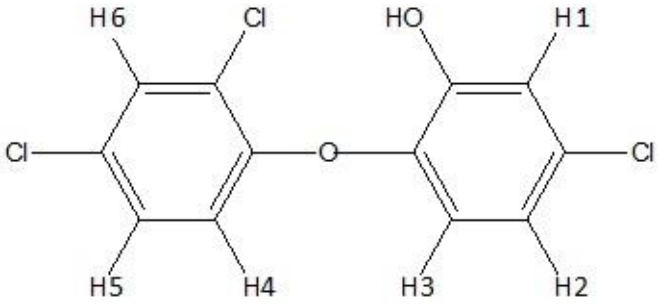

Figure 4.6 Identification of the protons in the molecular structure of triclosan

- **ESI-MS**

The ionization of TCS generates the ion peak m/z 310 with 85% relative abundance by the addition of Na^{+}, the peak m/z 325 (20%) is referred to the addition of K^{+}. These two ions appear as part of contamination present in the equipment.

The ion peak m/z 287 characterized the radical TCS with the abundance of 45%. The loss of a Cl (M–35) gives the peak m/z 255 (70% relative abundance) from here there is a loss of a CO (M–28), respecting the ion peak of m/z 227 with 25% relative abundance. The ion peak m/z 191 is regarding the loss of a HCL (M–36) with the relative abundance of 25%. The tallest peak in the chromatogram is the addition of a $OH^{\bullet}$ in the ion base peak m/z 304 with the highest relative abundance, 100%. The chromatogram is exposed in the Figure 4.7.

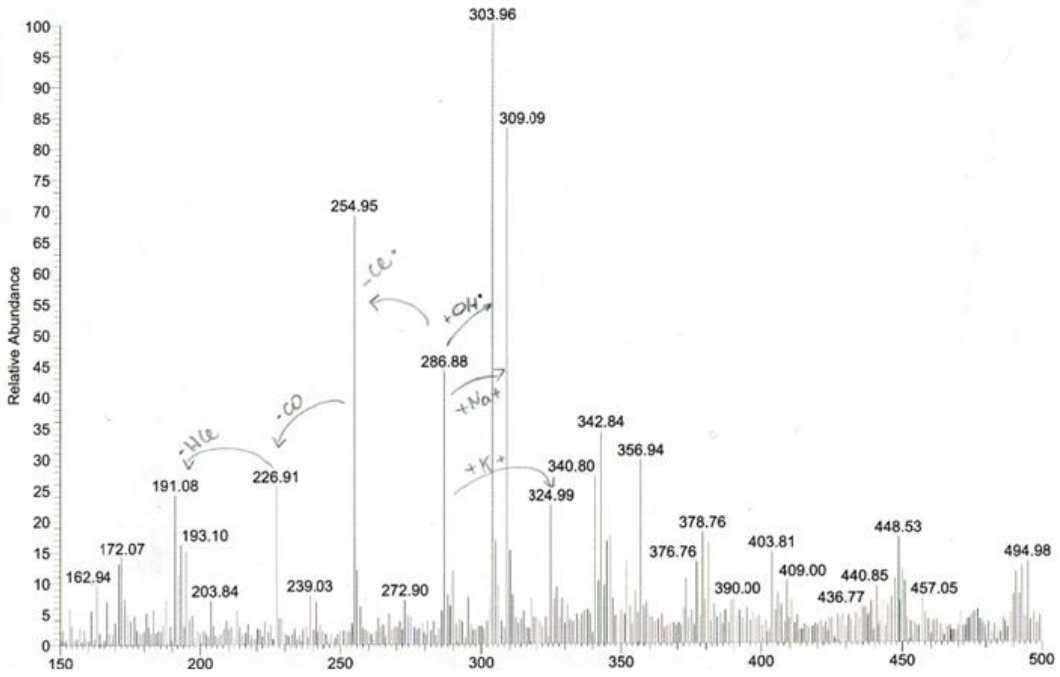

Figure 4.7 Chromatogram of TCS in positive ion mode

- **UV-Vis spectrophotometer**

A solution with the concentration of TCS of 10^{-4} M was prepared for analysis in the UV–Visible spectrophotometer. One peak appears in the range of 280 to 340 nm and the maximum peak is established approximately between 300 and 310 nm. The UV-Visible spectrum of TCS is showed in the Figure 4.8.

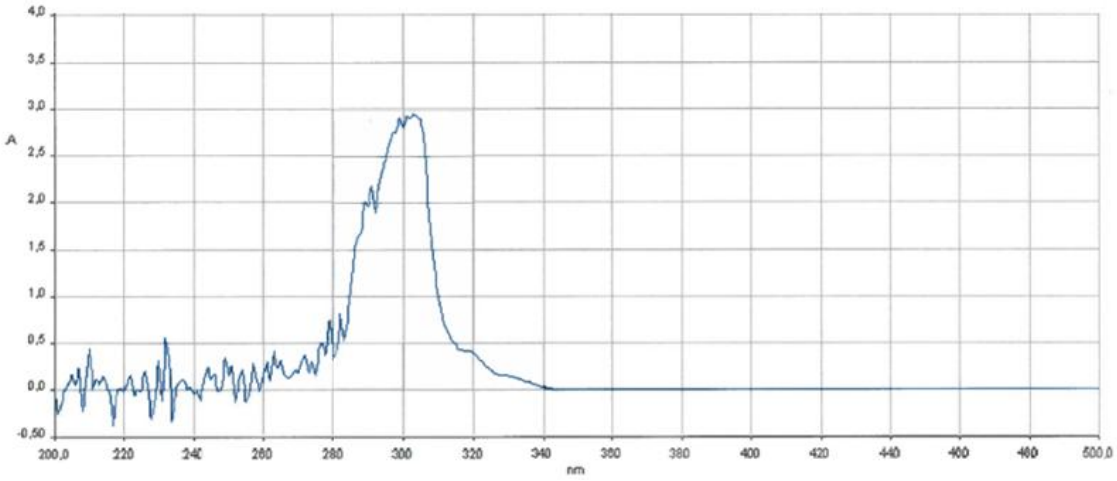

Figure 4.8 Emission spectra of TCS

4.2 TCS degradation and by-products by GC/MS

4.2.1 Rhodamine B as operational control

Photocatalytic degradation of Rhodamine B

The efficiency of the photocatalytic system was demonstrated by the gradual changed of color, from pink to white as showed in the Figure 4.9.

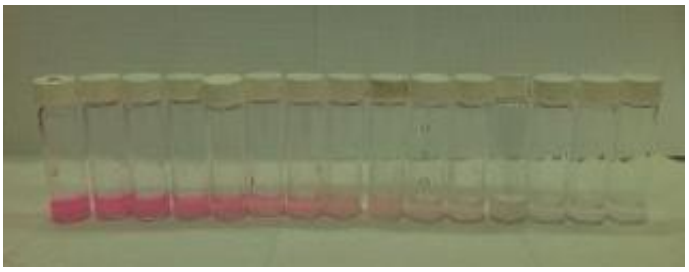

Figure 4.9 Picture of degradation samples of Rhodamine B during the time of experiment

The blank experiments showed in the Figure 4.10 confirmed no degradation of Rhodamine B.

Figure 4.10 Picture of the blank samples

4.2.2 Photocatalysis by UV light

- **1 hour**

The chromatograph resulting from the photocatalytic degradation with UV lamps reveals 5 peaks, two higher peaks in the retention time 20.361 and 20.995 with the abundance of 100% and 70% (Figure 4.11). The other 3 peaks are at the retention time 10.477, 12.227 and 17.461 with the respective abundance of 12, 7 and 19%. In order to confirm if the small peaks that appear between the retention time 9 and 19 min are significant, an amplification was performed. This chromatograph is exposed in the Appendix II, Figure II.1. The degradation during this first hour achieved 68% of removals of TCS, (Figure III.1, Appendix III).

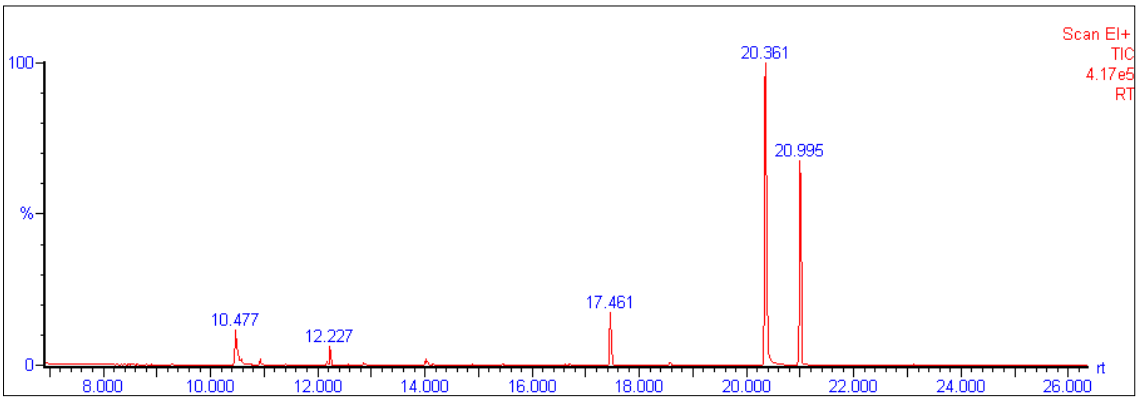

Figure 4.11 Chromatogram of the UV lamps degradation of 1 hour experiment

→ Peak at the retention time 10.477:

The peak in the retention time 10.477 min has been identified has $C_8H_6Cl_2O_2$, this compound was a result of 2,4–DCP and acetic anhydride reaction.

The base peak ions typical of 2,4–DCP are m/z 162 (100% abundance) and the 164 (about 60%) (Figure 4.12). A comparison with the mass spectrum of 2,4-DCP obtained by Yu *et al.*, 2006 confirms the 2,4-DCP presence (Figure 4.13). The ratio between the m/z 162, 164 and 166, the m/z 63, 98 and 126 are also visible in both mass spectra. The final compound $C_8H_6Cl_2O_2$ is characterized by the base peaks ions 204 and 206.

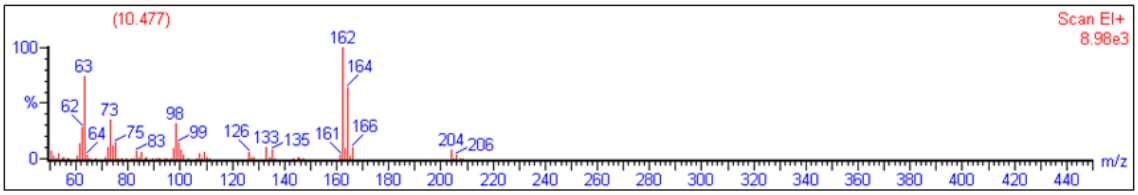

Figure 4.12 Peak 10.477: $C_8H_6Cl_2O_2$

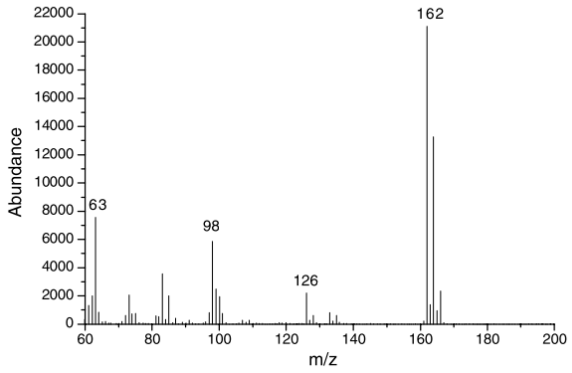

Figure 4.13 Mass spectrum of 2,4-DCP by Yu *et al*., 2006

The identified $C_8H_6Cl_2O_2$ compound, was a result of the acetic anhydride reaction from the treatment of the analysis and the by-product 2,4–DCP (a) and b) in Figure 4.14). The molecular structure of $C_8H_6Cl_2O_2$ was proposed and is presented in point c) Figure 4.14.

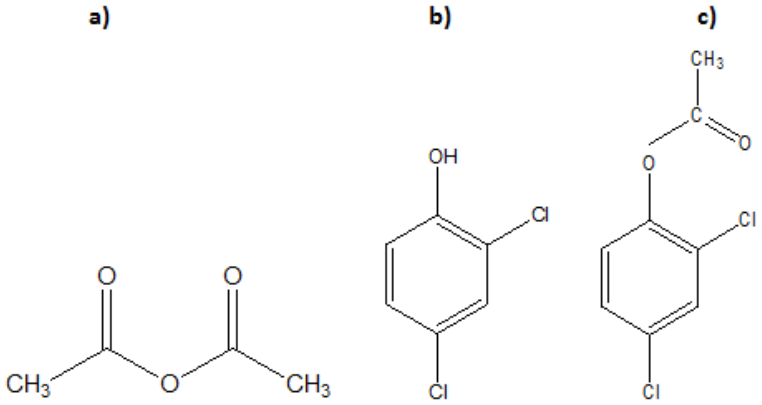

Figure 4.14 a) Molecular structure of acetic anhydride b) Molecular structure of 2,4-DCP, c)Molecular structure suggested for $C_8H_6Cl_2O_2$

The appearance of 2,4–DCP is verified in the literature as being one common intermediate as presented in the table IV.1, Appendix IV by the authors: Sankoda *et al*., 2011; Yang *et al*., 2011; Rafqah *et al*., 2006 and Yu *et al*., 2006. In the case study of Yu *et al*., 2006 2,4–DCP was the major intermediate. The nature of the this compound was a result of the homolytic scission of carbon – oxygen bond leading directly to the formation of 2,4–DCP (Rafqah *et al*., 2006). Even being referred as a by-product in the Fenton reaction by Yang *et al*., 2011, in this study 2,4–DCP was only identified in the UV experiment after 1 hour of degradation.

→ Peak at the retention time 12.227:

In the retention time 12.227 the mass spectrum has the base peak ion m/z 114 with 100% abundance, is characterized by the C_8H_2O radical cation (Figure 4.15).

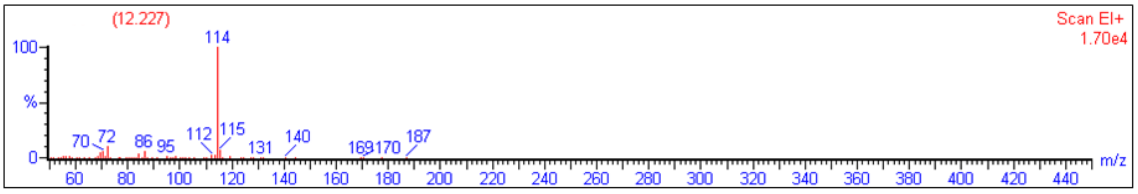

Figure 4.15 Peak 12.227: C_8H_2O radical cation

→ Peak at the retention time 17.461:

The peak at the retention time 17.461 characterize by the base ion peak m/z 149 (abundance at 100%) is suggested as a C_7O_4H and possibly is a contaminant (Figure 4.16). The identification of this peak was extremely difficulty. The ion peak m/z 105 is represented of the aromatic compound C_6O_2H. The addition of a COO reveals the ion peak m/z 149. This ion peak appears once again in the amplified chromatogram at the retention time 18.561 (Figure I.3 in the Appendix I).

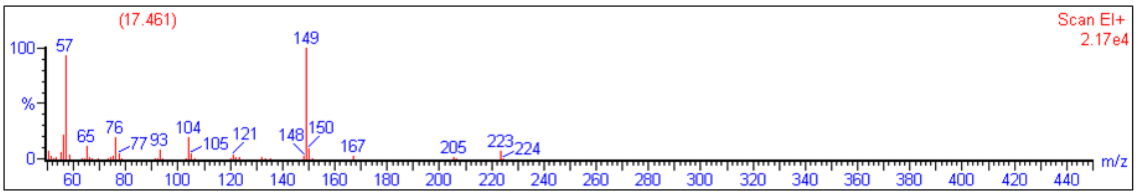

Figure 4.16 Peak 17.461

→ Peak at the retention time 20.361 and 20.995:

The peaks at the retention time 20.361 and 20.995 are TCS (Figure I.4 and Figure I.5 in the Appendix I).

→ Amplified chromatograph; peak at the retention time 10.927:

From the amplified chromatograph (Figure II.1, Appendix II); the peak at the retention time 10.927 the m/z 89 was associated to a C_6OH (Figure 4.17). $C_3H_3O_2$ radical cation is identified at the m/z 71, the difference between the m/z 56 and 71 denotes the addition of a CH_3. The compound $C_{12}H_7Cl_3O_5$ was identified in this mass spectrum. The m/z 336 verifies the presence of this compound.

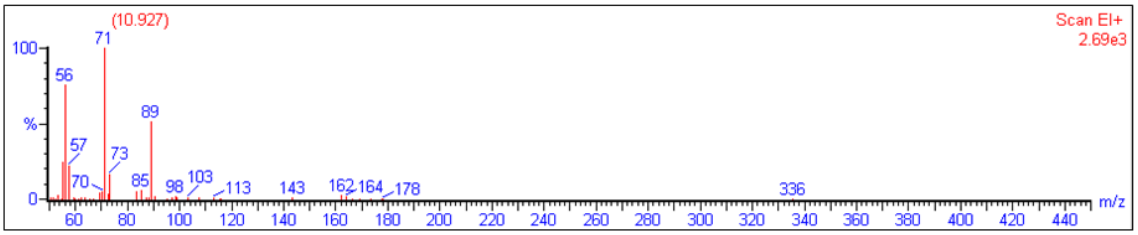

Figure 4.17 Peak 10.927: $C_{12}H_7Cl_3O_5$

Based in the article of Rafqah *et al*., 2006 this compound probably is the result of successive oxidations. The proposal structure (a) in Figure 4.18) and the molecular base peak ion (m/z 336) belong to the type of product identified in the article of Rafqah *et al*., 2006 (b) in Figure 4.18). These species are hydroquinone's and are formed due to the very few protons found in the presence of a lot of fragments.

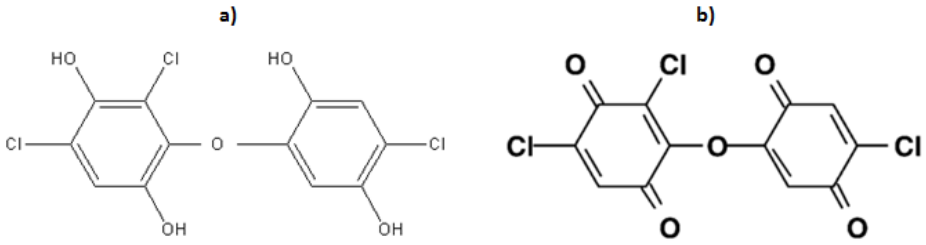

Figure 4.18 Hydroquinine`s species, a) Proposal structure b) Proposal structure by Rafqah *et al*., 2006

Other two peaks present the amplified chromatogram; at retention time 12.177 and 14.011 min.

→ Amplified chromatograph; peak at the retention time 12.177:

By the retention time 12.177 the ion base peak m/z 57 (100% abundance) denotes the presence of a C_2HO_2 (Figure 4.19).

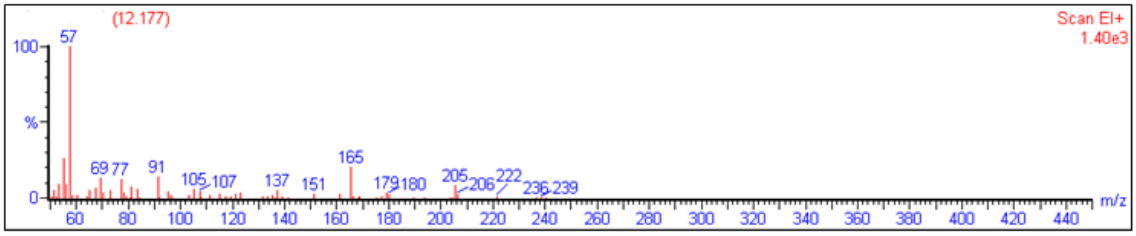

Figure 4.19 Peak 12.177: C_2HO_2

→ Amplified chromatograph; peak at the retention time 14.011:

The ion peak m/z 71 at the peak in the retention time 14.011 correspond to $C_3H_3O_2$ radical cation. Here the difference between the m/z 56 and 71 represents a CH_3 (Figure 4.20).

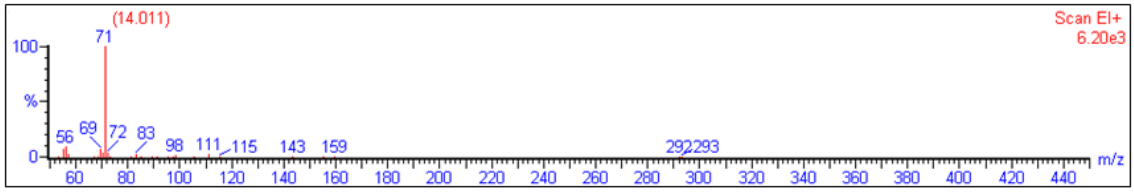

Figure 4.20 Peak 14.011: $C_3H_3O_2$ radical cation

- **3 hours**

After 3 hours of degradation, four peaks appear at the retention times 14.011, 17.461, 20.345 and 20.995 with respective abundance of 11, 62, 100 and 91% (Figure 4.21). The major abundance peaks (retention time 20.345 and 20.995) match TCS peaks as portrayed in the Figure I.8 and I.9 from the Appendix I.

In the peak in the retention time 14.011 the mass spectrum revealed the base peak ion m/z 71 in the abundance of 100%, identified as $C_3H_3O_2$ radical cation. Here the difference between the m/z 56 and 71 represents a CH_3. The mass spectrum is presented in the Appendix I, Figure I.6. The peak in the retention time 17.461 is characterized by the mass spectrum with a base peak ion m/z 149 in the abundance of 100% (Appendix I, Figure I.7). The C_7O_4H compound is recognized to be a contaminant.

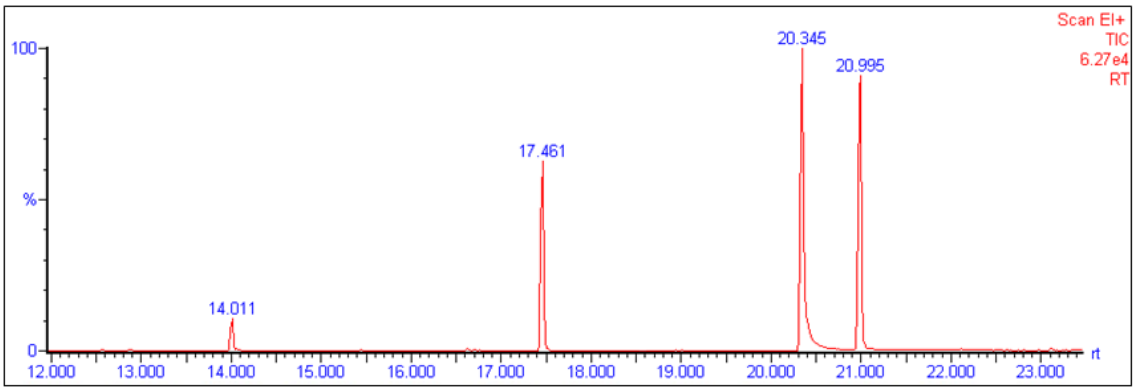

Figure 4.21 Chromatogram of the UV lamps degradation of 3 hours experiment

- **4 hours**

In the 4 hour experiment the chromatograph showed 4 peaks (Figure 4.22). The peaks in the retention time 20.346 and 20.963 with the respective abundance of 100 and 11% are TCS as the matching mass spectrum reveals in the Figure I.12 and I.13 in the Appendix I. The two peaks at the retention time 17.429 and 18.529 with the abundance of 11 and 4% have the same peaks in the mass spectra; the base ion peak of m/z 149 is identical in the abundance of 100%. These peaks are identified has C_7O_4H compound as contaminant. The respective mass spectrum is exposed in the Figure I.10 and I.11 in the Appendix I.

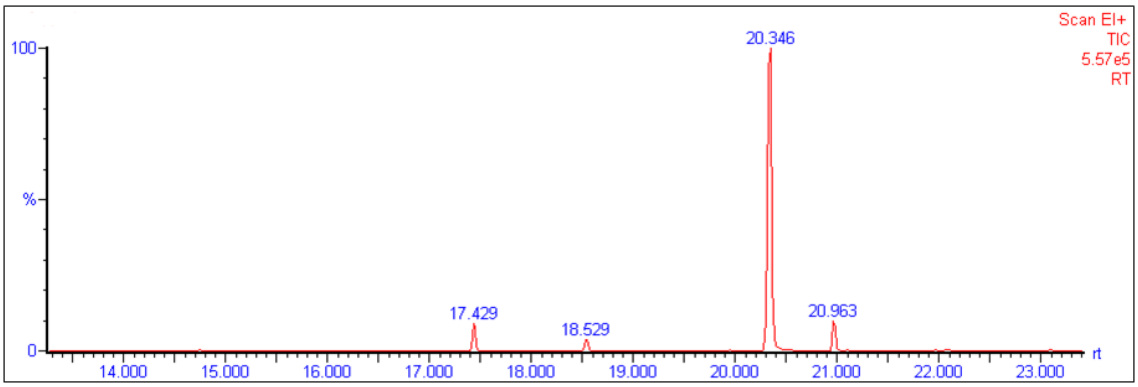

Figure 4.22 Chromatogram of the UV lamps degradation of 4 hours experiment

- **5 hours**

For the 5 hours experiment, TCS was present at the retention time 20.430 and 21.064 with the abundance of 100 and 20% (Figure 4.23). The mass spectra presented in the Figure I.16 and I.17 in the Appendix I verified the TCS compound. The peaks in the retention time 17.546 and 18.630 (43 and 11% of abundance) have the base ion peak m/z 149 at 100%, the peaks that appear are the same so we conclude to be in the presence of isomers. The identified compound was the C_7O_4H compound, a contaminant; the respective mass spectra are present in the Figure I.14 and I.15 in the Appendix I.

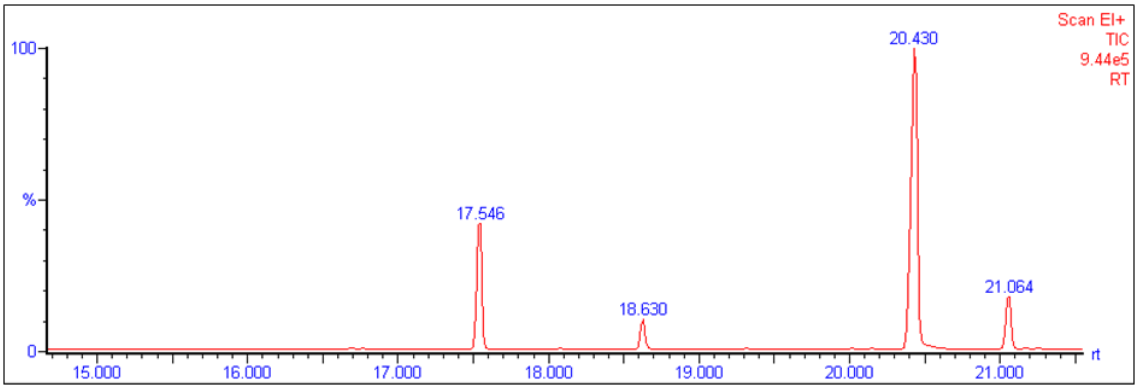

Figure 4.23 Chromatogram of the UV lamps degradation of 5 hours experiment

The pH values measure in the standard solution and in the different time experiments realized are exposed in the Table 4.1.

Table 4.1 pH measurements from the photocatalytic experiment under UV light

Time (h)	0	1	3	4	5	8
pH	7,5	7	7	7	7	7

The concentration of TCS by UV lamps had the higher percentage of degradation during the first hour, equivalent to 68% degradation (Table 4.2). The major degradation during the first

hour is present in the studies by Sankoda *et al*., 2011; Rafqah *et al*., 2006 and Yu *et al*., 2006. The presented percentages in these articles were always above to the percentage of degradation achieved, Yu *et al*., 2006 had an estimated degradation rate of 96% within 6h, and after 5h a total of 92% was achieved in this work. These differences could be due to different operational conditions.

Table 4.2 Degradation percentages of the UV experiment

Time (h)	1	3	4	5
Degradation (%)	68	73	84	92

4.2.3 Photocatalysis by sunlight

The chromatogram of the photocatalytic degradation of TCS with sunlight exposes 4 peaks (Figure 4.24). The peaks in the retention time 20.395 and 21.011 with the respective abundance of 100% and 22% are characteristic of the TCS compound proven by the respective mass spectra in the Figure I.20 and I.21 in the Appendix I. The peaks 17.461 and 18.561 with the abundance of 12 and 3% are identified by the same base peak ion of m/z 149 (100% abundance) which is representative of the C_7O_4H compound, a contaminant (Figure I.18 and I.19 in the Appendix I).

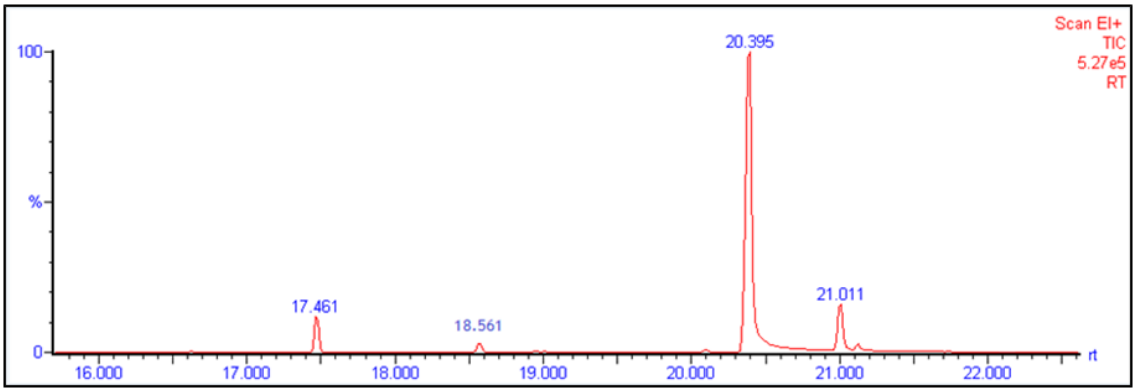

Figure 4.24 Chromatogram of the photocatalytic sunlight degradation for the 8 h experiment

The operational conditions related to sunlight are very difficult to control since they directly depend from the weather conditions. However, when photocatalytic degradation was performed under the best weather conditions, the degradation of TCS achieved a degradation of 90% in 8 hours (Figure III.2, Appendix III).

The pH measure in the standard solution and after 8h of photocatalytic degradation under sunlight is presented in the Table 4.3.

Table 4.3 pH measurement under photocatalytic degradation under sunlight

Time (h)	0	8
pH	7,5	7

4.2.4 Photocatalysis by LEDs

In the chromatogram of the photocatalytic LEDs experiment (Figure 4.25), the peaks at the retention times 17.529, 18.613 and 21.046 were produced. The peaks 1.626 and 4.610 are referring to the solvent n-hexane and the internal standard benzonitrile.

Peaks at the retention time 17.529 and 18.613 with the abundance of 20% reveal similar mass spectra (Appendix I Figure I.22 and I.23). This mass spectrum is characterized by the base ion peak 149 at 100% abundance and was identified as C_7O_4H compound, a contaminant The peak related to triclosan appear at the retention time of 21.046 in the abundance of 28%, the related mass spectrum is in the Appendix I, Figure I.24.

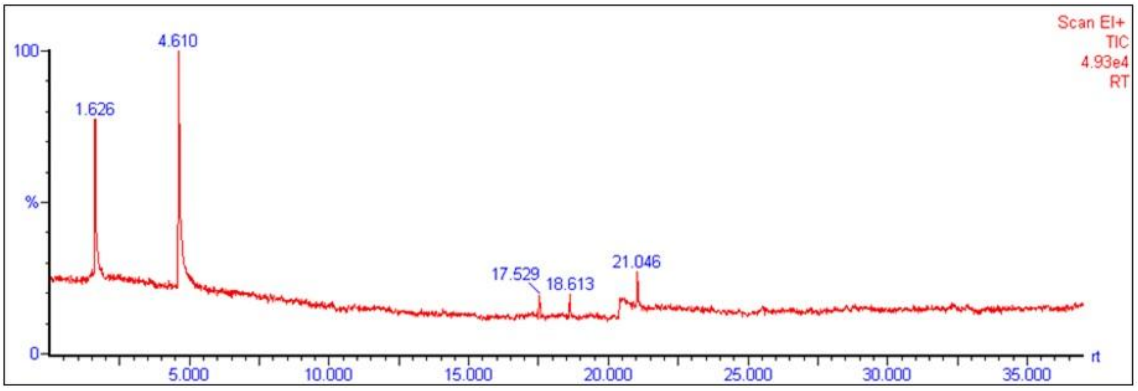

Figure 4.25 Chromatogram of the photocatalytic LEDs degradation of 8h experiment

In the chromatogram of 8h photocatalysis only one peak of TCS appear (Figure 4.25), in the opposite at what happened in the chromatograms of the photocatalytic experiments by UV, sunlight and Fenton reaction. In these reactions TCS appears always in two peaks, chromatograms were presented in Figure 4.11, Figures 4.21 to 4.24 and Figures 4.28 to 4.31. Although since the intensity signal is lower in the chromatogram of the Figure 4.25 when compared with the others, it is possible that the quantity it is to low to be detected by the signal and for this only one peak appears..

Comparing the ratio of the base peak ions on the mass spectrum of TCS in photocatalysis by LEDs (Figure I.24 in Appendix I) and the mass spectra of TCS produced in all the other experiments, with the exception of photo-Fenton, was notable some differences. The degradation rate was low, when compared with the other methods, this could indicate a changed to the mechanisms of action in photocatalysis by LEDs.

The pH measure in the standard solution and after 8h of photocatalytic degradation under LEDs is presented in the Table 4.4.

Table 4.4 pH measurement under photocatalytic degradation under LEDs

Time (h)	0	8
pH	7,5	7

The degradation of TCS on photocatalysis by TiO_2 with LEDs was possible and the rate of removal reached 53% after 8h (Figure III.3, Appendix III). By comparing the degradation rate of LEDs with sunlight, LEDs yield almost twice less degradation than sunlight.

There are only a limited number of papers that study the LED photocatalysis applied in the field of environmental engineering (Yu *et al*., 2013). No paper on LED photocatalysis performed in triclosan was found at the time of this written study.

LED photocatalytic degradation of phenols, specifically of 4–chlorophenol (4-CP) and 2,4–DCP might be a good approximation to what could happen with TCS. These compounds are structurally related to TCS due to its aromatic character and phenol presence. Yu *et al*., 2013 had percentages of removal of 4-CP and 2,4–DCP in the order of 25% and 28% after 1 hour of irradiation, showed in the Table 4.5.

Table 4.5 Percentage of removal of pesticides (4 - CP and 2,4-DCP) (Adapted from: Yu *et al*., 2014)

Pesticides	4-CP	2,4-DCP
Degradation (%)	25	28

When comparing LEDs with UV lamps, LEDs confirmed to be more energy-efficient and the emissions of LEDs have the advantage that they can be matched with the absorption band of TiO_2 (Yu *et al*., 2013).

Different authors studied the feasibility of the application of LEDs in the degradation of hazardous compounds through photocatalysis (Jo & Tayade, 2014; Yu *et al*., 2013 ; Levine *et al*., 2011; Ghosh *et al*., 2009; Shie *et al*., 2008; Wang & Ku, 2006; Han *et al*., 2004). The degradation always occurred, demonstrating that LEDs are a viable photon source for photocatalytic process. Even if the rates of removal are minor than fluorescent lamps the potential of LEDs could be improved by optimizing operational conditions, such as the light distribution over the catalyst, like TiO_2 nanotubes, is a good solution to increase the contact surface with the catalyst (Levine *et al*., 2011).

4.2.5 Photo-Fenton reaction

The chromatogram resulted of the degradation by photo–Fenton reaction experiment showed no peaks in the area expected for the retention time of triclosan (Figure 4.26). Two peaks appeared which resulted from the treatment for analysis, the extraction and derivatization made with hexane arises at the retention time 1.526 min and the adding of the internal standard at the retention time of 4,410 min. The initial pH of the suspension with $FeSO_4.7H_2O$ and TCS before the drop by the addition of H_2SO_4 was 6, and after 3.

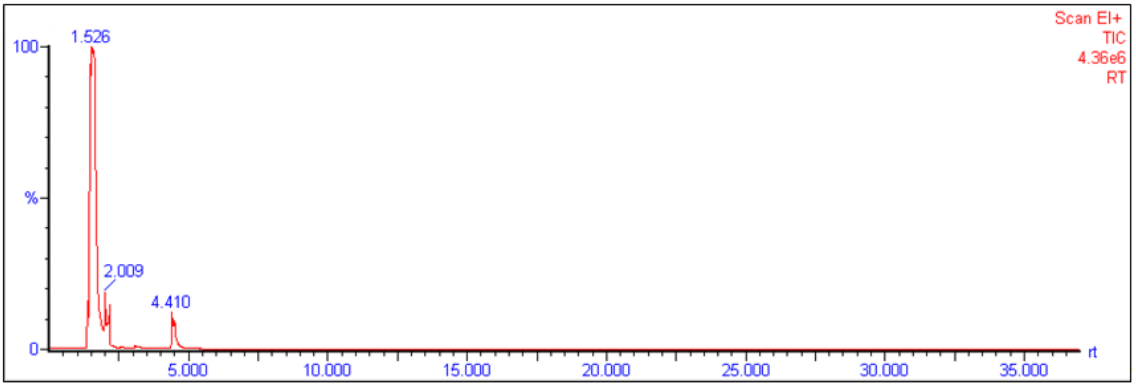

Figure 4.26 Chromatogram of the photo-Fenton reaction experiment

In the photo-Fenton experiment no degradation products were detected, evidencing that there was a complete degradation of the products and a high conversion to CO_2. One option is the fast degradation that makes harder the follow-up of the evolution products. Klamerth *et al*., 2009 only gathered two experimental points due to the rapid evolution of the compounds during photo-Fenton reaction. Bear in attention that this chromatogram has a very high signal when compared with all the others.

The photo-Fenton reaction revealed a full degradation of the TCS compound by the end of the 2nd hour (Figure III.4 in Appendix III). In Son *et al*., 2010 photo-Fenton reaction experiment, triclosan was almost completely removed within the 1st hour. The photo-Fenton experiment performed by Klamerth *et al*., 2009 by sunlight over a mixture of emerging contaminants (acetaminophen, antipyrine, atrazine, caffeine, diclofenac, isoproturon, progesterone, sulfamethoxazole, and triclosan), showed degradation of TCS in 20 minutes in demineralized water and degradation of the total of the other contaminants over 38 minutes.

Bauer & Fallmann, (1997) compared the systems $UV/O_2/Fe^{2+}$, UV/TiO_2, $UV/O_3/Fe^{2+}$ and $UV/H_2O_2/ Fe^{2+}$ (photo-Fenton reaction), in the degradation of 10^{-3} mol/l 4-CP). The degradation was followed by total organic carbon analysis, results are exposed in the Figure 4.27. The photo-Fenton reaction was the most effective method in the degradation of 4-CP.

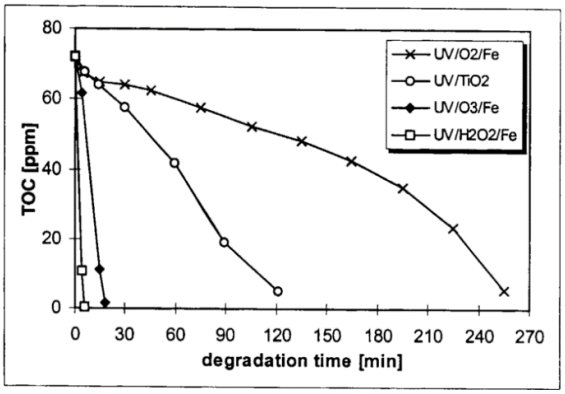

Figure 4.27 Degradation of 10^{-3} mol/l 4-CP by different AOPs (Adapted from Bauer & Fallmann, 1997)

Once again, photo-Fenton achieved removals of 96,4% in dipyrone, an analgesic drug with aromatic character, having the best degradation rate when compared with Fenton reaction, UV/H_2O_2 photolysis and UV/TiO_2 photocatalysis in the study performed by Giri & Golder, (2014).

Photo–Fenton reaction has proven to be a method that brings rapid and complete degradation of the compounds even in different operational conditions.

4.2.6 Fenton Reaction

- **Single addition of H_2O_2**

The Fenton experiment with the addition of H_2O_2 with all the volume released at once was performed twice, firstly for the duration of 2 hour experiment and then for 4 hours experiment. In both no peaks appear apart from TCS peaks.

At the 2 hours experiment TCS appears at the retention time 20.395 and 21.061 (Figure 4.28). For the 4h experiment, TCS appears at the retention time 20.478 and 21.095 (Figure 4.29).

The mass spectra that allowed to confirm the TCS identification, are exposed in Figure I.25, I.26, I.27 and I.28 of the Appendix I. The initial pH of before the drop of the suspension with $FeSO_4.7H_2O$ and TCS by the addition of H_2SO_4 was 6, and after 2.8, and had the same values in the experiment of 2 and 4 hours. After 2 hours, the degradation of TCS achieved 92%, at the end of the 4^{th} hour, it was 95% (Figure III.5, Appendix III).

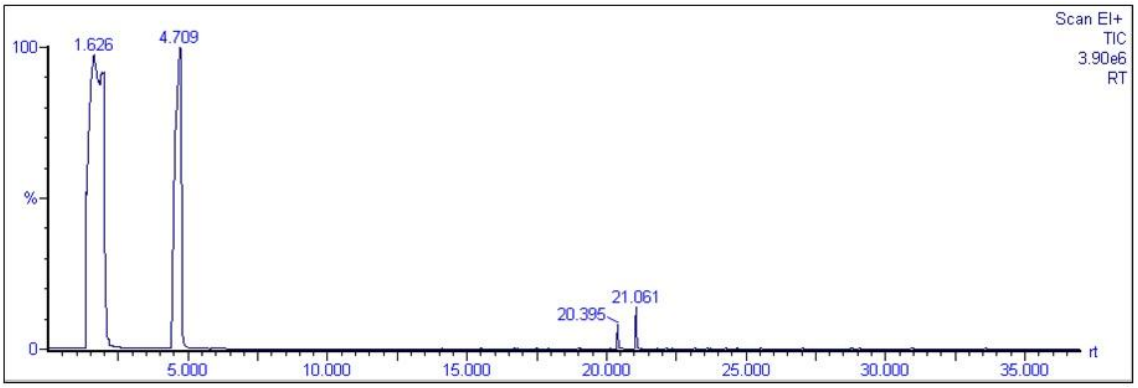

Figure 4.28 Chromatogram of the Fenton reaction of 2 hour experiment

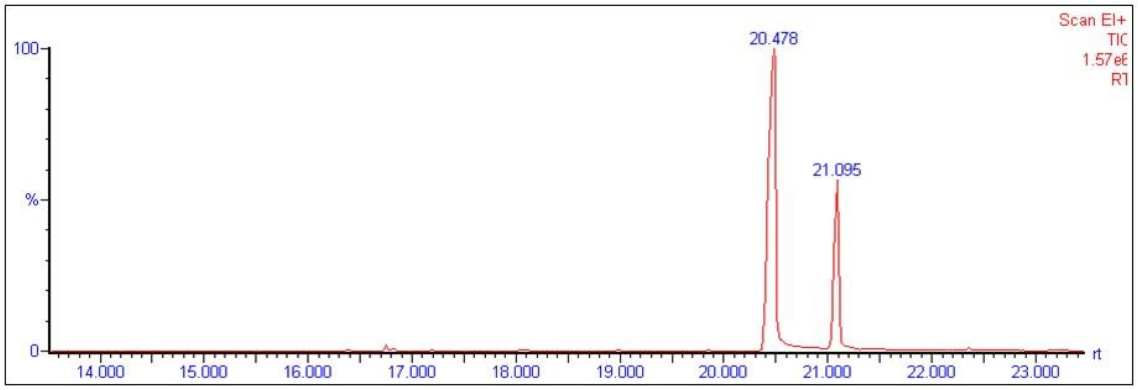

Figure 4.29 Chromatogram of the Fenton reaction of 4 hour experiment

- **Triple addition of H_2O_2**

The Fenton reaction experiment performed in 2 and 4 hours, by adding H_2O_2 in three instants throughout the duration of the experiment; exposed only TCS peaks. The 2 hour experiment showed TCS peaks at the retention time 20.345 and 20.995 in the abundance of 100% and 38% (Figure 4.30). The 4 hour experiment revealed the TCS peaks at the retention time 20.378 and 21.011 with the respectively abundance of 100% and 22% (Figure 4.31).

The corresponding peaks mass spectra are present in the Figures I.29, I.30, I.31 and I.32 in the Appendix I. The initial pH of the $FeSO_4.7H_2O$ and TCS suspension was 6, after the addition of H_2SO_4, was 2.8, and had the same values in the experiment of 2 and 4 hours. After 2 hours, the degradation of TCS achieved 90%, at the end of the 4th hour, it was 93% (Figure III.6, Appendix III).

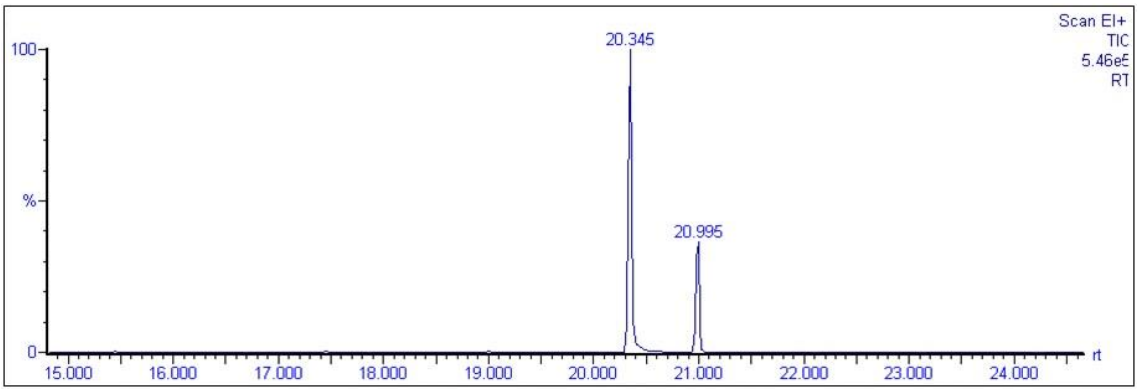

Figure 4.30 Chromatogram of the Fenton reaction of 2 hour experiment by adding H_2O_2 in three instants of time

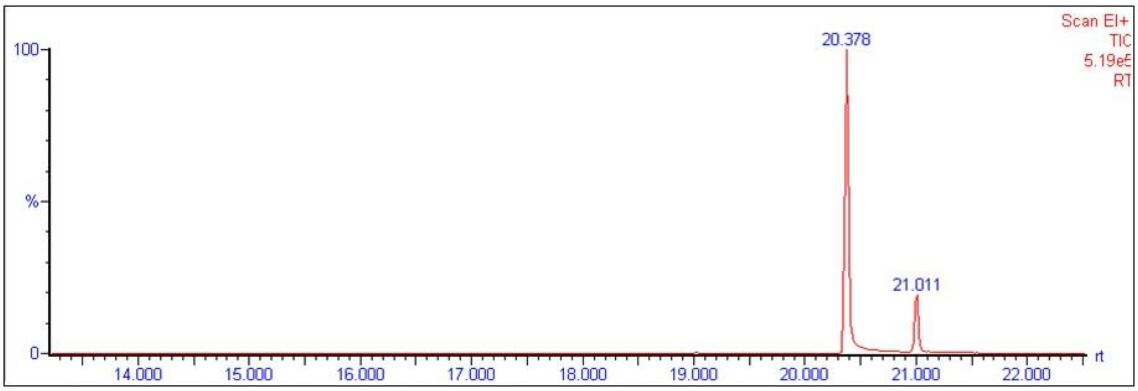

Figure 4.31 Chromatogram of the Fenton reaction of 4 hour experiment by adding H_2O_2 in three instants of time

The degradation of TCS under Fenton reaction by adding H_2O_2 once or in three instants of time during the duration of the experiment, resulted in the same magnitude of degradation of the compound (Figure III.5 and III.6 in the Appendix III). Since Fenton reaction with the addition of H_2O_2 at once was more efficiency (95% versus 93%) the comparison of the methods only consider Fenton reaction by adding H_2O_2 once. The initial idea for adding H_2O_2 in three times was due to the curiosity of knowing if OH^- and $OH^\bullet$ species would accelerate the rate of degradation by being consumed during three separated phase in time. The catalytic degradation of H_2O_2 became inefficient if it is transformed in water.

4.2.7 Global aspects

→The suggested identification of C_7O_4H compound being a contaminant characterized by the ion peak m/z 149:

The ion peak m/z 149 appears repeatedly in the photodegradation experiments, except in the photo-Fenton and Fenton reaction. The identification of this peak was extremely difficulty; the NIST and Willey libraries gave very different compounds, showing some problems in the identification. The consultation of the literature revealed some inadequacy too. The ion peak m/z 149 must have in its composition one aromatic ring, constituted by carbon and hydrogen,

with the typical signature of chloride not present (M-2 and M-4). The final proposal is based on the assumption the ion peak m/z 105 is an aromatic compound of formula C_6O_2H and the addition of a COO presented the peak m/z 149 giving the C_7O_4H compound (Table 4.6). This compound is suspected to be a contaminant.

Table 4.6 Mass spectrum of the ion peak m/z 149 in the different experiments

Photocatalytic degradation by UV		
Hours (h)	Retention times	Descriptive Figure
1	17.461	Figure 4.16
	18.561	Figure I.3, Appendix I
3	17.461	Figure I.7, Appendix I
4	17.429	Figure I.10, Appendix I
	18.529	Figure I.11, Appendix I
5	17.546	Figure I.14, Appendix I
	18.630	Figure I.15, Appendix I
Photocatalytic degradation by sunlight		
Retention time		Descriptive Figure
17.461		Figure I.18, Appendix I
18.561		Figure I.19, Appendix I
Photocatalytic degradation by LEDs		
Retention time		Descriptive Figure
17.529		Figure I. 22, Appendix I
18.613		Figure I. 23, Appendix I

→ Dioxins

Dioxins are the by-products of the degradation of TCS that cause more general concern. According to the literature, dioxins are formed in the first minutes of irradiation (Latch *et al*., 2003), although after 1 hour in the UV experiment and all the others performed, no dioxins were detected.

Rafqah *et al*., 2006 defends dioxins only are formed if triclosan in its anionic form absorbs light at waveleght inferior of 300 nm. The technical features of fabrication of the model of the UV lamps indicates that the maximum wavelength is 310 nm, the UV–Visible spectra from the manufacturer show a narrow peak in this wavelength so no irradiation is emitted under 300 nm. Yu *et al*., 2006 detected chlorinated dibenzo-p-dioxin in samples exposed to 254 nm UV light but in the samples exposed to 365 nm no chlorinated dibenzo-p-dioxin congener was found.

The wavelength of the LEDs was not measured and no manufacturer features existed, the LED system was built in the Università degli Studi di Padova, and for the same reason either the

wavelength of the LEDs is higher than 300 nm or dioxins were produced in the first hour and were destroyed by the end of the experiment, which might account to no dioxins being visible.

The photo-Fenton reaction revealed a full degradation of the TCS compound. In the destruction of TCS the method that yields best results by source of light was photo-Fenton followed by UV, sunlight and finally LEDs (Figure 4.32). The degradation percentages were given by the following order: Photo-Fenton reaction→ Fenton reaction→ UV→ Sunlight and finally LEDs

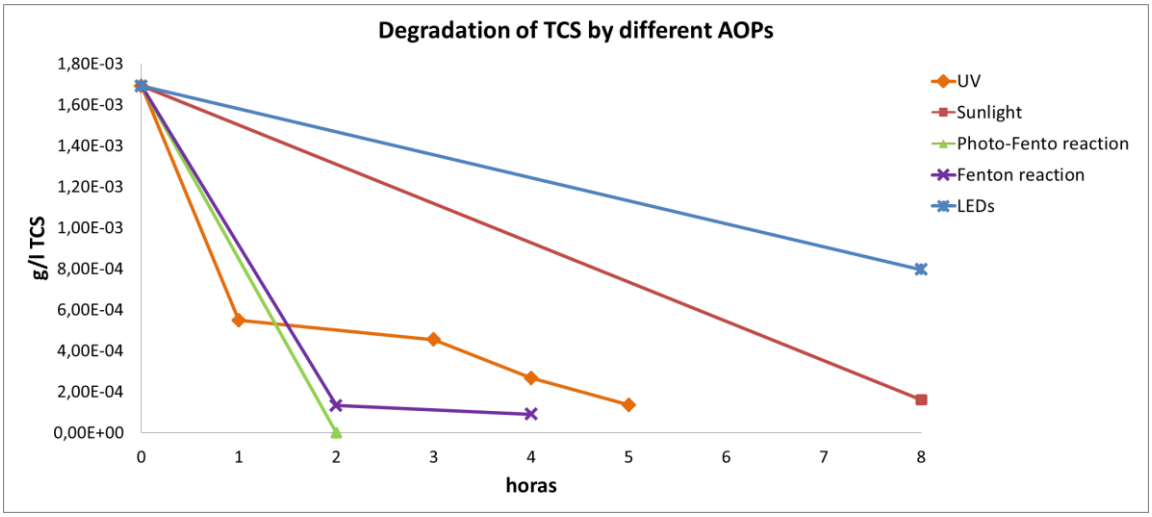

Figure 4.32 Degradation of TCS by different AOPs

In the Table 4.7, are presented the degradation percentages of the different methods used, this degradation had only in account the final concentration and the initial concentration since it was not possible to follow the reactions during the time, except in the UV experiment. We can gather the degradations in three groups, the photo-Fenton reaction with 100%, Fenton, UV and sunlight degradation in the range of the 90% and LEDs with a degradation of 53%.

Since there was not a sufficient number of experiments to make a statistical study it's possible the that the three methods of degradation, Fenton reaction, UV and sunlight, have very similar degradation rates.

Table 4.7 Degradation percentages of the different methods used

AOPs	photo-Fenton	Fenton	UV	Sunlight	LEDs
Degradation (%)	100	95	92	90	53

5 Conclusions and future work

Throughout the course of this study, several methods of degradation of TCS, known as AOPs were evaluated. The analysis of the result and literature lead to the following conclusions:

- Photon-Fenton reaction was the best AOPs, having a degradation rate of 100% of TCS within 2 hours, and no by-products were detected;
- The degradation was given by the following order: photo-Fenton → Fenton reaction → UV → Sunlight → LEDs;
- The photocatalytic degradation under UV produced by-products after the first hour. It was not possible to compare with the other methods since samples were not gathered after one hour;
- Hydroquinone specie and 2,4–DCP intermediates were identified in the first hour of the photocatalytic degradation under UV;
- A common contaminant, identified has C_7O_4H compound, was present at the degradation by UV, sunlight and LEDs;
- Photocatalytic degradation by using LEDs is a viable possibility in the destruction of TCS. The degradation percentage was 53% after 8h;
- Photocatalytic degradation under LEDs could follow different mechanisms of action when comparing the degradation rate with other degradation sources;
- The addition of H_2O_2 once or in three separate times gave the same magnitude of degradation of the TCS;
- No dioxins where detected in the operational conditions used.

Future work and recommendations:

- The study work with LEDs is worthwhile to continue given the advantages of long durability and low consumption of energy making the future potential for these lamps very high; fluorescent lamps in the ending of their life cycle carry the risk of spread of mercury in the environment and as governments make these lamps unavailable new solutions are required; Fenton and photo-Fenton reaction can be also a costly process due to the reagents cost used.
- More studies in the use of LEDs should be performed in order to better define the kinetics reactions;
- LEDs allowed a variable possibility to design devices. An industrial scale pilot can be used to research;
- Improve the extraction and derivatization techniques to understand the degradation products;

- Following degradation of TCS through time in different AOPs and the by–products generated is an interesting point to have in considerer;
- In the case of photo-Fenton process, possibly high quantities of TCS were transformed in $CO_{2;}$ the measurement of CO_2 levels can be quantified on the absorption of CO_2 by sodium hydroxide.

6 References

Adolfsson-Erici, M., Pettersson, M., Parkkonen, J. & Sturve, J. (2002). Triclosan, a commonly used bactericide found in human milk and in the aquatic environment in Sweden. *Chemosphere*, **46**(9-10), 1485–1489.

Aguillon, C., Newman, J. & Machado, A. (2010). Pharmaceuticals and Personal Care Products (PPCPs):triclosan. http://www.csun.edu/~vchsc006/triclosan.pdf.

Aliabadi, M. & Sagharigar, T. (2011). Photocatalytic removal of Rhodamine B from aqueous solutions using TiO_2 nanocatalyst. *Journal of Applied Environmental and Biological Sciences,* **1**(12), 620–626.

Allmyr, M., Adolfsson-Erici, M., McLachlan, M. S. & Sandborgh-Englund, G. (2006). Triclosan in plasma and milk from Swedish nursing mothers and their exposure via personal care products. *Science of the Total Environment*, **372**(1), 87–93.

Aranami, K. & Readman, J. W. (2007). Photolytic degradation of triclosan in freshwater and seawater. *Chemosphere*, **66**(6), 1052–1056.

Bauer, R. & Fallmann, H. (1997). The photo-Fenton oxidation — A cheap and efficient wastewater treatment method. *Research on Chemical Intermediates*, **23**(4), 341–354.

Bester, K. (2003). Triclosan in a sewage treatment process-balances and monitoring data. *Water Research*, **37**(16), 3891–3896.

Bhargava, H. N. & Leonard, P. A. (1996). Triclosan : Applications and safety. *American Journal of Infection Control*, **24**(3), 209 – 218.

Bovey, F. A., Mirau, P. A. & Gutowsky, H. S. (1988). *Nuclear Magnetic Resonance Spectroscopy*: Academic Press, INC.

Bruins, A. P. (1998). Mechanistic aspects of electrospray ionization. *Journal of Chromatography A*, **794**(1), 345–357.

Carp, O., Huisman, C. L. & Reller, A. (2004). Photoinduced reactivity of titanium dioxide. *Progress in Solid State Chemistry*, **32**, 33–177.

Catrinescu, C., Arsene, D., Apopei, P. & Teodosiu, C. (2012). Degradation of 4-chlorophenol from wastewater through heterogeneous Fenton and photo-Fenton process, catalyzed by Al–Fe PILC. *Applied Clay Science*, **58**, 96–101.

Cech, N. B. & Enke, C. G. (2002). Practical implications of some recent studies in electrospray ionization fundamentals. *Mass Spectrometry Reviews*, **20**, 362–387.

Chalew, T. E. A. & Halden, R. U. (2009). Environmental exposure of aquatic and terrestrial biota to triclosan and triclocarban. *Journal of the American Water Resources Association*, **45**(1), 4–13.

Coogan, M. A., Edziyie, R. E., La Point, T. W. & Venables, B. J. (2007). Algal bioaccumulation of triclocarban, triclosan, and methyl-triclosan in a North Texas wastewater treatment plant receiving stream. *Chemosphere*, **67**, 1911–1918.

Czaplicka, M. (2001). Determination of phenols and chlorophenols in bottom sediments. *Chromatographia*, **53**, 470–473.

Dann, A. B. & Hontela, A. (2011). Triclosan: environmental exposure, toxicity and mechanisms of action. *Journal of Applied Toxicology*, **31**, 285–311.

Dayan, A. D. (2007). Risk assessment of triclosan [Irgasan] in human breast milk. *Food and Chemical Toxicology* , **45**(1), 125–129.

Fang, J.L., Stingley, R. L., Beland, F. A., Harrouk, W., Lumpkins, D. L. & Howard, P. (2010). Occurrence, efficacy, metabolism and toxicity of triclosan. *Journal of Environmental Science and Health. Part C, Environmental Carcinogenesis & Ecotoxicology Reviews*, **28**(3), 147–171.

Foran, C. M., Bennett, E. R. & Benson, W. H. (2000). Developmental evaluation of a potential non-steroidal estrogen: triclosan. *Marine Environmental Research*, **50**,153–156.

Fuertes, V. C., Negre, C. F. A., Oviedo, M. B., Bonafé, F. P., Oliva, F. Y. & Sánchez, C. G. (2013). A theoretical study of the optical properties of nanostructured TiO_2. *Journal of Physics: Condensed Matter*, **25**, 1-7.

Fujishima, A. & Murakami, T. (2010). Expanding industrialization of photocatalysts. *Sangakukan*, **6**.

Ghosh, J. P., Sui, R., Langford, C. H., Achari, G. & Berlinguette, C. P. (2009). A comparison of several nanoscale photocatalysts in the degradation of a common pollutant using LEDs and conventional UV light. *Water Research*, **43**, 4499–4506.

Giri, A. S. & Golder, A. K. (2014). Fenton, photo-Fenton, H_2O_2 photolysis, and TiO_2 photocatalysis for dipyrone oxidation : drug removal, mineralization, biodegradability and degradation mechanism. *Industrial & Engineering Chemistry Research*, **53**, 1351 - 1358.

Glaser, A. (2004). The Ubiquitous Triclosan A common antibacterial agent exposed. *Pesticides and You*, **24**(3), 12-17.

Gómez, M. J., Gómez-Ramos, M. M., Agüera, A., Mezcua, M., Herrera, S. & Fernández-Alba, A. R. (2009). A new gas chromatography/mass spectrometry method for the simultaneous analysis of target and non-target organic contaminants in waters. *Journal of Chromatography A*, **1216**, 4071–4082.

Hakura, A., Suzuki, S., Sawada, S., Motooka, S. & Satoh, T. (2002). An improvement of the Ames test using a modified human liver S9 preparation. *Jornal of Pharmacological Methods*, **46**, 169-172.

Hakura, A., Suzuki, S. & Satoh, T. (1999). Advantage of the use of human liver S9 in the Ames test. *Mutation Research*, **438**, 29-36.

Halden, R. U. (2014). On the need and speed of regulating triclosan and triclocarban in the United States. *Environmental Science & Technology*, **48**, 3603–3611.

Han, W., Zhu, W., Zhang, P., Zhang, Y. & Li, L. (2004). Photocatalytic degradation of phenols in aqueous solution under irradiation of 254 and 185nm UV light. *Catalysis Today*, **90**, 319–324.

Heath, R. J., Rubin, J. R., Holland, D. R., Zhang, E., Snow, M. E. & Rock, C. O. (1999). Mechanism of triclosan inhibition of bacterial fatty acid synthesis. The *Journal of Biological Chemistry*, **274**(16), 11110–11114.

Heidler, J. & Halden, R. U. (2007). Mass balance assessment of triclosan removal during conventional sewage treatment. *Chemosphere*, **66**(2), 362–369.

Ho, C. S., Lam, C. W. K., Chan, M. H. M., Cheung, R. C. K., Law, L. K., Lit, L. C. W., Ng, K. F., Suen, M. W. M. & Tai, H. L. (2003). Electrospray ionisation mass spectrometry: principles and clinical applications. *The Clinical Biochemist Reviews,* **24**(1), 3–12.

Hontela, A. & Habibi, H. R. (2013). 8 - Personal care products in the aquatic environment: a case study on the effects of triclosan in fish. In *Organic Chemical Toxicology of Fishes* (pp. 411– 437): Academic Press.

Jabrou, S. N. (2012). Extraction of phenol from industrial water using different solvents. *Research Journal of Chemical Sciences*, **2**(4), 1–12.

Jo, W. & Tayade, R. J. (2014). New generation energy-efficient light source for photocatalysis : LEDs for environmental applications. *Industrial & Engineering Chemistry Research,* **53**, 2073-2084.

Júnior, A., Quina, F., Gozzi, F., Silva, V., Friedrich, L. & Moraes, J. (2012). Fundamental mechanistic studies of the photo-Fenton reaction for the degradation of the organic pollutants. In T. Puzyn (Ed.)*, Organic Pollutants Ten Years After the Stockholm Convention - Environmental and Analytical Update*: Intech.

Kaneko, M. & Okura, I. (2002). *Photocatalysis: science and technology*. Japan: Kodansha/ Springer.

Katz, D. R., Cantwell, M. G., Sullivan, J. C., Perron, M. M., Burgess, R. M., Ho, K. T. & Charpentier, M. A. (2013). Factors regulating the accumulation and spatial distribution of the emerging contaminant triclosan in the sediments of an urbanized estuary: Greenwich Bay, Rhode Island, USA. *Science of the Total Environment*, **443**, 123–133.

Kim, K., Park, H., Yang, W. & Lee, J. H. (2011). Urinary concentrations of bisphenol A and triclosan and associations with demographic factors in the Korean population. *Environmental Research*, **111**(8), 1280–1285.

Klamerth, N., Miranda, N., Malato, S., Agüera, A., Fernández-Alba, A. R., Maldonado, M. I. & Coronado, J. M. (2009). Degradation of emerging contaminants at low concentrations in MWTPs effluents with mild solar photo-Fenton and TiO_2. *Catalysis Today*, **144**(1-2), 124–130.

Kola, R. K., Rasheed, A. & Yalavarthy, P. D. (2013). Evaluation of antibacterial activity of triclosan against human patogens. *The Ecoscan*, **4**, 273–276.

Kudo, A. & Miseki, Y. (2009). Heterogeneous photocatalyst materials for water splitting. *Chemical Society Reviews*, **38**(1), 253–278.

Latch, D. E., Packer, J. L., Arnold, W. A. & McNeill, K. (2003). Photochemical conversion of triclosan to 2,8-dichlorodibenzo-p-dioxin in aqueous solution. *Journal of Photochemistry and Photobiology A: Chemistry*, **158**, 63–66.

Levine, L. H., Richards, J. T., Coutts, J. L., Soler, R., Maxik, F. & Wheeler, R. M. (2011). Feasibility of ultraviolet-light-emitting diodes as an alternative light source for photocatalysis. *Journal of the Air & Waste Management Association*, **61**(9), 932–940.

Li, X., Ying, G., Zhao, J., Chen, Z., Lai, H. & Su, H. (2013). 4-Nonylphenol, bisphenol-A and triclosan levels in human urine of children and students in China, and the effects of drinking these bottled materials on the levels. *Environment International*, **52**, 81–86.

Ling, L., Xian, J., Ali, S., Geng, B., Fan, J., Mills, D. M., Arvanites, A.C., Orgueira, H., Ashwell, M. A., Carmel, G., Xiang, Y. & Moir D. T. (2004). Identification and characterization of

inhibitors of bacterial enoyl-acyl carrier protein reductase. *Antimicrobial agents and chemotherapy*, **48**(5), 1541-1547.

Liu, F., Ying, G., Yang, L. & Zhou, Q. (2009). Terrestrial ecotoxicological effects of the antimicrobial agent triclosan. *Ecotoxicology and Environmental Safety*, **72**, 86–92.

McAvoy, D. C., Schatowitz, B., Jacob, M., Hauk, A. & Eckhoff, W. S. (2002). Measurement of triclosan in wastewater treatment systems. *Environmental Toxicology and Chemistry*, **21**(7), 1323–1329.

Mezcua, M., Gómez, M. J., Ferrer, I., Aguera, A., Hernando, M. D. & Fernández-Alba, A. R. (2004). Evidence of 2,7/2,8-dibenzodichloro-p-dioxin as a photodegradation product of triclosan in water and wastewater samples. *Analytica Chimica Acta*, **524**, 241–247.

Mortelmans K. & Zeiger E. (2000). The Ames *Salmonella*/microsome mutagenicity assay. *Mutation Research*, **455**(1-2), 29-60.

Nakata, K. & Fujishima, A. (2012). TiO_2 photocatalysis: design and applications. *Journal of Photochemistry and Photobiology C: Photochemistry Reviews*, **13**(3), 169–189.

Nassef, M., Matsumoto, S., Seki, M., Khalil, F., Kang, I. J., Shimasaki, Y., Oshima, Y. & Honjo, T. (2010). Acute effects of triclosan, diclofenac and carbamazepine on feeding performance of Japanese medaka fish (*Oryzias latipes*). *Chemosphere*, **80**, 1095–1100.

Australian Government - Department of Health and Ageing/ National Industrial Chemicals Notification and Assessment Scheme. (2009). *Triclosan*. Priority Existing Chemical Assessment Report nr.30.

Ohtani, B., Prieto-Mahaney, O. O., Li, D. & Abe, R. (2010). What is Degussa (Evonik) P25? Crystalline composition analysis, reconstruction from isolated pure particles and photocatalytic activity test. *Journal of Photochemistry and Photobiology A: Chemistry*, **216**, 179–182.

Orvos, D. R., Versteeg, D. J., Inauen, J., Capdevielle, M., Rothenstein, A. & Cunningham, V. (2002). Aquatic toxicity of triclosan. *Environmental Toxicology and Chemistry*, **21**(7), 1338–1349.

Rafqah, S., Wong-Wah-Chung, P., Nelieu, S., Einhorn, J. & Sarakha, M. (2006). Phototransformation of triclosan in the presence of TiO_2 in aqueous suspension : mechanistic approach. *Applied Catalysis B: Environmental*, **66**, 119–125.

Ricart, M., Guasch, H., Alberch, M., Barceló, D., Bonnineau, C., Geiszinger, A., la Farré, M., Ferrer, J., Ricciardi, F., Romaní, A. M., Morin, S., Proia, L., Sala, L., Sureda, D. & Sabater, S. (2010). Triclosan persistence through wastewater treatment plants and its potential toxic effects on river biofilms. *Aquatic Toxicology*, **100**, 346–353.

Russel, A.D. (2004). Whither triclosan?*Journal of Antimicrobial Chemotherapy*, **53**, 693-695.

Sanchez-Prado, L., Llompart, M., Lores, M., García-Jares, C., Bayona, J. M. & Cela, R. (2006). Monitoring the photochemical degradation of triclosan in wastewater by UV light and sunlight using solid-phase microextraction. *Chemosphere*, **65**, 1338–1347.

Sankoda, K., Matsuo, H., Ito, M., Nomiyama, K., Arizono, K. & Shinohara, R. (2011). Identification of triclosan intermediates produced by oxidative degradation using TiO_2 in pure water and their endocrine disrupting activities. *Bulletin of Environmental Contamination and Toxicology*, **86**, 470–475.

SCCS. (2010). *Opinion on triclosan: antimicrobial resistance* (Publication No. 1251/09). European Commission, Brussels: Angerer, J., Bernauer, U., Chambers, C., Chaudhry, Q., Degen, G., Eisenbrand, G., Platzek, T., Rastogi, S. C., Rogiers, V., Rousselle, C., Sanner, T., Savolainen, K., Engelen, J., Vinardell, M. P., Waring, R. & White, I. R.

Shie, J., Lee, C., Chiou, C., Chang, C., Chang, C. & Chang, C. (2008). Photodegradation kinetics of formaldehyde using light sources of UVA, UVC and UVLED in the presence of composed silver titanium oxide photocatalyst. *Journal of Hazardous Materials*, **155**, 164–72.

Silverstein, R. M., Webster, F. X. & Kiemble, D. J. (2005). *Spectrometric identification of organic compounds*. United States of America, USA: Jon Willey & Sons, INC.

Singer, H., Müller, S., Tixier, C. & Pillonel, L. (2002). Triclosan: occurrence and fate of a widely used biocide in the aquatic environment: field measurements in wastewater treatment plants, surface waters, and lake sediments. *Environmental Science & Technology*, **36**(23), 4998–5004.

Skoog, D., West, D., Holler, F. & Crouch, S. (2004). *Fundamentals of Analytical Chemistry*. United States of America, USA: Thomson Brooks/Cole.

Son, H., Khim, J. & Zoh, K. (2010). Degradation of triclosan in the combined reaction of Fe^{2+} and UV-C: Comparison with the Fenton and photolytic reactions. *Environmental Progress & Sustainable Energy*, **29**(4), 415–420.

Song, Z., Wang, N., Zhu, L., Huang, A., Zhao, X. & Tang, H. (2012). Efficient oxidative degradation of triclosan by using an enhanced Fenton-like process. *Chemical Engineering Journal,* **198-199**, 379-387.

Sun, Q. & Xu, Y. (2010). Evaluating intrinsic photocatalytic activities of anatase and rutile TiO_2 for organic degradation in water. *Journal of Physical Chemistry*, **114**(44), 18911–18918.

Tatarazako, N., Ishibashi, H., Teshima, K., Kishi, K. & Arizono, K. (2004). Effects of triclosan on various aquatic organisms. *Environmental Sciences*, **11**(2), 133–140.

Thompson, A., Griffin, P., Stuetz, R. & Cartmell, E. (2005). The fate and removal of triclosan during wastewater treatment. *Water Environment Research,* **77**(1), 63–67.

Tixier, C., Singer, H. P., Canonica, S. & Müller, S. R. (2002). Phototransformation of triclosan in surface waters: a relevant elimination process for this widely used biocide-laboratory studies, field measurements and modeling. *Environmental Science & Technology*, **36**(16), 3482–3489.

Toms, L. L., Allmyr, M., Mueller, J. F., Adolfsson-Erici, M., McLachlan, M., Murby, J. & Harden, F. A. (2011). Triclosan in individual human milk samples from Australia. *Chemosphere*, **85**, 1682–1686.

U.S, EPA (2013). *Priority pollutants*. From URL: http://water.epa.gov/scitech/methods/cwa/pollutants.cfm (acceded: 9 -09-2014)

Villalaín, J., Mateo, C. R., Aranda, F. J., Shapiro, S. & Micol, V. (2001). Membranotropic effects of the antibacterial agent triclosan. *Archives of Biochemistry and Biophysics*, **390**(1), 128–136.

Waller, N. J. & Kookana, R. S. (2009). Effect of triclosan on microbial activity in Australian soils. *Environmental Toxicology and Chemistry*, **28**(1), 65–70.

Wang, L., Falany, C. N. & James, M. O. (2004). Triclosan as a substrate and inhibitor of 3` - phosphoadenosine 5` - phosphosulfate-sulfotransferase and udp-glucuronosyl transferase in human liver fractions, *The American Society for Pharmacology and Experimental Therapeutics*, **32**(10), 1162–1169.

Wang, W. & Ku, Y. (2006). Photocatalytic degradation of Reactive Red 22 in aqueous solution by UV-LED radiation. *Water Research*, **40**, 2249–2258.

Xie, Z., Ebinghaus, R., Flöser, G., Caba, A. & Ruck, W. (2008). Occurrence and distribution of triclosan in the German Bight (North Sea). *Environmental Pollution*, **156**, 1190–1195.

Yang, B., Ying, G., Zhao, J., Zhang, L., Fang, Y. & Nghiem, L. (2011). Oxidation of triclosan by ferrate: reaction kinetics, products identification and toxicity evaluation. *Journal of Hazardous Materials*, **186**, 227–235.

Yazdankhah, S. P., Scheie, A. A., Hoiby, E. A., Lunestad, B. T., Heir, E., Fotland, T. O., Naterstand, K. & Kruse, H. (2006). Triclosan and antimicrobial resistance in bacteria: an overview. *Microbial Drug Resistance*, **12**(2), 83 – 90.

Ying, G. & Kookana, R. S. (2007). Triclosan in wastewaters and biosolids from Australian wastewater treatment plants. *Environment International*, **33**, 199–205.

Yu, J. C., Kwong, T. Y., Luo, Q. & Cai, Z. (2006). Photocatalytic oxidation of triclosan. *Chemosphere*, **65**, 390–399.

Yu, L., Achari, G. & Langford, C. H. (2013). LED-based photocatalytic treatment of pesticides and chlorophenols. *Journal of Environmental Engineering*, **139**, 1146–1151.

Appendixes

Appendix I – Mass spectra

Characterization of the standard solution

- **GC/MS**

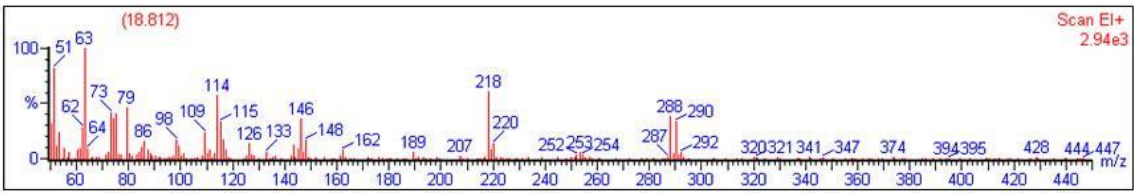

Figure I.1 Peak at 18.812: Triclosan isomer

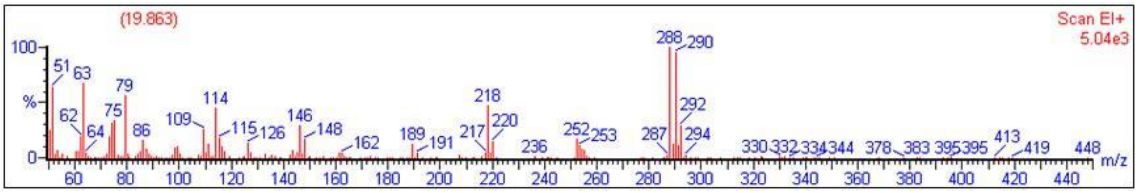

Figure I.2 Peak at 19.863: Triclosan isomer

- **Photocatalytic degradation with UV lamps**

1 hour:

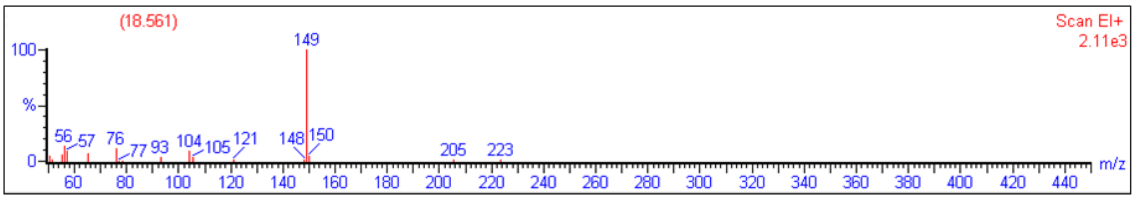

Figure I.3 Peak 18.561

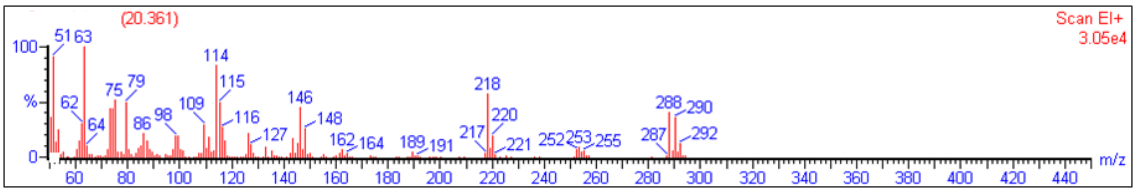

Figure I.4 Peak 20.361: Triclosan

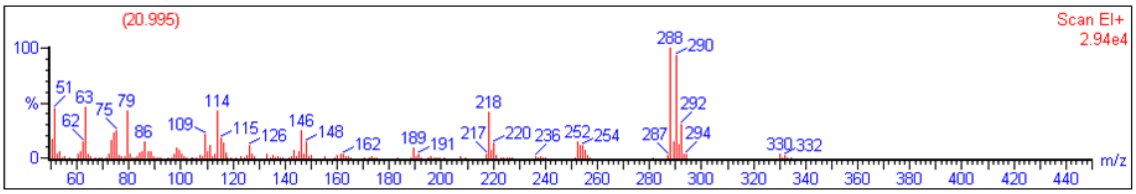

Figure I.5 Peak 20.995: Triclosan

3 hours:

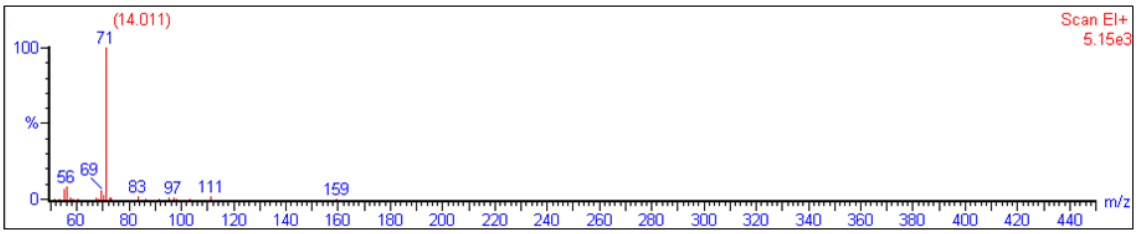

Figure I.6 Peak 14.011: $C_3H_3O_2$ radical cation

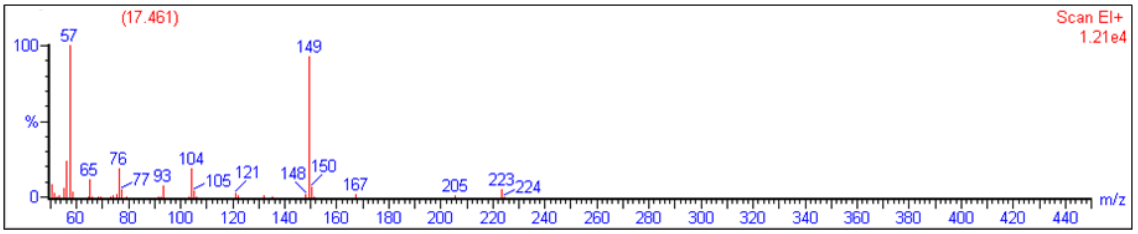

Figure I.7 Peak 17.461

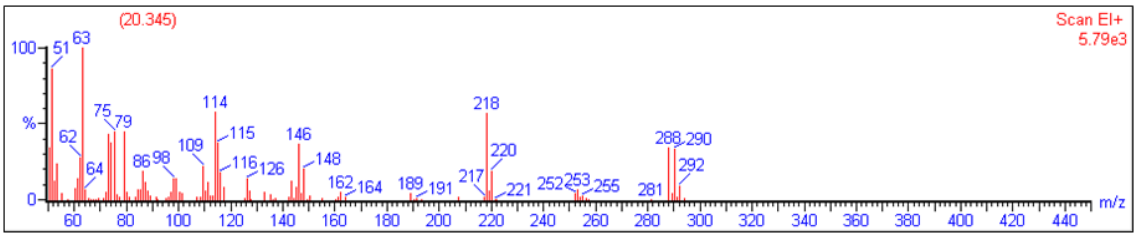

Figure I.8 Peak 20.345: Triclosan

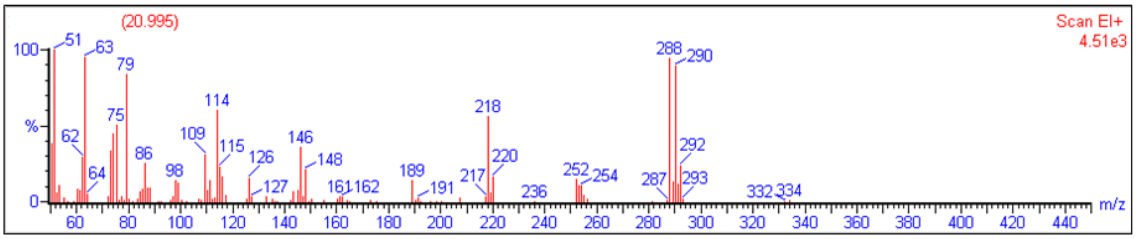

Figure I.9 Peak 20.995: Triclosan

4 hours:

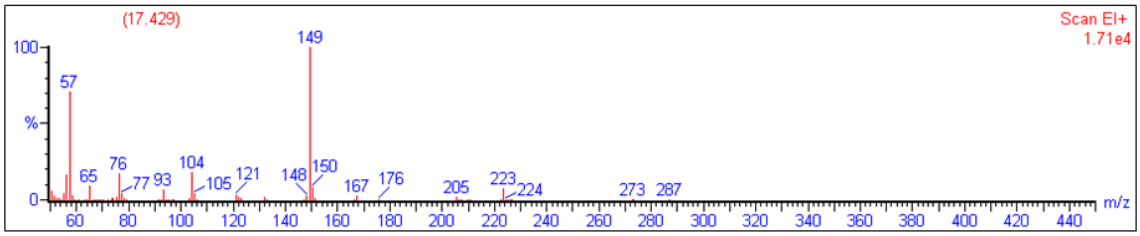

Figure I.10 Peak 17.429

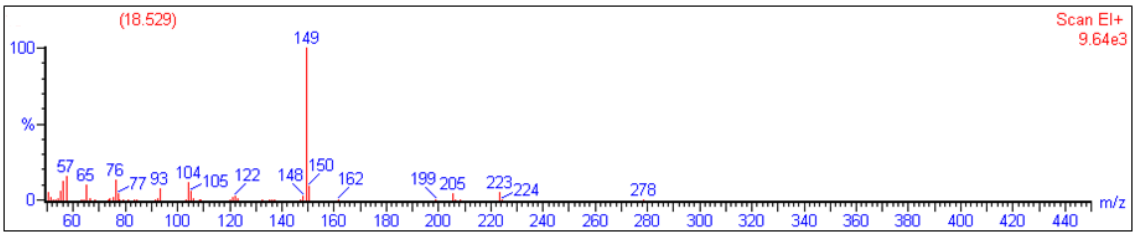

Figure I.11 Peak 18.529

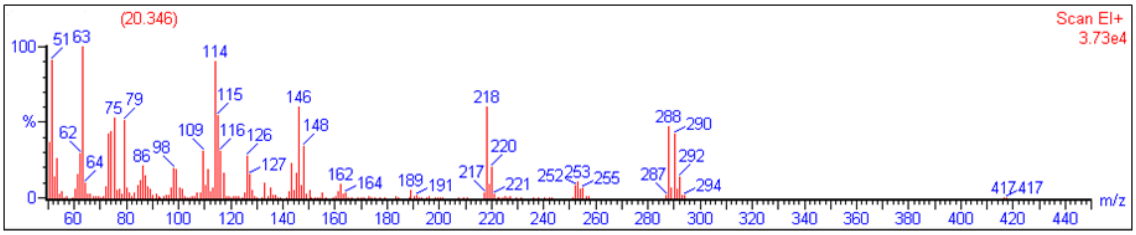

Figure I.12 Peak 20.346: Triclosan

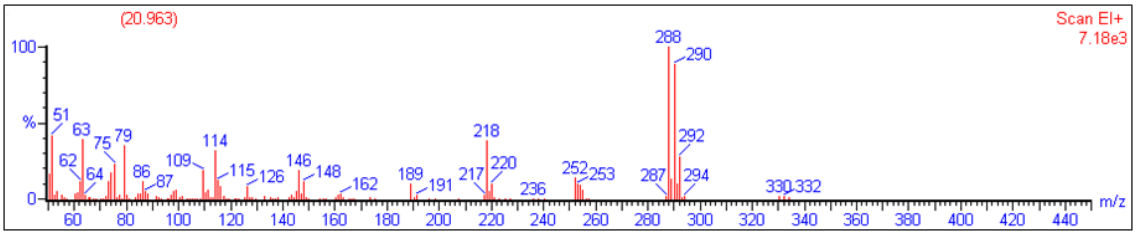

Figure I.13 Peak 20.963: Triclosan

5 hours:

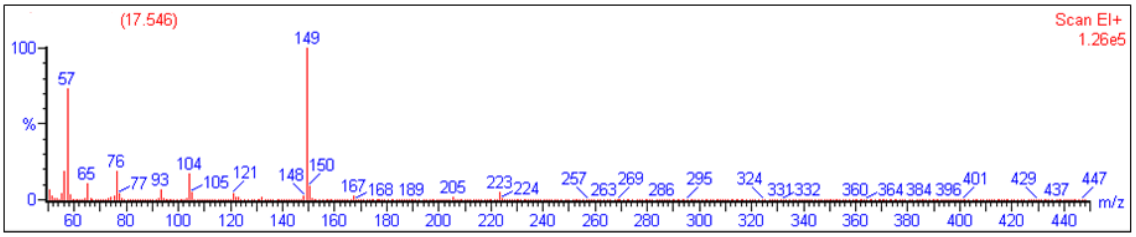

Figure I.14. Peak 17.546

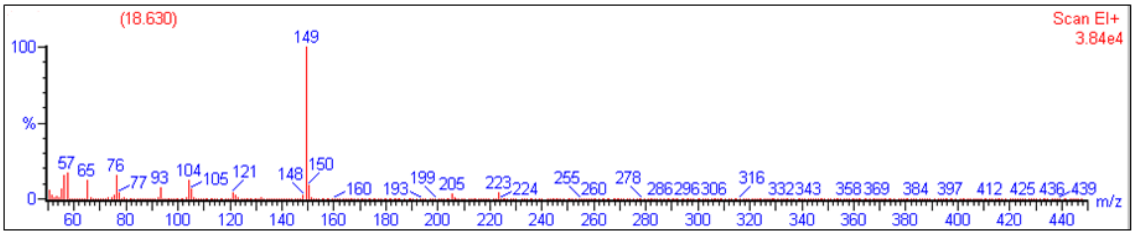

Figure I.15 Peak 18.630

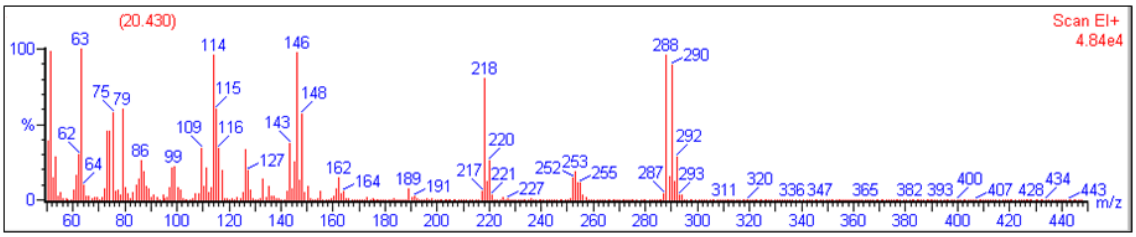

Figure I.16 Peak 20.430: Triclosan

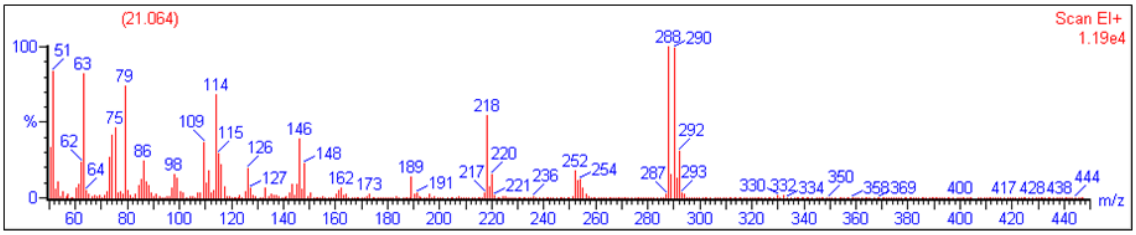

Figure I.17 Peak 21.064: Triclosan

- **Photocatalytic degradation with sunlight**

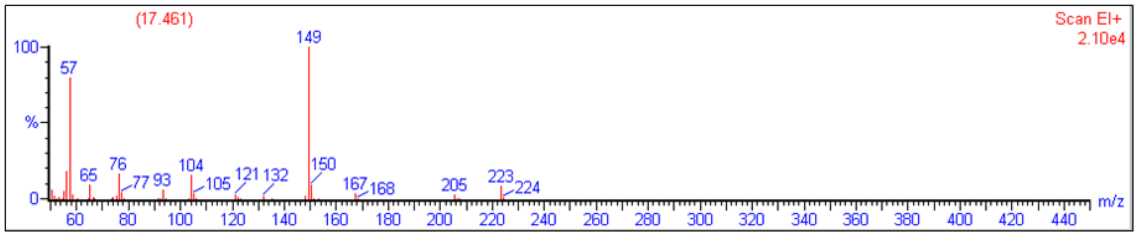

Figure I.18 Peak 17.461

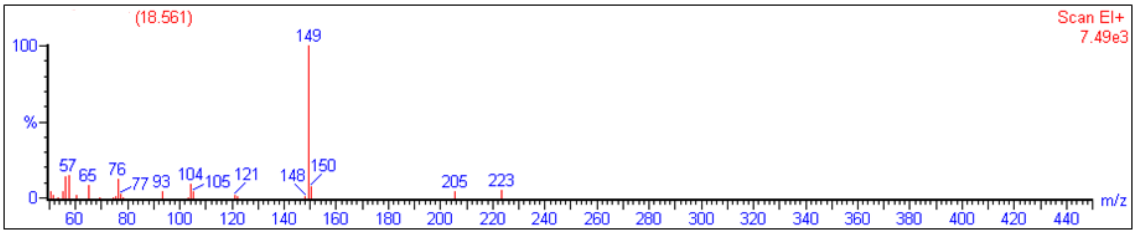

Figure I.19 Peak 18.561

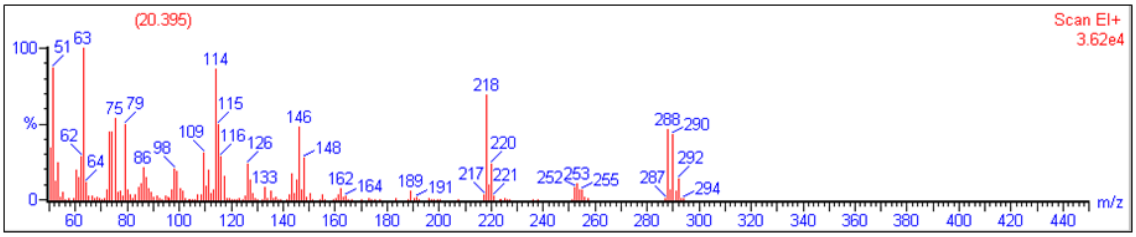

Figure I.20 Peak 20.395: Triclosan

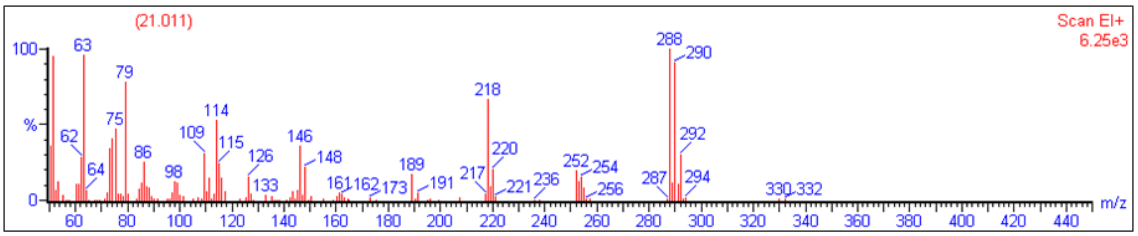

Figure I.21 Peak 21.011: Triclosan

- **Photocatalytic degradation with LEDs**

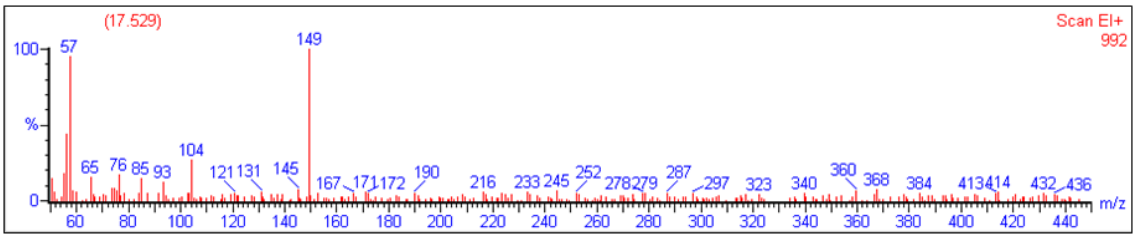

Figure I.22 Peak at 17.529

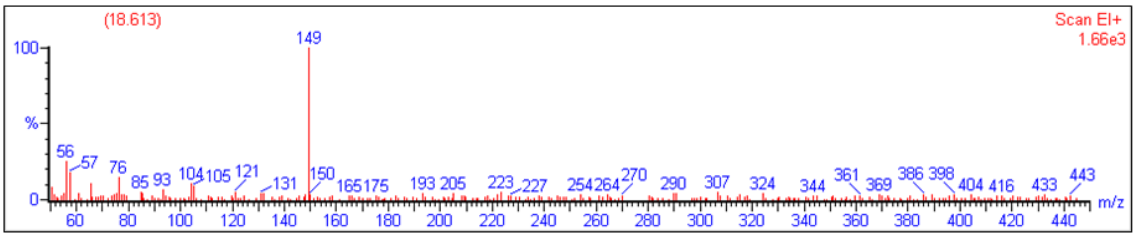

Figure I.23 Peak at 18.613

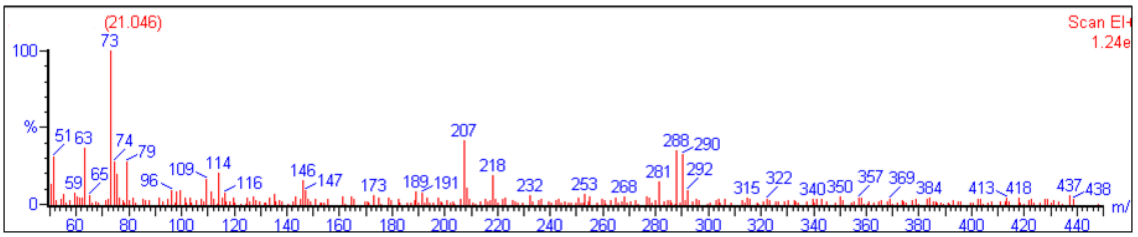

Figure I.24 Peak 21.046: Triclosan

- **Degradation by the Fenton reaction**

  - <u>Used of H_2O_2 at once:</u>

2 hours:

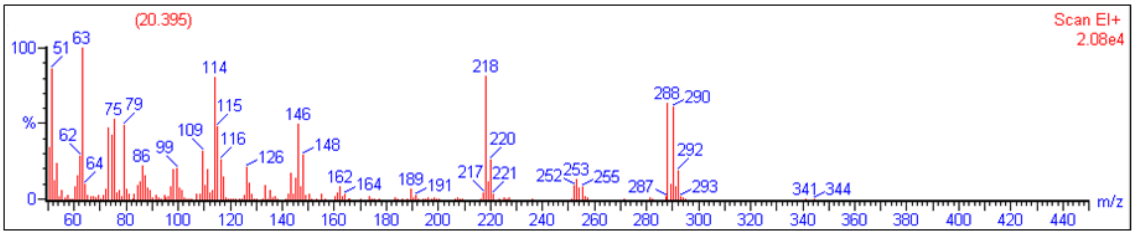

Figure I.25 Peak 20.395: Triclosan

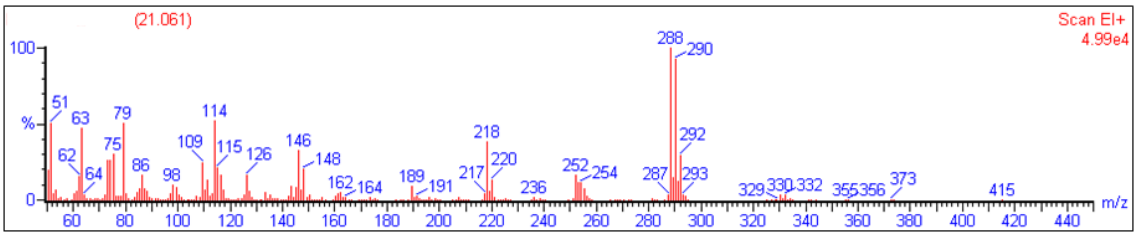

Figure I.26 Peak 21.061: Triclosan

4 hours:

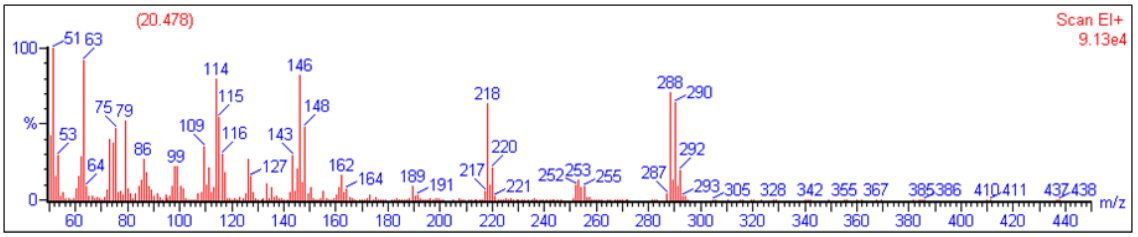

Figure I.27 Peak 20.478: Triclosan

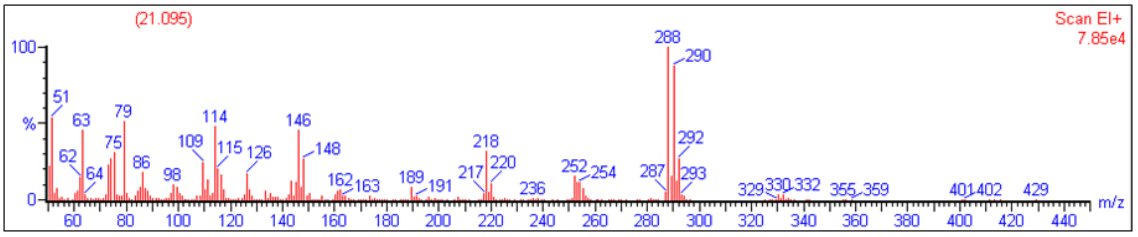

Figure I.28 Peak 21.095: Triclosan

- <u>Used of peroxide hydrogen in three times</u>

2 hours:

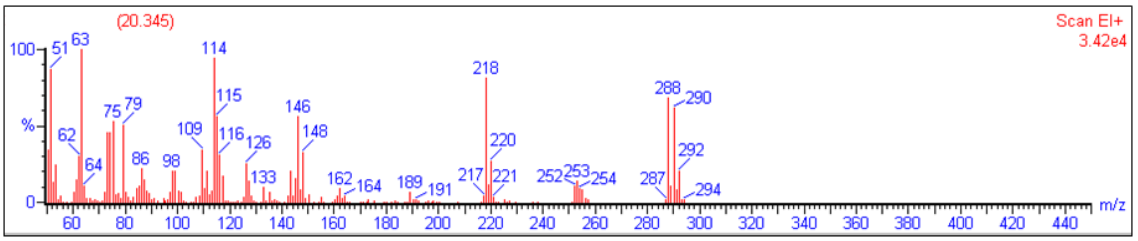

Figure I.29 Peak 20.345: Triclosan

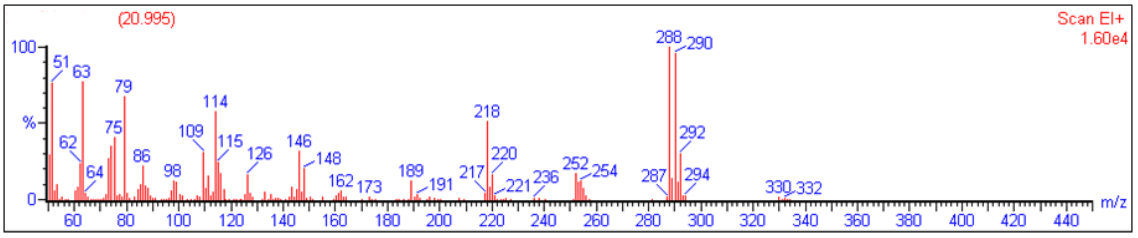

Figure I.30 Peak 20.995: Triclosan

4 hours:

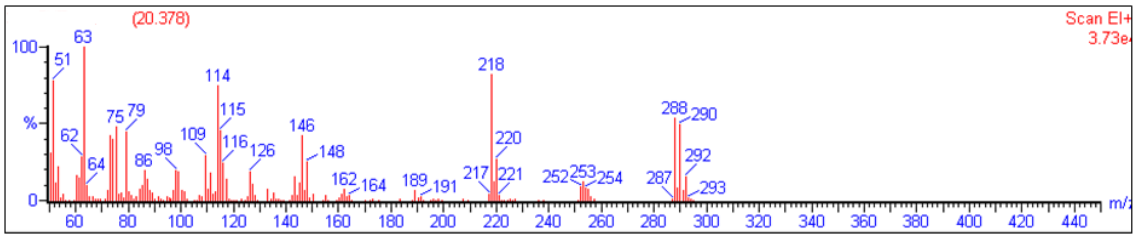

Figure I.31 Peak 20.378: Triclosan

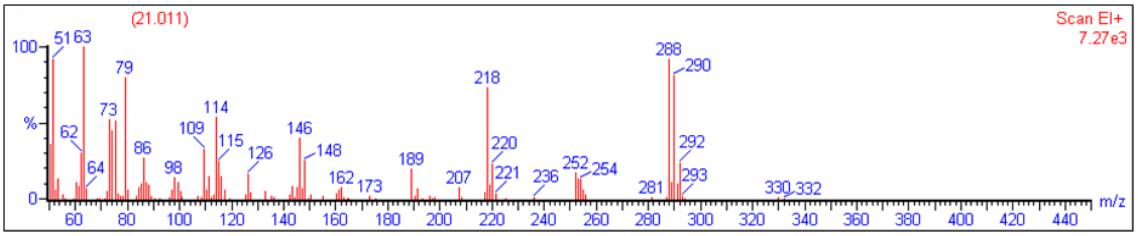

Figure I.32 Peak 21.011: Triclosan

Appendix II – Chromatograms

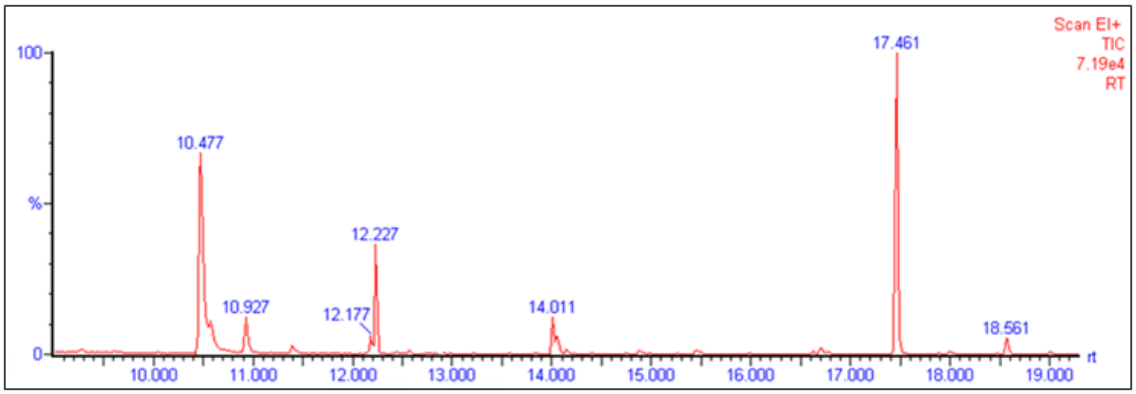

Figure II.1 Amplified chromatogram of the photocatalytic degradation by UV lamps experiment between the retention time 9 and 19 min

Appendix III – Quantitative Results

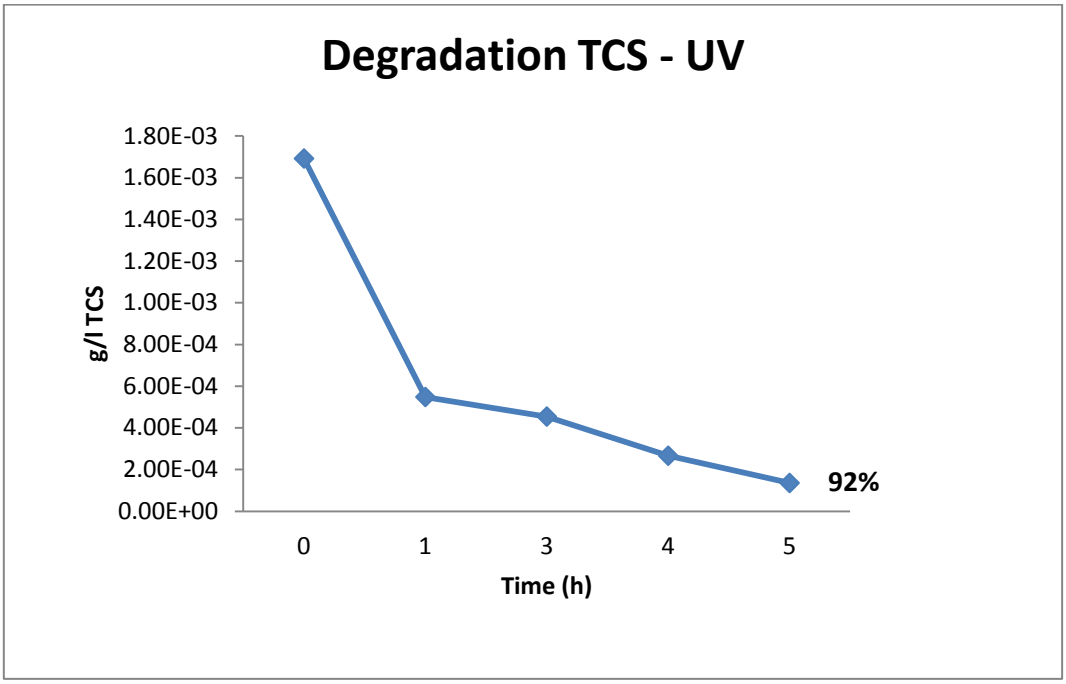

Figure III.1 Degradation of TCS under UV light

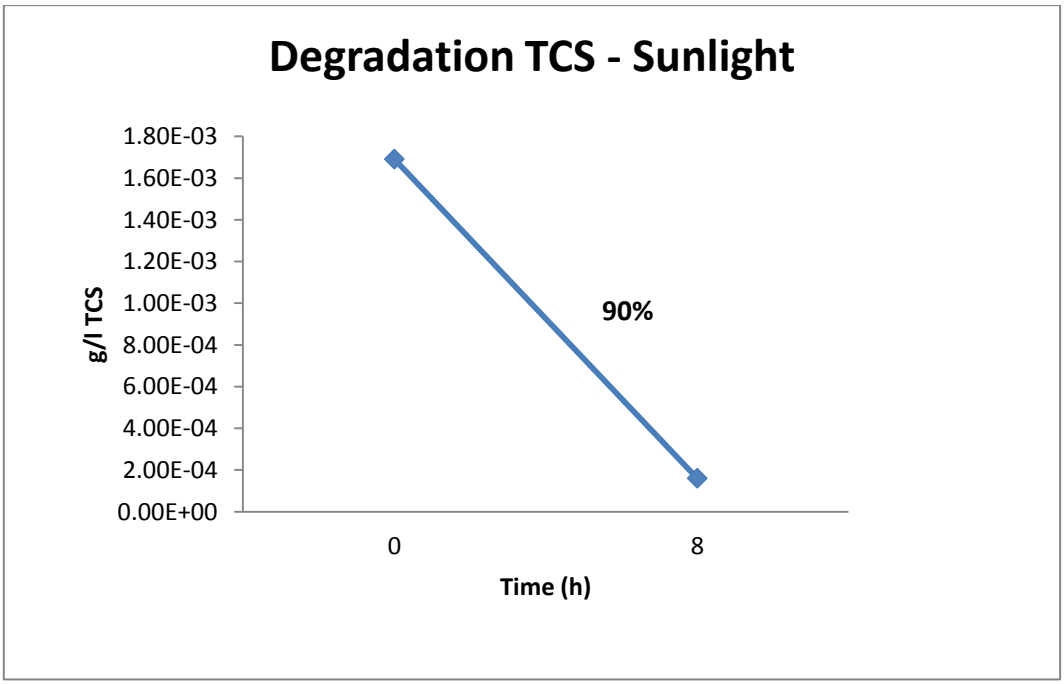

Figure III.2 Degradation of TCS under sunlight

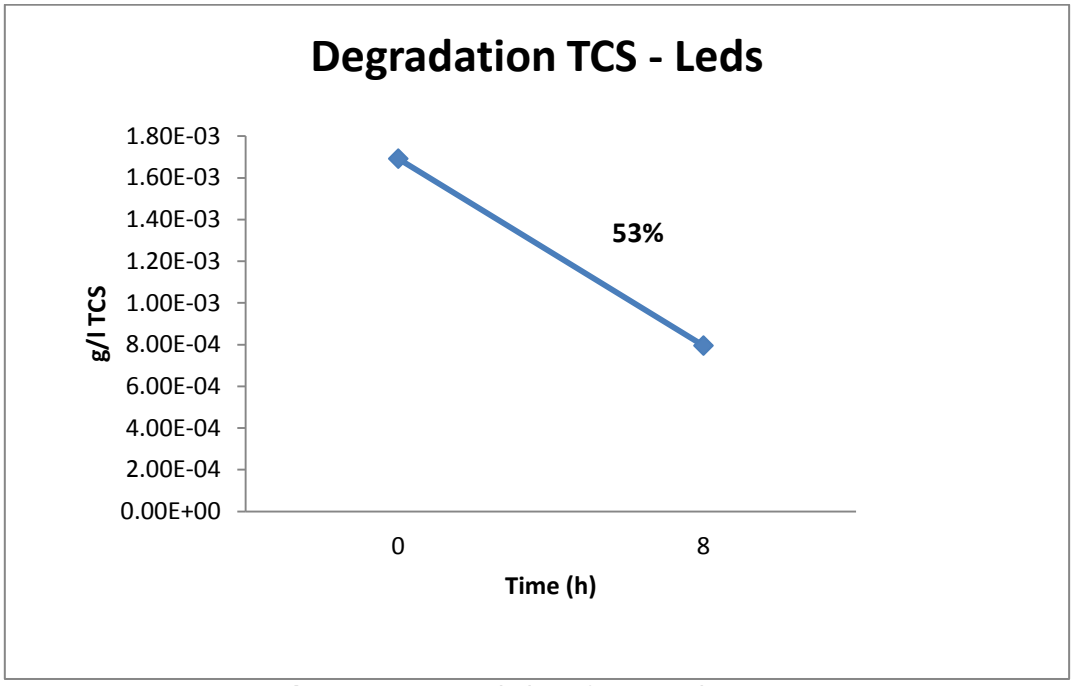

Figure III.3 Degradation of TCS under LEDs

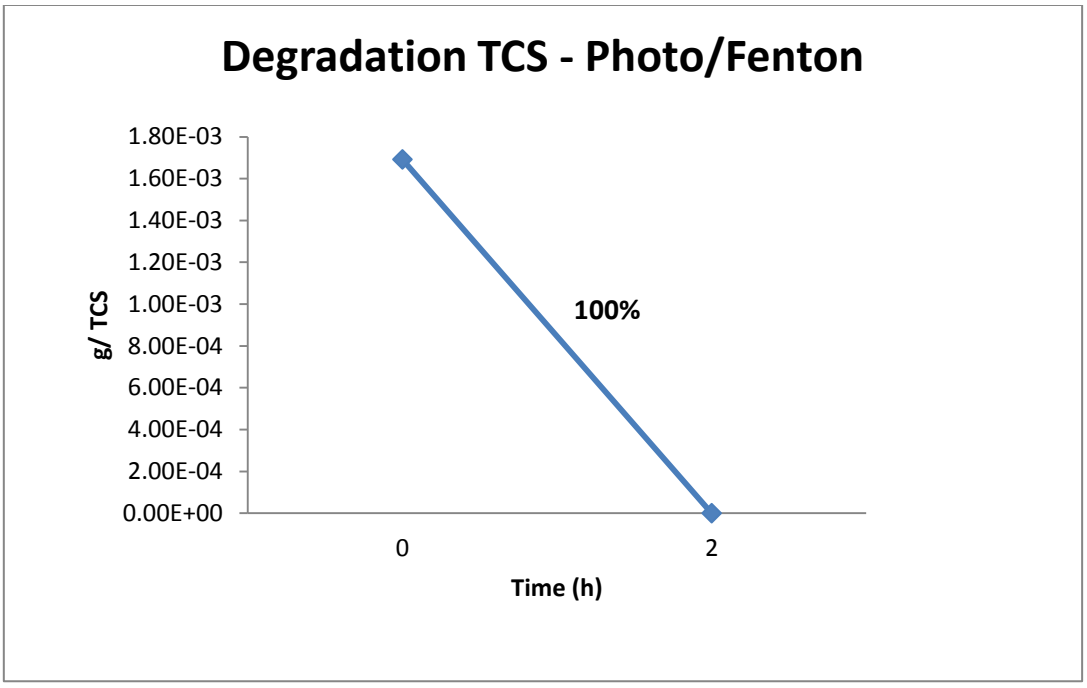

Figure III.4 Degradation of TCS under photo - Fenton reaction

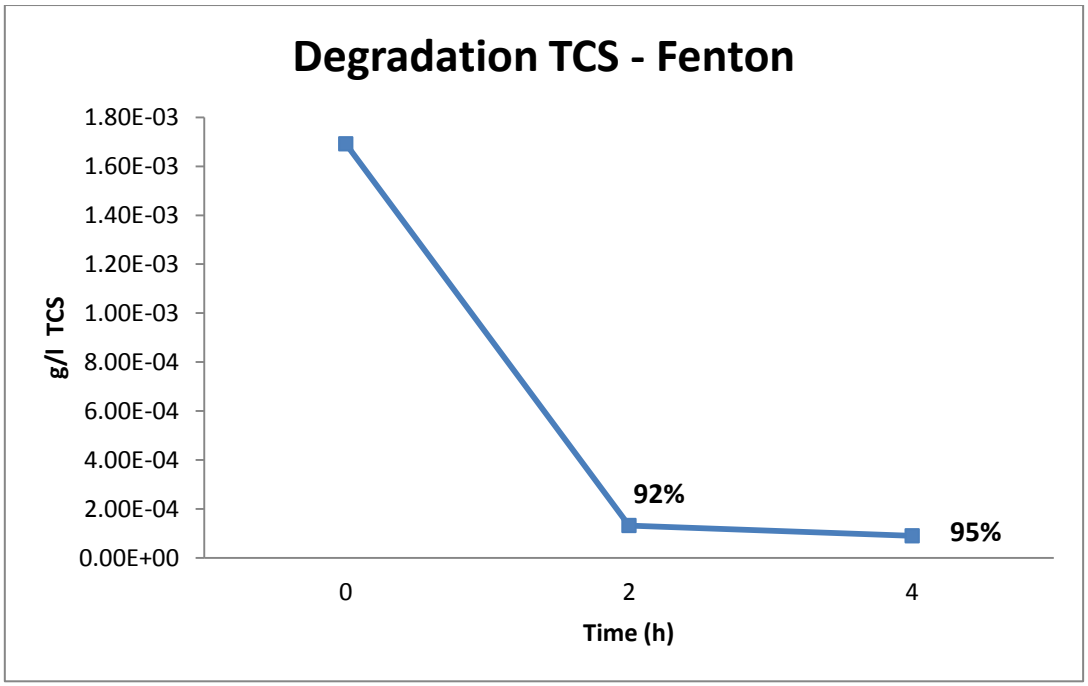

Figure III.5 Degradation of TCS under Fenton reaction (addition of H_2O_2 at once)

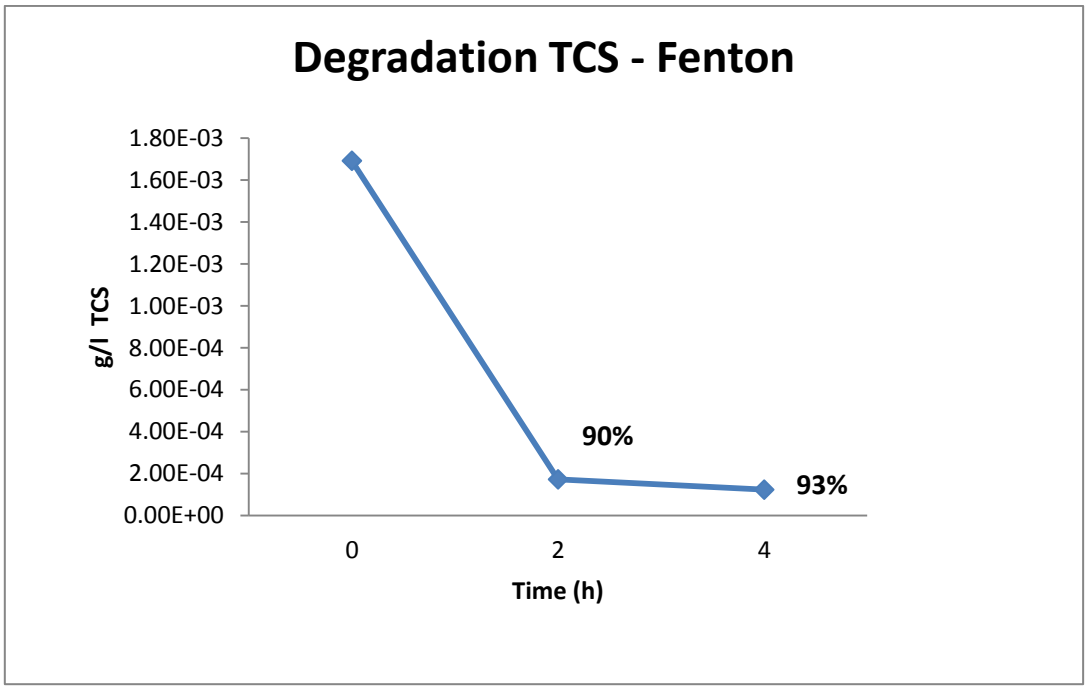

Figure III.6 Degradation of TCS under Fenton reaction (addition of H_2O_2 in 3 instants of time)

Appendix IV – Resume of the main intermediate products founded in the literature

Table IV.1 Main Intermediate products reported in the literature

Identified Intermediates	Reaction	Author
Dichlorophenols (2,4-DCP), tetraclosans, mono-chlorinated derivative of TCS, hydroxylated TCS and 2,8–DCDD	Photochemical degradation by UV	Sankoda *et al*., 2011
2,4–DCP, chlorocatechol hydroxylated TCS and 5 – chloro – 2 – (4 – chlorophenoxyl)phenol	Photochemical degradation by UV	Rafqah *et al*., 2006
2,4–DCP, quinone of TCS (2-chloro-5-(2,4-dichlorophenoxy)-[1,4]benzoquinone) and hydroquinone of TCS (2-chloro-5-(2,4-dichlorophenoxy)benzene-1,4-diol)	Photochemical degradation by UV	Yu *et al*., 2006
2,4–DCP, 2-chlorobenzoquinone, chlorophenol and hydroquinone of TCS;	Degradation by Fenton reaction	Yang *et al*., 2011
Chloride (ionic intermediate of TCS)	Degradation by Fenton reaction	Son *et al*., 2010
Chloride (ionic intermediate of TCS)	Degradation by photo-Fenton reaction	Son *et al*., 2010
2,8–DCDD, another di-chlorinated dioxin or dichlorohydroxydibenzofuran, dichlorohydroxydiphenyl ether, monochlorophenol and dichlorophenol;	Photochemical degradation by sunlight	Sanchez-Prado *et al*., 2006